


1-1-2010

# Investigating The Metal Binding Sites In Znta, A Zinc Transporting Atpase

Sandhya Muralidharan  
*Wayne State University*

Follow this and additional works at: [http://digitalcommons.wayne.edu/oa\\_dissertations](http://digitalcommons.wayne.edu/oa_dissertations)

 Part of the [Biophysics Commons](#), and the [Molecular Biology Commons](#)

---

## Recommended Citation

Muralidharan, Sandhya, "Investigating The Metal Binding Sites In Znta, A Zinc Transporting Atpase" (2010). *Wayne State University Dissertations*. Paper 110.

This Open Access Dissertation is brought to you for free and open access by DigitalCommons@WayneState. It has been accepted for inclusion in Wayne State University Dissertations by an authorized administrator of DigitalCommons@WayneState.

**INVESTIGATING THE METAL BINDING SITES IN ZNTA,  
A ZINC TRANSPORTING ATPASE**

by

**SANDHYA MURALIDHARAN**

**DISSERTATION**

Submitted to the Graduate School

of Wayne State University,

Detroit, Michigan

In partial fulfillment of the requirements

for the degree of

**DOCTOR OF PHILOSOPHY**

2010

MAJOR: BIOCHEMISTRY AND  
MOLECULAR BIOLOGY

Approved by:

\_\_\_\_\_  
Advisor Date

\_\_\_\_\_

\_\_\_\_\_

\_\_\_\_\_

## DEDICATION

*To my Amma and Achan*

## ACKNOWLEDGEMENTS

The work presented in this dissertation is the result of several years of learning and the support and encouragement of several people. The years I spent at Wayne State University working through this dissertation have been a wonderful experience. First and foremost, I would like to thank, my parents Indira and Muralidharan and my sister Smitha for their endless love, motivation, support in every decision I have made and for believing me in all my dreams. I would also like to thank all my teachers who have taught me through school and college, and channel my thirst for knowledge.

A very special thank you to my grandmothers, my paternal grandmother whom I lost during my PhD, for all the love, and affection and my late maternal grandmother for constantly encouraging and motivating me towards higher education.

I would like to thank my advisor, Dr Bharati Mitra who supported, and encouraged me throughout this work, for the freedom to pursue my ideas. The work presented in this thesis would not have been possible without her guidance.

I would like to thank, Dr. David Evans, Dr Timothy Stemmler and Dr Larry Matherly for their direction as committee members, their comments and suggestions have contributed vastly to this dissertation. Thanks also to the Department of Biochemistry and Molecular Biology and Wayne State University School of Medicine for all the facilities and financial support. I would also like to thank Dr Barry Rosen for expressing interest in my work. Special thanks to Dr Marilyn Doscher for continued support and advice as the graduate student advisor. A very big thank you to Mr. Joe Fiore, Ms. Roselle Cooper, Ms. Yanna Marsh and Ms. Judy Thomas for all the

administrative help and making the life of an international graduate student very comfortable.

To my lab mates both past and present, the support and encouragement that I received from them has been enormous. I would like to thank Aster Dewanti and Junbo Liu, for helping me during my early days in the lab and teaching me skills of membrane protein purification and molecular biology. Shyamalee Kandegedara is a great friend and colleague, she is one of the most intelligent, unassuming and humble persons I have met. I will miss her company, the long scientific and philosophical conversations with her I will always remember. Thanks to Dhaval Joshi and Iryna King for all the help. I would also like to thank Suranjana Haldar for all the help with the EXAFS data analysis. I was lucky to have an opportunity to mentor several undergraduate students, my interactions with them helped sharpen my teaching skills. Suzan Hadwan and Brian Rutledge are two undergraduate students I will always remember. It was a joy to teach them, and I wish them all the very best in their future pursuits.

Very special thanks to all my friends who made my life in Detroit enjoyable and fun-filled. Smriti Anand, my former roommate for being a very good friend and a sisterly figure. Madhura Chakrabarti who has supported me in so many ways, for being there in good and bad, for all the crazy movies, endless hours of shopping and yapping, I wish her all the very best in the pursuit of her PhD degree. I am also very grateful to Shreyashi Ganguly, Jayprakash Saha, for being such good friends and Shreyashi, especially for providing loads of laughter at the end of a tiring day.

At the Department of Biochemistry, I have had the opportunity to meet people of different nationalities; some of them over the years have become very close friends. I

would like to thank Kristina Bencze for being a great friend and helping me during the initial days in graduate school. Ying, Poorna Subramanian, Andrea Rodrigues, Ana Jankovic, Song Chen, Jianbo Yang, Masafumi Yoshinaga, Jeremy Cook, Asmita Vaishnav and Elizabeth Masko for all the joyful times, late nights in the department and endless discussions about experiments.

I would also like to thank all my friends and family outside Detroit for their constant support, with a special thanks to Dr.Shridhar and Mrs.Nirmala Bhat, Mr.V.C.Pisharody and Mrs.Rajalakshmi Pisharody, Ms.Vasumathi Bharathan, Mr.T.P.Narayanan and Mrs.Vijayalaskshmi Narayanan, Mr. Val Narayanan and Mrs.Latha Narayanan, Mr.Sankaranarayanan and Mrs.Kamala Sankaranarayanan, Mr.Gopalakrishnan and Mrs.Devaki Gopalakrishnan, Mr.Sreejith Ramachandran, Dr.Kavitha Chendil Kumar, Dr.Pankhuree Verma, Ms.Shilpa Ramanujam and Mr.Dinesh Rabindran.

And finally, to my husband, Santosh Pisharody for the unconditional love, patience and optimism, to continue with my degree. I do not have enough words to express my thanks, for all the support and confidence he has provided.

## TABLE OF CONTENTS

Dedication . . . . .	ii
Acknowledgements . . . . .	iii
List of Tables . . . . .	xiv
List of Figures . . . . .	xv
<b>Chapter 1:</b> An Introduction to Transition Metal Homeostasis. . . . .	1
1.1 Inorganic Physiology . . . . .	2
1.2 Cellular Metal Homeostasis . . . . .	3
1.2.1 Metallochaperones. . . . .	4
1.2.2 Metal Sensors. . . . .	5
1.2.3 Metal Sequestering Proteins. . . . .	5
1.2.4 Transcriptional and Translational metal regulation. . . . .	6
1.2.5 Post translational metal regulation. . . . .	6
1.2.6 Metal transporters. . . . .	7
1.2.7 Examples of how these metalloproteins regulate copper and iron homeostasis. . . . .	8
1.3 Chemistry of Transition Metals. . . . .	9
1.3.1 Irving-William Series. . . . .	9
1.3.2 Chemical Properties of Metals. . . . .	10

1.4	Background on Zinc. . . . .	12
1.4.1	Chemistry of Zinc. . . . .	12
1.4.2	Biology of Zinc. . . . .	13
1.5	Transport systems for zinc. . . . .	14
1.6	Zinc homeostasis in <i>E.coli</i> . . . . .	17
1.7	P-type ATPases. . . . .	19
1.8	Classification of P-type ATPases. . . . .	24
1.9	Classification of P <sub>IB</sub> ATPases. . . . .	25
1.10	Background on ZntA. . . . .	28
1.11	Lead and Cadmium. . . . .	36
1.12	Aims of the thesis. . . . .	36
1.13	Significance of the thesis. . . . .	39
1.14	References. . . . .	40
<b>Chapter 2:</b>	<b>Conserved motifs in the amino terminal domain of ZntA: their role in metal binding and selectivity. . . . .</b>	<b>50</b>
2.1	Introduction. . . . .	50
2.2	Materials. . . . .	53
2.3	Experimental Methods. . . . .	53



2.3.1	Construction N1-ZntA with carboxyl - terminal strep tag. . . . .	53
2.3.2	Construction of C29A, C30A, C31A, D32A, D32N, C35A, D58A, D58N, C59A, C62A. . . . .	53
2.3.3	Protein expression and Purification of the ZntA mutants. . . . .	55
2.3.4	Protein expression and purification of N1-ZntA and N1-ZntA mutants. . . . .	57
2.3.5	Determination of Protein Concentration. . . . .	58
2.3.6	ATPase Activity Measurements. . . . .	58
2.3.7	Measurement of Metal Binding Affinity of the N1-ZntA mutants. . . . .	59
2.3.8	Preparation of Metal bound N1 and N1-mutants. . . . .	59
2.3.9	Measurement of Metal Binding Stoichiometry of the N1-ZntA mutants by ICP-MS. . . . .	60
2.3.10	Sensitivity to metal salts. . . . .	60
2.3.11	X-Ray Absorption Spectroscopy (XAS) . . . . .	60
2.4	Results. . . . .	63
2.4.1	The in vivo resistance activity of N1-ZntA mutants to Pb <sup>+</sup> , Zn <sup>2+</sup> and Cd <sup>2+</sup> in the growth medium. . . . .	63
2.4.2	Activity of the Purified N1-ZntA mutants. . . . .	66
2.4.3	Stoichiometry of Metal Binding to N1-ZntA mutants	

	using ICP-MS. . . . .	70
2.4.4	Affinity of $Pb^{2+}$ , $Zn^{2+}$ and $Cd^{2+}$ for the amino terminal metal binding site mutants using direct fluorescence quenching. . . . .	71
2.4.5	Analysis of Lead, Zinc, Cadmium, Cobalt and Copper binding by X-ray absorption spectroscopy. . . . .	75
2.5	Discussion. . . . .	86
2.6	References. . . . .	91
<b>Chapter 3:</b>	<b>The N-terminal domain of ZntA: it's role as a chaperone to the transporter. . . . .</b>	<b>95</b>
3.1	Introduction. . . . .	95
3.2	Materials. . . . .	98
3.3	Methods. . . . .	99
3.3.1	Construction of ZntA and $\Delta N$ with a carboxyl-terminal strep tag. . . . .	99
3.3.2	Construction N1-ZntA with carboxyl - terminal strep tag. . . . .	99
3.3.3	Construction of Co-expression vector containing both $\Delta N$ -ZntA (Membrane domain) and N1-ZntA (N-terminal domain) in pBADmycHisP. . . . .	100
3.3.4	Construction of double and single cysteine mutants in $\Delta 46$ -ZntA. . . . .	101
3.3.5	Expression and purification of N terminal domain of ZntA (N1-ZntA) . . . . .	103

3.3.6	Expression and Purification of ZntA and $\Delta$ N- ZntA. . . . .	104
3.3.7	Protein concentration determination. . . . .	105
3.3.8	Metal bound sample preparation for ATPase activity measurements and Transport Assay. . . . .	105
3.3.9	Measurement of Metal Concentration by ICP-MS. . . . .	106
3.3.10	ATPase activity assay. . . . .	106
3.3.11	Transport Assays in everted membrane vesicles. . . . .	107
3.3.12	Fluorescence Studies to monitor intermolecular crosslinking. . . . .	108
3.3.13	Fluorescence studies to monitor intramolecular crosslinking. . . . .	109
3.3.14	Competition Survival Assay. . . . .	109
3.3.15	Sensitivity to metal salts. . . . .	110
3.4	Results. . . . .	110
3.4.1	N1-ZntA confers a Competitive Advantage to ZntA. . . . .	110
3.4.2	The resistance profile of co-expression vector in the presence of $Pb^{2+}$ , $Cd^{2+}$ , and $Zn^{2+}$ . . . . .	112
3.4.3	ZntA and $\Delta$ N membrane vesicles supplied with N1-bound metal as the substrate catalyze ATP- dependent transport of lead, zinc and cadmium. . . . .	115
3.4.4	Metal bound N-terminal domain activates the transmembrane	

	domain of ZntA. . . . .	117
3.4.5	Interaction of N1 with $\Delta$ N. . . . .	121
3.4.6	Proximity of the two metal binding domains. . . . .	123
3.5	Discussion. . . . .	125
3.6	References. . . . .	129
<b>Chapter 4:</b>	<b>Characterizing the metal binding properties of a truncated form of ZnTa that is structurally similar to the pineal night-specific ATPase encoded by the Wilson Disease Gene . . . . .</b>	<b>133</b>
4.1	Introduction. . . . .	133
4.2	Materials. . . . .	137
4.3	Methods. . . . .	138
4.3.1	Construction of Del231-ZntA with a carboxyl-terminal His tag and carboxyl terminal strep tag. . . . .	138
4.3.2	Protein expression of Del231-ZntA. . . . .	138
4.3.3	Protein Purification of Del231-ZntA. . . . .	139
4.3.4	Determination of Protein Concentration. . . . .	140
4.3.5	Sensitivity to metal salts. . . . .	141
4.3.6	ATPase Activity Measurements. . . . .	141

4.3.7	Preparation of Metal bound Del231-ZntA. . . . .	142
4.3.8	Measurement of Metal Binding Stoichiometry of Del231-ZntA by ICP-MS. . . . .	142
4.4	Results. . . . .	143
4.4.1	The in vivo resistance activity of Del231-ZntA mutant to Pb <sup>2+</sup> , Zn <sup>2+</sup> and Cd <sup>2+</sup> in the growth medium. . . . .	143
4.4.2	Activity of the purified Del231-ZntA. . . . .	145
4.4.3	Stoichiometry of Metal Binding to Del231-ZntA using ICP-MS. . . . .	147
4.5	Discussion. . . . .	147
4.6	References. . . . .	149
<b>Chapter 5: Conclusions and Future Directions. . . . .</b>		<b>152</b>
Abstract. . . . .		155
Autobiographical Statement. . . . .		157

## LIST OF TABLES

Table 1.1.	The Composition of some common elements in the human body. . . . .	1
Table 1.2	Chemical Properties of Transition Metals. . . . .	11
Table 1.3	Chemical Properties of some Non Essential Metals. . . . .	12
Table 1.4	Hard-Soft Acid Base Classification of Metal ions and Ligands . . . . .	35
Table 2.1	Kinetic parameters for N1-mutants in the presence of lead. . . . .	67
Table 2.2	Kinetic parameters for N1-mutants in the presence of zinc . . . . .	68
Table 2.3	Kinetic parameters for N1-mutants in the presence of cadmium . . . . .	69
Table 2.4	Metal binding stoichiometry of N1-mutants. . . . .	71
Table 2.5	Association Constants for binding of Lead, Zinc and Cadmium to mutants . . . . .	75
Table 2.6	EXAFS Fitting results . . . . .	85
Table 3.1	Kinetic parameters for $\Delta N$ and ZntA . . . . .	118
Table 4.1	Kinetic parameters obtained for ZntA and Del231-ZntA. . . . .	146
Table 4.2.	Metal binding stoichiometry of Del231-ZntA . . . . .	147

## LIST OF FIGURES

Figure 1.1.	Zinc Homeostasis in <i>E.coli</i> . . . . .	19
Figure 1.2.	The Post-Albers Cycle based on the Na <sup>+</sup> /K <sup>+</sup> ATPase. . . . .	21
Figure 1.3.	Calcium ATPase Structure. . . . .	22
Figure 1.4.	Classification of P <sub>IB-2</sub> ATPases. . . . .	28
Figure 1.5.	Schematic representation of ZntA. . . . .	29
Figure 1.6.	Sequence Alignment of N-terminal domain of P <sub>IB-2</sub> subgroup. . . . .	30
Figure 1.7.	Solution structures of N-terminal domain of CadA, ZntA and CopA. . . . .	32
Figure 1.8.	Sequence alignment of Helix 6 of ZntA and its close homologues. . . . .	33
Figure 1.9.	Sequence alignment of Helix 7 and 8 of ZntA and its close Homologues. . . . .	33
Figure 1.10.	Sequence Alignment of Helix8 of ZntA compared to Helix 6 of Ca <sup>2+</sup> ATPase and Na <sup>+</sup> /K <sup>+</sup> ATPase. . . . .	34
Figure 2.1.	Sequence Alignment of N-terminal domain of P <sub>IB-2</sub> subgroup. . . . .	52
Figure 2.2.	Resistance profile of the N-ZntA mutants to lead, zinc and cadmium. . . . .	64
Figure 2.3.	Fluorescence Spectra obtained for titration of N1-ZntA with Lead. . . . .	73
Figure 2.4.	Plot of change in fluorescence emission. . . . .	74
Figure 2.5.	EXAFS and Fourier transforms of lead bound N1-ZntA. . . . .	76
Figure 2.6.	EXAFS and Fourier transforms of zinc bound N1-ZntA. . . . .	78

Figure 2.7	EXAFS and Fourier transforms of copper bound N1-ZntA. . . . .	80
Figure 2.8	EXAFS and Fourier transforms of cobalt bound N1-ZntA. . . . .	81
Figure 2.9	EXAFS and Fourier transforms of cadmium bound N1-ZntA. . . . .	83
Figure 2.10	Sequence alignments of the N-terminal domain of P <sub>B</sub> ATPases. . . . .	90
Figure 3.1.	Metal Binding sites in ZntA. . . . .	97
Figure 3.2	Scheme for construction of co-expression vector. . . . .	101
Figure 3.3	Location of restriction sites in the position of cysteine residues. . . . .	103
Figure 3.4	Model for Transport Assay in everted membrane vesicles. . . . .	108
Figure 3.5	Agarose gel picture of Molecular competition assay. . . . .	112
Figure 3.6	Resistance profile of co-expression vector. . . . .	114
Figure 3.7	Plots of the Transport Assay. . . . .	116
Figure 3.8	Representative ATPase activity assay plots obtained for $\Delta$ N. . . . .	119
Figure 3.9	Representative ATPase activity assay plots obtained for ZntA. . . . .	120
Figure 3.10	Fluorescence resonance energy transfer spectra. . . . .	122
Figure 3.11	Model showing cysteine residues in $\Delta$ 46-ZntA. . . . .	123
Figure 3.12	Fluorescence emission spectra showing the pyrene excimer. . . . .	125
Figure 3.13	Model for metal delivery to the transmembrane metal binding site in ZntA. . . . .	129



Figure 4.1	Membrane topology of PIB and P2/P3 ATPases. . . . .	133
Figure 4.2	Structure of PINA. . . . .	137
Figure 4.3	Structure representing ZntA and Del231-ZntA. . . . .	137
Figure 4.4	Resistance profile of Del231-ZntA. . . . .	143

## CHAPTER 1

### AN INTRODUCTION TO TRANSITION METAL HOMEOSTASIS

All living organisms are maintained by constant chemical processes which require many of the elements of the periodic table. Metals play different roles in living systems (1). Organisms have evolved to make use of the special properties of metals to perform many important functions. Some of these are for biological signaling processes, charge maintenance, structural roles, electron transfer, enzyme catalysis, dioxygen transport (2-3). The metal ions are made available to the organisms by various methods depending upon the surrounding conditions; these elements can be made bioavailable or the organisms accumulate the necessary nutrients by several processes.

**Table 1.1.** The Composition of some common elements in the human body(2).

ELEMENT	PERCENTAGE(by weight)
Sodium, Potassium, Sulfur	0.1
Chlorine	0.09
Silicon, Magnesium	0.04
Iron, Fluorine	0.005
Zinc	0.003
Copper, Bromine	$2 \times 10^{-4}$
Selenium, Manganese, Arsenic, Nickel	$2 \times 10^{-5}$
Lead, Cobalt	$9 \times 10^{-6}$

## 1.1 INORGANIC PHYSIOLOGY

Living cells constantly acquire, store and transport metal ions such that the optimal concentrations of these metals are readily available for metalloproteins and also to protect themselves from the toxic effects of metal excess (3). The optimal concentrations of different metals can vary widely. The concentration of calcium is very high in the human body and its major use is the stabilization of the endoskeleton (2). Also are present large amounts of potassium, sodium and magnesium which function to maintain charge and osmotic balance or as structural elements (2). These elements belong to Groups I and II of the periodic table and are called macro nutrients (2, 4). Some elements like iron, zinc, copper, molybdenum, cobalt, chromium, vanadium and nickel are less abundant. These transition metals are called trace metals (2). Iron, copper, zinc, cobalt, and nickel are essential for organisms and play several important biological roles. Iron is involved in dioxygen transport in hemoglobin and myoglobin and in electron transfer (2, 4). Copper serves as an electron carrier in cytochrome c oxidase, as a facilitator of oxygen transport in hemocyanin, and also as a catalytic site for enzymes such as superoxide dismutase (2, 4). Zinc functions as a structural element in zinc finger proteins; it plays a regulatory role (in superoxide dismutase) and catalytic roles in several enzymes. Cobalt serves in alkyl group transfer in Vitamin B<sub>12</sub> and oxidases (2). Nickel is involved in nitrogen fixation, oxo transfer in oxidases, and plays a catalytic role in hydrogenases and hydrolases (2, 4).

Studies in bacterial cells have shown that they maintain transition metal ions in a fixed and narrow range; this is represented as the total number of metal atoms per cell, and this value is called the metal quota (5). *E.coli*, for instance concentrates transition metal ions down to a narrow range as follows: iron and zinc (~0.1mM), and copper, manganese, molybdenum and selenium (~ 0.01mM) (6). Other metal ions such as sodium, potassium and magnesium are highly abundant in bacterial cells (~10mM) (6). Some toxic metals like cadmium, mercury, lead are also found in organisms but do not have any specific or known biological role. For this reason, metal ion concentrations have to be very tightly controlled since they are essential for survival but at the same time any change in concentration can cause havoc. Essential transition metal levels in a cell have to be precisely regulated such that there is a sufficient supply of the metal, at the same time an excess of essential and the non essential metals must be avoided since it would lead to metal toxicity. This process of maintaining the concentration of essential metal ions in the right concentration range is called homeostasis, and detoxification or resistance is the removal of toxic concentrations of non essential metal ions (7). All organisms have to maintain metal homeostasis for survival.

## 1.2 Cellular Metal Homeostasis

Metal ion regulation is a very important cellular function performed in unison by several proteins: metallochaperones, metalloregulators and metal transporters (8). These proteins are involved in the tightly regulated processes of uptake, storage and secretion. Two decades ago, the discovery of the genes

responsible for Wilsons, Menkes, and Lou Gehrig's diseases threw light on cellular metal homeostasis mechanisms (9). Wilsons disease is an autosomal recessive disorder characterized by the accumulation of toxic amounts of copper in the liver, kidney and brain (10). ATP7B, a 1411 – amino acid copper transporting ATPase, is the gene responsible for this disease; it is located on chromosome 13 (10). Menkes disease is an X-linked disorder characterized by a deficiency of copper and is caused by defects in the *ATP7A* gene (11). Both these proteins are involved in copper transport. Some other proteins which were subsequently studied were transferrin that transports iron into the cell, its counterpart being ferritin which is involved in iron efflux (11). Studies on the Wilsons and Menkes proteins and similar proteins in several organisms have lead to models showing how chaperones, sensors and transporters work towards metal delivery, and positioning metals in the required location in the cell.

### 1.2.1 Metallochaperones

Metallochaperones are helper proteins which bind to metal ions and transfer them to the target proteins (12). Copper, nickel and iron chaperones are well documented. Examples of chaperone proteins are Atx1 which is the first copper chaperone to have been identified in *S.cerevisiae*; the human homolog of this protein is Atox1 which transfers copper to the Menkes and Wilsons disease proteins (9). The bacterial homolog of Atox1 and Atx1 is CopZ in *E.coli* which interacts with CopA and CopY (9, 12). CCS is a copper chaperone for superoxide dismutase which inserts copper directly into the target protein (12). So far only two known iron chaperones have been documented in literature.

Frataxin, a protein implicated in a neurological disease Friedreich's ataxia, is a mitochondrial iron chaperone (13). Human poly(rc) binding protein 1 (PCPB1) is a cytosolic iron chaperone that binds to iron and loads ferritin (13). The nickel chaperone UreE delivers the metal to the active site of the enzyme Urease (14). Chaperone proteins for very few metals are known, so it is thought that most proteins get their metals from the cytoplasmic metal pools. But then, how do the cells sense the need for metal ions?

### 1.2.2 Metal Sensors

Metal sensors are transcriptional regulators; they detect and respond to metal deficiency or excess in the cells. There are several bacterial sensors which have been identified they are classified as metal de-repressors, co-repressors and metal activators (15). ArsR-SmtB, CsoR-RcnR and CopY are some of the metal de-repressors and Fur, NikR and DtxR are co-repressors, and MerR is an example of an activator (15).

### 1.2.3 Metal Sequestering Proteins

Cells can control the transport of metal ions but at the same time they can also control the free metal ion concentrations with the help of metal sequestering proteins. The example of Metallothionein illustrates the role of a metal sequestering protein. It participates in the process of sequestering metals such as zinc and thus serves as a reservoir for zinc ions (16). In addition to zinc, metallothionein can also bind to cadmium, and lead. Metallothionein is a cysteine rich protein that can bind to seven zinc ions in two zinc/thiolate clusters. In one cluster, three zinc ions are bound to nine cysteines ( $Zn_3S_9$ ) and the other has

four zinc bound to eleven cysteines ( $Zn_4S_{11}$ ) (16). In these clusters, zinc is in a tetrahedral coordination environment with the sulfurs (16). The different zinc ions bind to metallothionein with a range of affinities. Cadmium also binds to metallothionein with four coordinate geometry. Unlike zinc and cadmium, metallothionein binds to lead in trigonal geometry (17).

#### **1.2.4 Transcriptional and Translational metal regulation**

Metal regulatory transcription factor (MTF1) genes are induced in response to metals such as copper, cadmium and zinc. Studies have reported that zinc stabilizes a complex between MTF1 and its DNA binding site (15). The *Drosophila* MTF1 has a copper cluster and zinc fingers, the cysteine residues that coordinate the cluster when replaced by alanine do not upregulate the transcription of copper metallothionein gene in response to a high concentration of copper (15). Also are present several proteins that control translation or mRNA stability for different gene products. Some examples are the iron responsive proteins IRP1 and IRP2; they bind to iron responsive elements in mRNAs that encode ferritin and transferrin receptor. Ferritin is required when there is excess iron and transferrin is needed when there is low amount of iron (15).

#### **1.2.5 Post translational metal regulation**

Degradation of proteins involved in metal homeostasis is a way of post translational metal regulation; this applies to several proteins such as the iron responsive protein IRP2, the copper chaperone CCS, the copper importer CTR1, the iron efflux protein ferroportin and the zinc uptake transporter ZIP4 (15). ZIP4

is a good example to explain the phenomenon of post translational metal regulation. When zinc is low, the extracellular amino terminal domain of ZIP4 undergoes proteolytical degradation (15). When zinc is absent ZIP4 is removed from the plasma membrane to a perinuclear location and when zinc is very high ZIP4 is degraded. ZIP4 has a histidine rich motif that is responsible for ubiquitination and proteolytic degradation (15). This motif also responds to cadmium by triggering degradation.

### 1.2.6 Metal transporters

Metal transporters are important members of the metal trafficking machinery. The uptake and efflux transporters are expressed under decreased and high metal conditions, respectively. Some of the transporters at the cytoplasmic membrane are ABC (ATP-binding cassette)-type ATPases, P-type ATPases, cation diffusion facilitator proteins, NRAMPs (natural resistance associated with macrophage protein) and ZIPs (Zrt /Irt – like protein) (18). The ABC transporters and the P-type ATPases utilize the energy from ATP hydrolysis to pump metal ions. ABC transporters are uptake pumps, they import manganese, zinc, nickel and iron across the cell membrane (18). These pumps work in unison with proteins located in the periplasm. P-type ATPases are efflux pumps that export a wide variety of metals. The CDF proteins export ions from the cytoplasm, through a coupled transport of two ions in the opposite direction (18). Nramp is a large family of proton coupled transporters that have roles in uptake of iron and manganese (18). Mammalian members of the ZIP family of proteins have been identified.



Thus, metallochaperones, metal sensing proteins and metal transporters together play an important role in regulating the intracellular transition metal concentration and helping cell survival.

### **1.2.7 Examples of how these metalloproteins regulate copper and iron homeostasis**

#### *Copper homeostasis*

In mammals, copper is absorbed from the gastrointestinal tract by a P-type copper transporting ATPase, *ATP7A* (Menkes protein) (19).  $\text{Cu}^+$  is then transported into the cell by the human copper transporter(hCTR1), and from here is further delivered to other targets by other copper chaperone proteins like Atox1, Ccs1, Cox17 and glutathione for delivery to Wilsons protein (*ATP7B*), superoxide dismutase, cytochrome oxidase, and metallothionein (19-20). *ATP7B* then transports copper to the luminal side of the secretory network (19).

#### *Iron homeostasis*

Like copper, iron is another vital metal that is required for the formation of hemoglobin and myoglobin; it helps maintain a healthy immune system (21). The iron homeostasis machinery mainly involves transferrin, iron that is absorbed is bound to transferrin (22). Transferrin receptors assist transferrin in shuttling the iron to cellular targets. Some other proteins involved in iron homeostasis are DMT1(divalent metal transporter1), ferroportin, ceruloplasmin, Nramp2 (21-22).

Unlike the copper and iron metabolism and homeostasis, which have been well studied and documented, very little is known about the uptake and storage of other metal ions. In the pursuit of understanding the details of other

metal homeostasis, our lab over the years has worked on metal transporters and my research over the past few years has focused on a zinc efflux pump in *E.coli* – the zinc transporting ATPase, *ZntA*.

### 1.3 Chemistry of Transition Metals

Transition metal ions in cells are found chelated to proteins or cofactors; the common metal ligands are O, N, S, or C. Within the cell there are present a large number of non specific binding sites for metals, thus it is truly a challenge to accommodate each metalloprotein with the correct metal ion (14). How does nature distinguish between the different transition metal ions and maintain a balance of ions? In order to understand this phenomenon one must first be familiar with the Irving-William series (the natural order of stability for divalent transition metals) and also the chemical properties of transition metals.

#### 1.3.1 Irving-William series

In the complex cellular environment, as per the Irving-William series copper and zinc form the tightest complexes, then nickel and cobalt, then ferrous iron and manganese and finally the weakest complexes are formed by calcium and magnesium ( $Mg^{2+} < Ca^{2+} < Mn^{2+} < Fe^{2+} < Co^{2+} < Ni^{2+} < Cu^{2+} > Zn^{2+}$ ) (14). But within the same cell some proteins bind to uncompetitive metals and some proteins bind to competitive metal ions. How do the proteins distinguish the wrong metals from the right ones? Cells overcome the problem imposed by the Irving-William series by compartmentalization and this was recently demonstrated by two periplasmic proteins in cyanobacteria, MncA for manganese and CucA for copper (23). Manganese and copper are at the

opposite ends of the Irving-William series, and both proteins prefer to bind to copper in vitro. The concentration of manganese in the cytoplasm is  $\sim 10 \mu\text{M}$  and that of copper is in the pM range (4). The MncA protein is a substrate for Tat (twin-arginine translocase) which helps MncA to fold in the cytoplasm to trap manganese; now MncA is folded and the metal binding site is buried inside the protein (23). On the other hand CucA is a substrate for Sec (general secretory pathway) which enables the CucA to fold in the periplasm after export thus binding to the competitive copper (23). Thus MncA and CucA can exist together and manganese cannot be replaced by the competitive copper.

### **1.3.2 Chemical Properties of Metals**

Transition metals are involved with many different metalloproteins. Most of these transition metals have more than one oxidation state. Some oxidation states are more common than the others. They also display different geometry and coordination which may govern metal selectivity and specificity.

**Table 1.2.** Chemical Properties of Transition Metals (2).

Oxidation State	Coordination Number	Geometry
Iron(II), d6	4-6	Tetrahedral, Octahedral
Iron(III), d5	3-8	Trigonal, Tetrahedral, Square planar, Trigonal bipyramidal, Octahedral
Cobalt(I), d8	6	Octahedral
Cobalt(II), d7	4,6	Tetrahedral, Octahedral
Cobalt(III), (d6)	6	Octahedral
Nickel(II), d8	4,6	Square planar, Octahedral
Copper(I), d10	3,4	Trigonal planar, Tetrahedral
Cu(II), d9	3-6	Trigonal planar, Tetrahedral, Square pyramid, Tetragonal, Square planar
Zinc(II), d10	4-6	Tetrahedral, Square pyramid, Octahedral

Knowledge of the chemical properties of non essential metal ions like cadmium, lead and mercury is very useful in understanding how these metals mimic essential metal ions leading to toxic side effects.

**Table 1.3.** Chemical Properties of some Non Essential Metals (2).

Oxidation State	Coordination Number	Geometry
Cadmium(II), d10	4,6	Tetrahedral, Octahedral
Lead(II),d10	3-6	Trigonal, Pyramidal, Square planar, Octahedral
Mercury(II),d10	2	Linear

#### 1.4 Background on Zinc

Zinc is the most common transition metal ion in the cytoplasm, but it is not as prevalent as group 1 and 2 metal ions (4). Zinc, which is essential for cell survival, serves as a cofactor for many enzymes. It plays a structural role as a scaffold for RNA polymerase, and tRNA synthetases (24). Zinc inhibits free radical formation and thus protects sulfhydryl groups. When the cellular concentration of zinc increases it has toxic effects; it blocks thiols and prevents disulfide bond formation and binding of other metals to their active sites (18, 24-25).

##### 1.4.1 Chemistry of Zinc

Zinc has an outer electronic configuration of  $3d^{10}4s^2$ . Zinc is a very small ion (radius  $0.65\text{\AA}$ ) and has a very concentrated charge to size ratio (4). It is also a good electron acceptor or Lewis acid, and its electron affinity is similar to copper and nickel (4). These metal ions bind to donors such as thiolates and amines with a high affinity. However, zinc does differ from copper and nickel in

its oxidation state (4). Both copper and nickel display multiple oxidation states. This redox inertness of zinc is perhaps a reason why it is a preferred metal ion in several biological reactions since redox activity introduces the risk of free radical formation (4). In addition to small size, high charge density and redox inertness, it also displays both hard and soft metal character. Zinc uses sulfur, oxygen and nitrogen as ligands in biological systems (17). Cys, His, Asp, and Glu are the most common amino acid ligands in zinc proteins. The coordination geometries preferred by zinc in biology are tetrahedral and trigonal bipyramidal (2). The diverse properties and flexible nature of zinc may explain why it is the only metal being represented in all six recognized classes of enzymes (17). The properties that make zinc valuable in biology relative to other metals are its availability, fast ligand exchange, redox inertness, flexible coordination geometry, good Lewis acid properties, and intermediate soft metal character; these are all put to particular uses in the cell.

#### **1.4.2 Biology of Zinc**

Zinc bound to proteins can play both structural and catalytic roles. Two well known zinc metalloproteins are Cu/Zn superoxide dismutase and alcohol dehydrogenase (Adh1). These are examples of high affinity zinc sites; low affinity zinc binding sites are present on proteins, lipids, and DNA and amino acids (histidine), glutathione and organic anions (citrate) (26). Since zinc is an integral part of so many proteins and reactions, the amount of free zinc in the cell must be very low. The term “free” is used to specify the labile zinc that is freely available for participating in reactions (26). Studies suggest that the total amount

of zinc present in the cell is in the millimolar range (6, 26). Many of the zinc metalloproteins have very high binding affinities, 1 nM zinc is equivalent to about 30 zinc ions per yeast cell and about 300 ions in a mammalian cell (26). Interestingly, free zinc is much lower in concentration (femtomolar range) despite the total amount of zinc being so much higher (6, 26-27). This underscores the perfect regulation of free zinc inside the cell and the delicate balance between zinc uptake, efflux, and sequestration.

Zinc regulators induce or repress specific operons or genes. These gene products are involved in zinc transport. In *E.coli* two zinc sensors Zur and ZntR have affinities in the femtomolar range for zinc which is much lower than the concentration of zinc in the cell (26-27). When the cell is zinc deficient, the Zur regulatory protein which is a member of the Fur family of bacterial metal responsive regulators, induces the expression of uptake transporters such as ZnuABC and ZupT (17, 26). Once the uptake stops, the accumulated zinc is used by the zinc proteins or the excess is exported out of the cell. ZntR which belongs to the MerR family of transcriptional regulators, induces the efflux transporter ZntA (17).

### **1.5 Transport systems for zinc**

Transporters are a major component of the zinc homeostasis machinery. The import of zinc and its transport out of the cell requires several membrane transport proteins. Zinc transport proteins belong to several families: some of them are ZIP proteins, ABC transporters, RND transporters, P-type ATPases, and CDF proteins (26, 28).

### **The ZIP proteins [(Zrt/Irt-like protein) ZIP (SLC39) family]**

The first identified members of this family were the yeast Zrt1 and the *Arabidopsis* Irt1 proteins. Mammalian ZIP proteins have been designated as SLC39 (26, 28). The ZIP proteins have 8 transmembrane domains (29). Many proteins that belong to this family have a histidine rich loop located between the 3<sup>rd</sup> and 4<sup>th</sup> transmembrane domains which may be involved in zinc binding (29). The mechanism of transport used by ZIPs is still not very clear. Zrt1 in yeast uses energy to transport zinc, whereas the human Zip2 (SLC39A2) is not energy dependent (29). Studies show that zinc uptake by the mammalian transporter may be due the HCO<sub>3</sub> gradient across the cell membrane (26).

### **The ABC transporter family**

This is a diverse group of active membrane transporters. Members of this group mediate a variety of transport processes in both prokaryotes and eukaryotes. They play a role in maintaining metal homeostasis by importing metal ions such as zinc; in addition they are also involved in the uptake of nutrients, resistance to cytotoxic drugs and antibiotics, and cholesterol and lipid trafficking (26). ABC transporters are a complex of three proteins, one or two of them being membrane embedded (30). These proteins form a pore in the membrane that permits the transport of specific substrates (28). Energy of ATP hydrolysis is used to transport substrate across the membrane (28).

### **The CDF proteins**

The mammalian members of the cation diffusion facilitator (CDF) family are called ZnT (SLC30) (26). CDF transporters are present bacteria, fungi, plants



and mammals. Most members of this family have six transmembrane domains (26, 28). The CDF proteins also have a histidine rich cytoplasmic loop between transmembrane domains 4 and 5. Many CDF proteins transport metals by antiport ( $Zn^{2+}/H^+$  or  $K^+$ ) (26).

### **The RND (Resistance-Nodulation-Division) family**

An example of the RND family is the CzcABC protein in *Ralstonia metallidurans*. The CzcD protein is induced under high  $Zn^{2+}$  concentrations (31). CzcA, CzcB and CzcC form a complex system that exports  $Zn^{2+}$ ,  $Co^{2+}$  and  $Cd^{2+}$  across the cytoplasmic and outer membrane. CzcA is a cation–proton antiporter that is located in the cytoplasmic membrane (31). CzcB is located in the periplasm. CzcC connects CzcB to the outer membrane to form CzcABC protein complex (31).

### **Other Efflux Transporters**

Zinc efflux transporters mediate the export of intracellular zinc to avoid the over accumulation of zinc and thus protects the cell from toxic side effects of zinc overload. In mammalian cells, Znt1/SLC30A1 which belongs to the CDF family plays a role in zinc efflux to maintain cellular zinc homeostasis and trans-epithelial zinc trafficking (26). In the brain, the zinc efflux transporters are very important after an ischemia or epileptic seizures as there is high accumulation of zinc (32). Yeast is different from other eukaryotes; it does not have any zinc efflux systems but the excess zinc is sequestered into vacuoles and this is a site for detoxification (26).

## 1.6 Zinc homeostasis in *E.coli*

*E.coli* is a very good model system to study zinc transporters. Our lab has for several years used *E.coli* transporters as model systems to characterize metal transporters. *E.coli* has a zinc quota of  $\sim 10^5$  atoms of zinc per cell (6, 26). *E.coli* has both high and low affinity transporters that work together to maintain cellular zinc homeostasis.

### Broad Spectrum Zinc uptake transporter in *E.coli*

When the zinc concentration in an *E.coli* cell is within the normal range, a broad substrate transporter ZupT is induced. ZupT is the first characterized bacterial uptake pump that belongs to the ZIP family of proteins (33). ZupT has eight transmembrane helices and studies have shown that ZupT is involved in the uptake of several ions such as  $Zn^{2+}$ ,  $Fe^{2+}$ ,  $Co^{2+}$ ,  $Cd^{2+}$  and  $Mn^{2+}$  (33-34). The energy source and the mechanism of transport are not clear.

### High affinity Zinc uptake pump in *E.coli*

When zinc concentrations are extremely low, the *E.coli* operon *znuABC* is induced by Zur. The ATP dependent uptake of zinc is catalyzed by ZnuABC. This pump depends on ZnuA which is a periplasmic binding protein having the ability to bind metal ions and ATP (18). ZnuB is the membrane permease and ZnuC is the subunit that catalyses ATP hydrolysis (18).

### Low Affinity zinc Efflux transporter in *E.coli*

Unlike the transporters involved in zinc uptake, the zinc export proteins have more specific substrates. Here too, there are high affinity and low affinity systems. ZitB (YbgR) a member of the CDF family is a low affinity zinc efflux

transporter (18). Sequence analysis and site directed mutagenesis studies suggest several residues such as His53, His159, Asp163 and Asp186 are essential for function (18). It has been observed that these residues are conserved in other CDF proteins even though the metal transported may vary suggesting that these residues may form a proton channel (17).

### **High Affinity Zinc Efflux transporter in *E.coli***

In *E.coli*, when there is an over accumulation of zinc, ZntR a zinc sensor activates the expression of an active transporter ZntA (Zinc transporting ATPase) which is a high affinity pump that is involved in zinc efflux (28). ZntA belongs to the P-type ATPase family of transporters. These are a class of ion pumps that are involved in many biological processes such as generating membrane potential, muscle contraction, removal of toxic ions from cells.

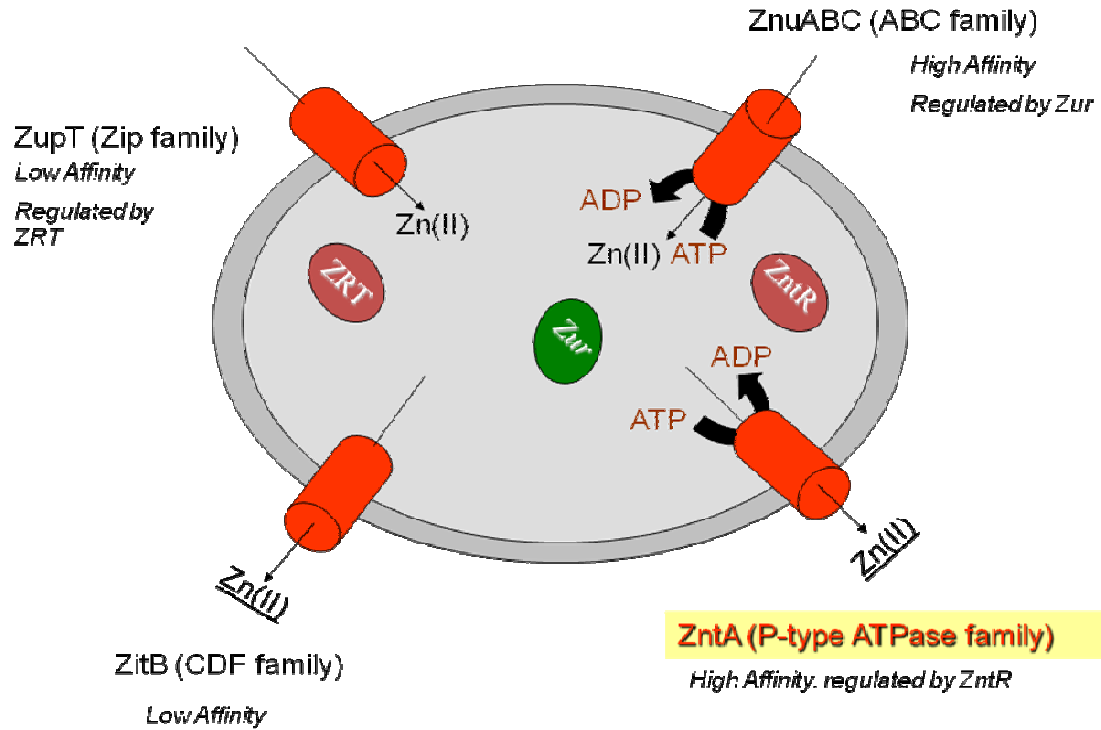


**Figure 1.1.** Zinc Homeostasis in *E.coli*.

### 1.7 P-type ATPases

In 1950's Jens Skou discovered the first P-type pump, the  $\text{Na}^+/\text{K}^+$  ATPase that uses ATP to transport  $\text{Na}^+$  and  $\text{K}^+$  ions across the axonal membrane (35). Through the years many other pumps with similar characteristics have been discovered such as the gastric  $\text{H}^+/\text{K}^+$  ATPase and the sarcoplasmic-reticulum  $\text{Ca}^{2+}$  ATPase that plays an important role in muscle contraction. A common feature of this class of transporters is the formation of a phosphorylated intermediate during the reaction cycle (36). The  $\text{Ca}^{2+}$ -ATPase,  $\text{Na}^+/\text{K}^+$  ATPase,  $\text{H}^+/\text{K}^+$  ATPase are very well studied and documented. Studies on these pumps have revealed several interesting details about the structure and mechanism of

this family of transporters. All the members of the P-type ATPase family have four well-defined domains.

### **The Phosphorylation (P) domain**

This domain contains the DKTGTLT motif, which is conserved throughout the P-type ATPase family. The *Asp* in this motif gets phosphorylated reversibly during the reaction. The P-domain in  $\text{Ca}^{2+}$  ATPase is roughly spherical and has a Rossman fold with a central seven stranded  $\beta$ -sheet flanked by  $\alpha$ -helices (37). This domain is homologous to bacterial ATPases (36).

### **The Nucleotide (N) domain**

As the name suggests it is here that ATP binds. The N-domain is a part of the P-domain. In the  $\text{Ca}^{2+}$  ATPase it is a  $\beta$ -sheet made of seven strands. The N-domain of  $\text{Na}^+/\text{K}^+$  ATPase has a similar fold as the  $\text{Ca}^{2+}$  ATPase except that the  $\beta$ -sheet is made up of six and not seven strands (37).

### **The Actuator (A) domain**

The sequence of this domain like the P-domain is highly conserved. It contains the conserved TGES motif. This domain is not involved in metal binding. Structural studies indicate that this domain has a  $\beta$ -sheet jelly roll fold which contains many conserved residues. This domain and especially the conserved TGES motif comes in close contact with the phosphorylation domain when the ion is being pumped (37).

### **The Membrane (M) domain**

The membrane domain consists of six to ten membrane helices depending on the P-type ATPase family. The  $\text{Ca}^{2+}$ -ATPase and  $\text{Na}^+/\text{K}^+$  ATPase

have 10 transmembrane helices (38). On comparing the sequences of the membrane region of various ATPases they were found to have very little sequence homology. However the overall structure of this region is similar. In the SR-  $\text{Ca}^{2+}$ -ATPase, Asp800 in M6 and Glu805 in M8 provide ligands for  $\text{Ca}^{2+}$  binding (37). The corresponding sites involved in ion translocation in *N.crassa*  $\text{H}^+$  ATPase are Asp730 and Glu 805, and in *A.thaliana*  $\text{H}^+$  ATPase, it is Asp 684 (39). In addition to these, Val304, Ala305 and Ile307 in M4 are also involved in binding  $\text{Ca}^{2+}$  (37).

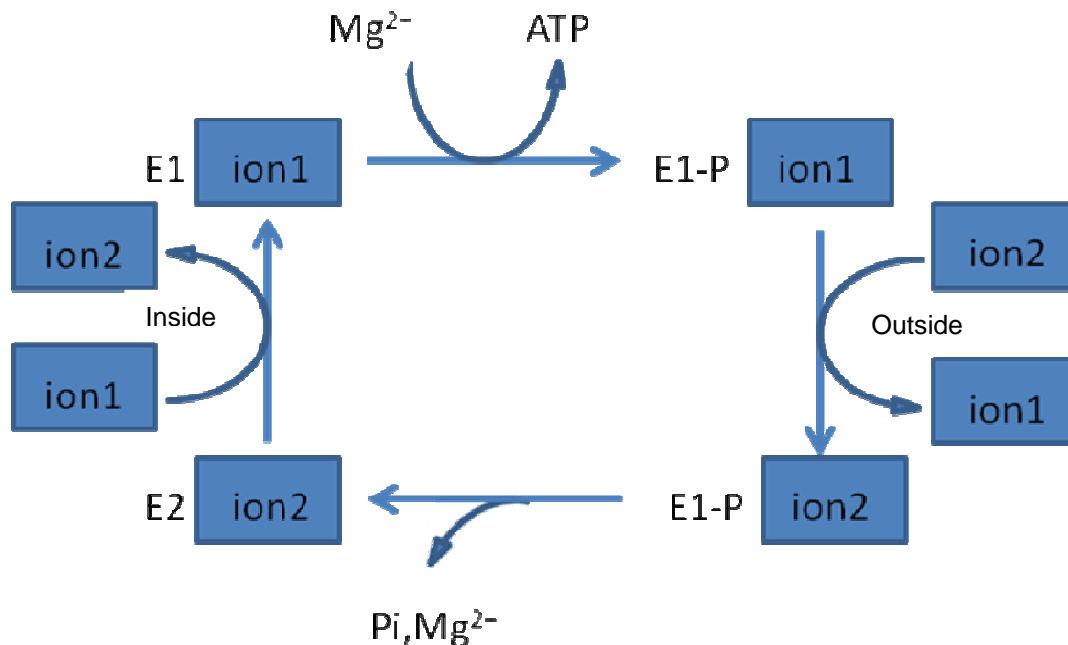


**Figure 1.2.** The Post-Albers Cycle based on the  $\text{Na}^+/\text{K}^+$  ATPase.

The ion 1 from the interior of the cell binds to the high affinity site in the ATPase which is the E1 state. Ion binding triggers phosphorylation of the enzyme by  $\text{Mg}^{2+}$ -ATP, which leads to the phosphorylated E1-P state. The phosphorylated E2-P state then forms, which is unable to phosphorylate ADP, and this state has

a reduced affinity for ion 1, and it goes outside the cell. Ion 2 binds from the outside and, on hydrolysis of the phosphorylated Asp, the enzyme releases ion 2 to the interior and rebinds ions 1. The enzyme is ready to start another cycle.

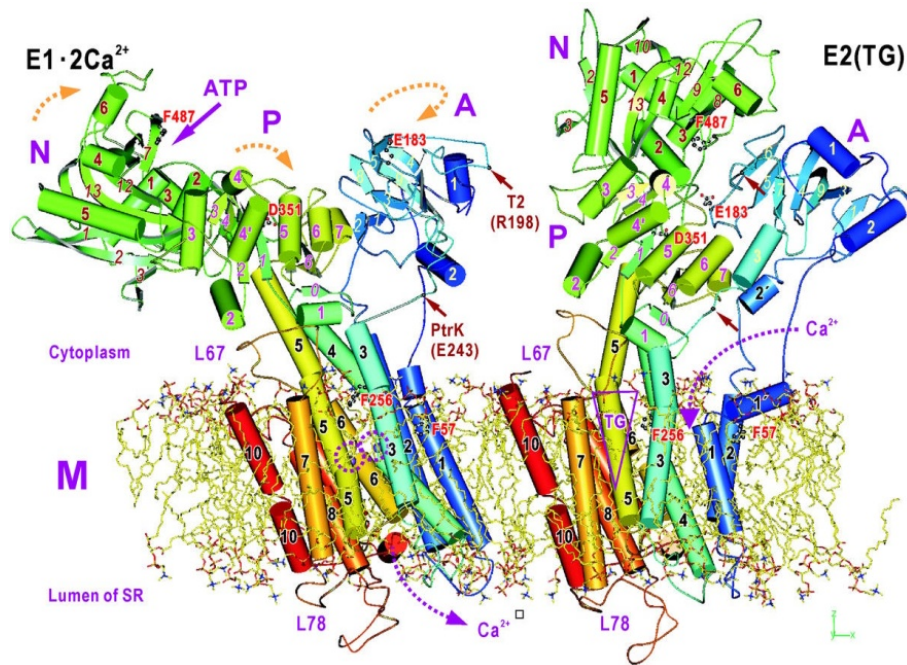


**Figure 1.3.** E1·2Ca<sup>2+</sup> and E2 (TG)2 forms of Ca<sup>2+</sup> ATPase in the lipid bilayer, generated by molecular dynamics simulation (37). E1·2Ca<sup>2+</sup> is the high affinity state when the two calcium ions from the interior of the cell are bound to the ATPase in the E1 state. Ion binding triggers the phosphorylation of the ATPase, this leads to formation of the E2-P state, which is unable to phosphorylate ADP and has low affinity for the metal ion. In the figure, the cylinders represent the  $\alpha$ -helices, arrows  $\beta$ -strands.

Ca<sup>2+</sup> ATPase is about 150 Å high and 80 Å thick, it is made up of a cytoplasmic head piece, a transmembrane domain which has 10  $\alpha$ -helices (M1-M10), and small luminal loops (40). Helices M2, M3, M4 and M5 have long cytoplasmic extensions (37, 40). The cytoplasmic headpiece is made up of the Actuator,

Nucleotide binding and Phosphorylation domains. In the  $\text{Ca}^{2+}$  ATPase the A domain controls the gating mechanism that in turn controls the  $\text{Ca}^{2+}$  binding and release (37). The N domain contains the ATP binding site. In the phosphorylation domain, the  $\gamma$ -phosphate reacts with the Asp351 (37). In the  $\text{E1.Ca}^{2+}$ , the A, N and P domains are wide apart. A domain is connected to helices M1 – M3, and P domain to helices M4 and M5. Helix M5 is very long, it functions as the backbone of the molecule (37). The SR  $\text{Ca}^{2+}$  ATPase has two high affinity  $\text{Ca}^{2+}$  binding sites in the transmembrane region (indicated by two purple circles in figure1.3). When the two  $\text{Ca}^{2+}$  ion dissociate to form the E2 state, the three domains which were wide apart come close together to form a compact structure (37). P domain inclines  $30^\circ$  with respect to the membrane, N domain rotates  $60^\circ$  with respect to the P domain and A domain shifts  $110^\circ$  horizontally (37). In the E2 state, helices M1, M3 and M5 are bent (37). Helices M1-M6 undergo major changes involving rearrangement (37). Thus, dissociation of  $\text{Ca}^{2+}$  ions leads to change in position of P domain which in turn leads to structural changes in the membrane region.

All P-type ATPases follow the same reaction mechanism. The Phosphorylation and Actuator domains all function in a similar manner. It is the N-terminal and the membrane domains that are involved in metal binding, depending of the class of ATPase their metal ion selectivity changes. Thus each ATPase has evolved to accommodate metal ions having different size and geometry (36).



## 1.8 Classification of P-type ATPases

On the basis of sequence alignment and substrate specificity this family is classified into five groups (group's I-V). Each group is further divided into subgroups on the basis of substrate specificity (36, 41).

### Type IA ATPases

This is a class of bacterial pumps, the *E.coli* Kdp K<sup>+</sup>- pump is an example of this group. Kdp is made up of four different proteins – KdpF, KdpA, KdpB and KdpC. KdpB is the ATPase that pumps K<sup>+</sup> ions and it has six membrane helices (42-43).

### Type IB ATPase

These transporters were discovered much later. They are simpler in terms of evolution especially the bacterial pumps. These ATPases are very widespread, and are present from archea to man. This group of ATPases has very broad substrate specificity; they are soft transition metal ions. Some of the examples of this class are the bacterial metal resistance proteins such as CopA, ZntA and CadA. These pumps assist in maintaining homeostasis of essential metal ions such as Cu<sup>+</sup> or Zn<sup>2+</sup> which may be toxic when they are in excess and also remove toxic ions such as Ag<sup>+</sup>, Cd<sup>2+</sup> and Pb<sup>2+</sup> from the cell thus maintaining the homeostasis of essential ions (36, 44-46).

### Type II and Type III ATPases

The previously mentioned sarcoplasmic reticular Ca<sup>2+</sup>- ATPase, and the Na<sup>+</sup>/K<sup>+</sup> ATPase belong to Type II and the H<sup>+</sup> ATPase is an example of class III.

## Type IV and V

Both type IV and V are groups of transporters which are not as well researched as the other classes of P-type ATPases. Type IV ATPases are found in eukaryotes, where they are involved in lipid transport and maintenance of lipid bilayer asymmetry (36). They are also known as lipid flippases. Studies in the red blood cell and *S.cerevisiae* have shown that these flippases translocate phospholipids from the outer to the inner leaflet of plasma membranes (36). These proteins have similar features as the metal ion transporting P-type ATPases. The type V family of transporters has features similar to other P-type ATPases, however their substrate specificities and biological roles are yet to be studied (36).

### 1.9 Classification of P<sub>1B</sub> ATPases

The Zinc Transporting ATPase (ZntA) was identified by our lab in 1997. ZntA belongs to the P<sub>1B</sub> family of ATPases. The discovery that the mutations in Cu<sup>+</sup> ATPases were responsible for Menkes and Wilsons disease first drew attention to this class of pumps in 1993. The widespread presence of these pumps from archaea to humans speaks of the important roles these proteins play in maintaining metal homeostasis. All the members of this class have 8 transmembrane regions. Helix 6 shows the characteristic CPC motif which is involved in metal binding (47). Based on the differences in their sequences and the metal ions they transport, they have been classified into several subgroups.

### Subgroup IB-1

Some of the well studied and characterized proteins such as the Menkes and Wilsons disease proteins belong to this group. Studies have shown that these are  $\text{Cu}^+$  ATPases that transport  $\text{Cu}^+$  out of the cytoplasm. These pumps can also transport  $\text{Ag}^+$  (48-49). These proteins have several metal binding domains (0-6) in the N-terminal region.

### Subgroup IB-2

ZntA belongs to this group. This subgroup of proteins consists of proteins that drive the efflux of divalent metals such as  $\text{Zn}^{2+}/\text{Cd}^{2+}/\text{Pb}^{2+}$ . Some of the proteins that belong to this class include *Synechocystis* ZiaA, *E.coli* ZntA, *S.aureus* CadA (50-52). The  $\text{P}_{1\text{B}2}$  type proteins have been found in archea, prokaryotes and plants. Both  $\text{P}_{1\text{B}1}$  and  $\text{P}_{1\text{B}2}$  have a CPC motif in helix 6 but distinct sequences in H7 and H8, which differentiates the two groups.

### Subgroup IB-3

CopB from *E.hirae* was the first characterized  $\text{P}_{1\text{B}3}$  type ATPase. Sequence analysis shows that members of this group have a conserved CPH motif in transmembrane helix 6 and also a histidine rich N-terminal metal binding domain (47). CopB was originally characterized as a  $\text{Cu}^+/\text{Ag}^+$  ATPase, but later studies showed it to be predominantly activated by  $\text{Cu}^{2+}$  transport and partially activated by  $\text{Cu}^+$  and  $\text{Ag}^+$  (45, 53).

### Subgroup IB-4

Sequence analysis using membrane prediction software has speculated that members of this group have only six transmembrane helices with only four

domains in the N-terminal half of the proteins and two domains downstream of the characteristic P-type ATPase cytoplasmic loop; however, there has been no experimental demonstration of this (47). These proteins do not have the N-terminal metal binding domain. Studies on *Synechocystis* PCC6803 CoaT, a member of this group have shown that this protein maybe involved in  $\text{Co}^{2+}$  transport (47).

### **Subgroup IB-5 and Subgroup IB-6**

Very few members of these groups have been characterized. Their substrate specificities and residues that participate in metal coordination are not known (45, 47).

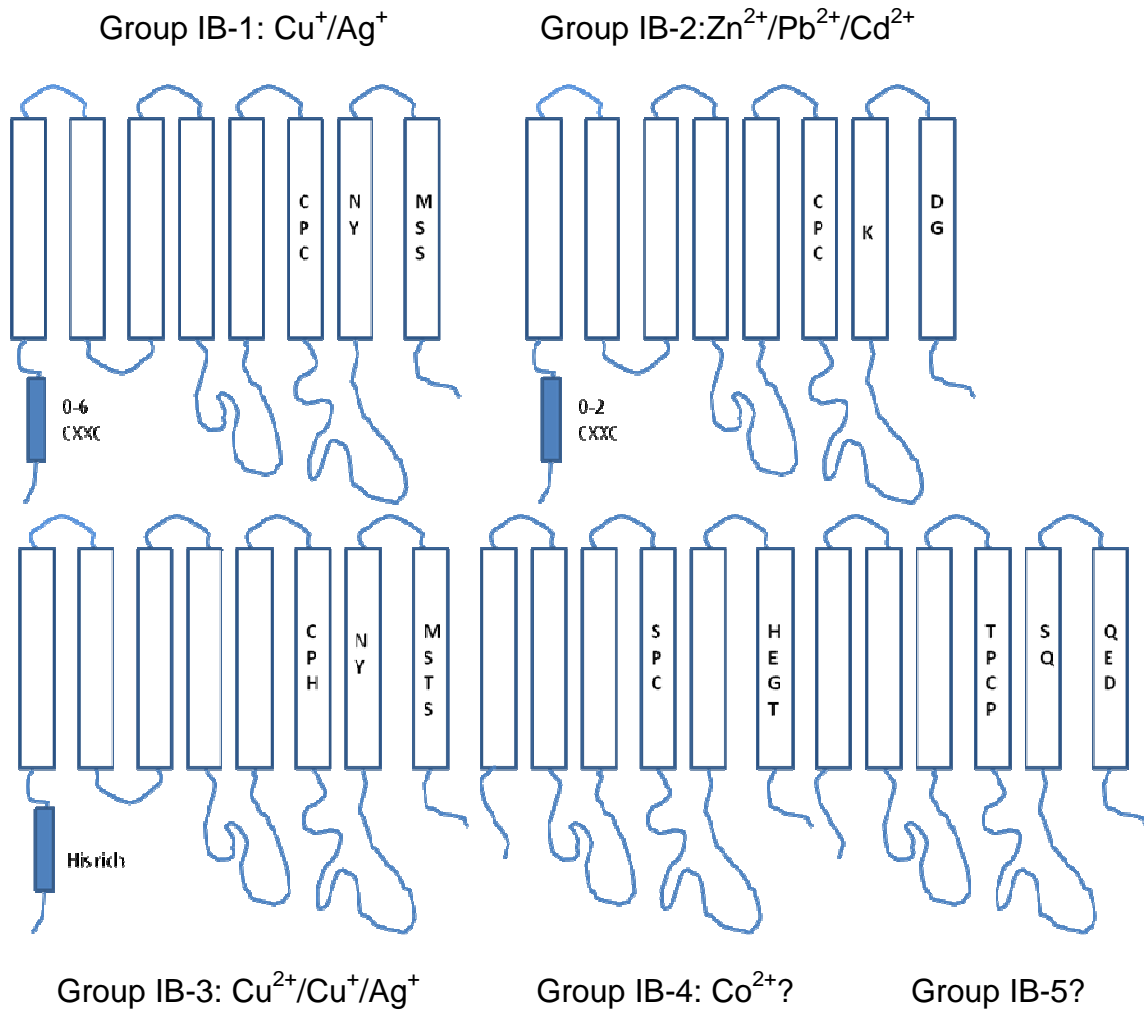


**Figure 1.4.** The metal specificity and structural characteristics of each subgroup.

### 1.10 Background on ZntA

ZntA a P-type ATPase is induced by ZntR, which exports not only  $\text{Zn}^{2+}$ , but also  $\text{Pb}^{2+}$  and  $\text{Cd}^{2+}$ . ZntA homologues are present in bacteria, archaea and plants. Early studies in our lab have shown that a *zntA* knock out strain results in sensitivity to zinc, lead and cadmium (54). This knock out strain did not show any sensitivity to copper and silver, indicating that in vivo ZntA is very specific for divalent metal ions (54). Purified ZntA is activated in the presence of  $\text{Zn}^{2+}$ ,  $\text{Pb}^{2+}$ ,  $\text{Cd}^{2+}$  and also  $\text{Hg}^{2+}$  (50). ATPase activity is highest in the presence of lead. Other

divalent metals such as  $\text{Cu}^{2+}$ ,  $\text{Ni}^{2+}$  and  $\text{Co}^{2+}$  also weakly activate the pump. ZntA has two high affinity metal binding sites one in the hydrophilic N-terminal domain and the other in the transmembrane region (55).

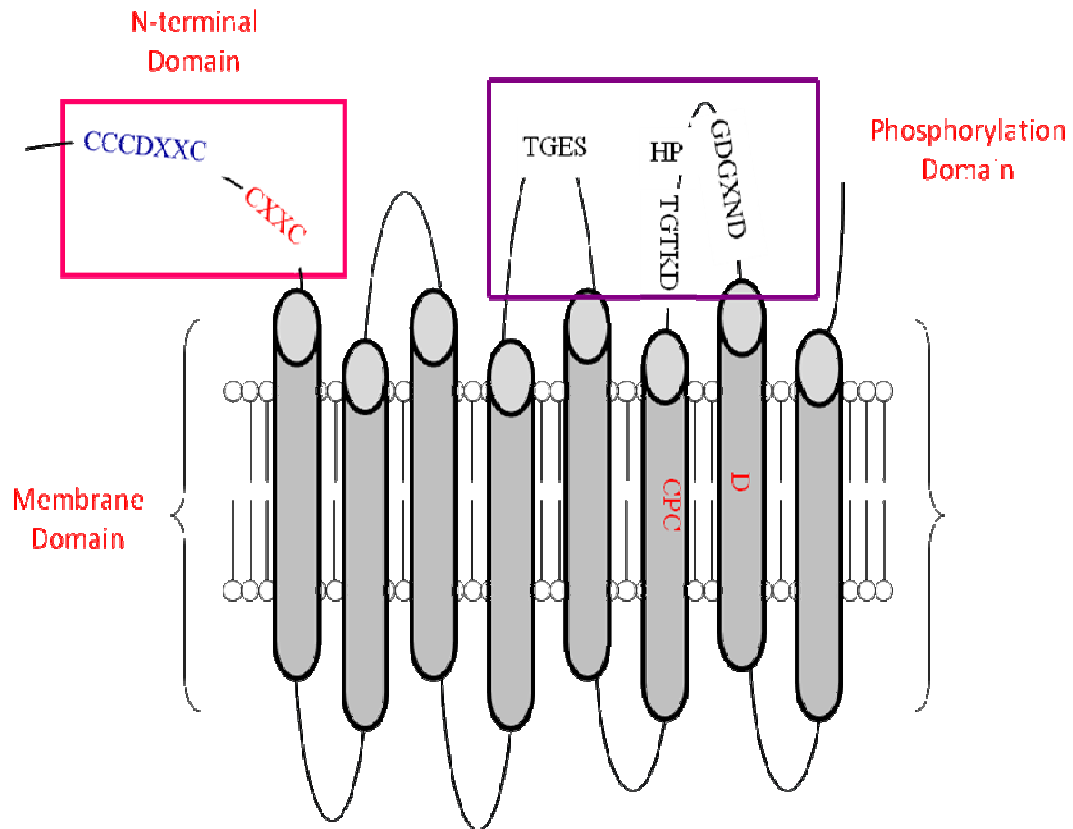


**Figure 1.5.** Schematic representation of ZntA showing the different domains and the conserved residues.

Studies on a truncated form of ZntA called  $\Delta\text{N-ZntA}$  which lacks the cytoplasmic N-terminal loop have shown that this truncated protein possesses in vitro activity although the activity is 2-3 fold lower than wild type ZntA for  $\text{Pb}^{2+}$ ,  $\text{Cd}^{2+}$  and  $\text{Zn}^{2+}$  (56).  $\Delta\text{N-ZntA}$  cloned into ZntA knock out strain when grown in media that has toxic concentrations of  $\text{Pb}^{2+}$ ,  $\text{Zn}^{2+}$  and  $\text{Cd}^{2+}$  was able to grow thus providing

resistance to these metal ions. However, when compared to ZntA the growth rate was rather slow (57). Stoichiometry measurements by ICP-MS have shown that  $\Delta$ N-ZntA can bind to only a single metal ion and the metal binding affinity is similar to the other metal binding site (56). Thus, although the N-terminal domain is not necessary for the overall activity of the protein it does provide a kinetic advantage to the enzyme. The N-terminal cytoplasmic region of proteins in the IB2 subgroup is about 100 residues long.

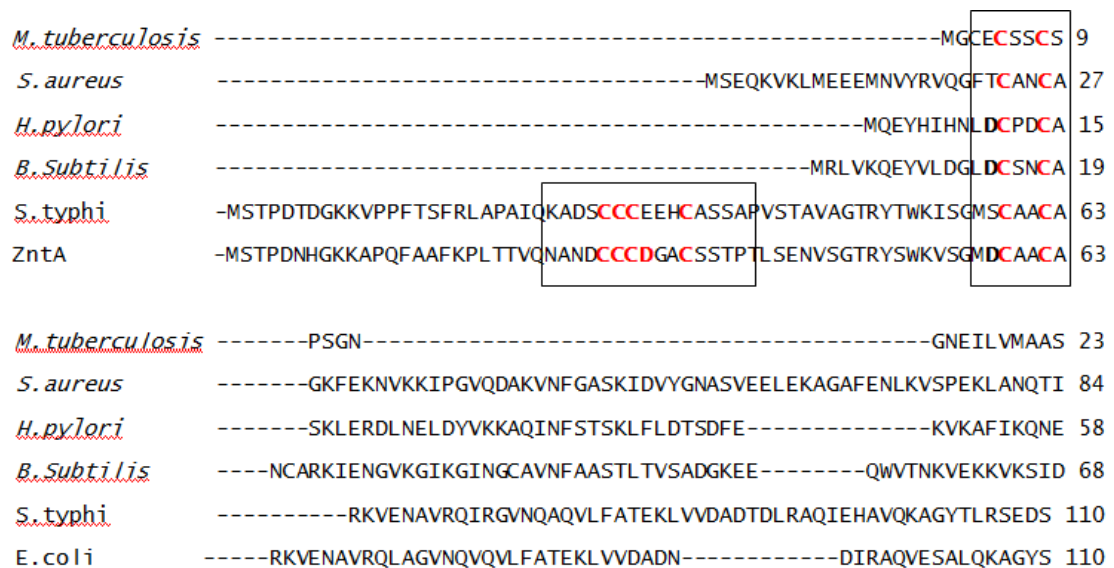


**Figure 1.6.** Alignments of the N-terminal domain of members of subgroup P<sub>1B-2</sub>.

Most of these proteins that belong to P<sub>1B2</sub> group have a hydrophilic cytoplasmic metal binding domain containing one to many copies of a metal binding motif CXXC. ZntA, in addition to the CXXC motif has an upstream conserved motif which is CCDXXC. In the Menkes and Wilsons disease proteins six copies of the CXXC motif are present (58). Studies on the N-terminal domain of the Menkes and Wilsons disease related proteins have shown that they can bind to

many metal ions (59). Solution structure of part of the N-terminal region of ZntA (residues 46-118) comparing the apo and zinc bound forms have shown that they have  $\beta\alpha\beta\beta\alpha\beta$ -ferredoxin like fold which is very similar to that of copper chaperones and to the N-terminal soluble domains of  $\text{Cu}^+$  ATPases (60).  $\text{Zn}^{2+}$  binds to the two cysteines and aspartate of the GMDCXXC motif with tetrahedral coordination (5). Structural and biochemical data on similar proteins from other laboratories have shown that presence of different residues changes the metal selectivity pattern (53, 59, 61).

Biochemical studies in the past have indicated that lead binding to the N-terminus of ZntA requires more than the two cysteines of CXXC; some cysteines from the upstream CCCDXXC motif may be involved in conferring high selectivity to lead (56). The N-terminal domain is involved in binding to different metal ions and when it is absent the activity of the transporter is reduced, indicating that it may have other functions.



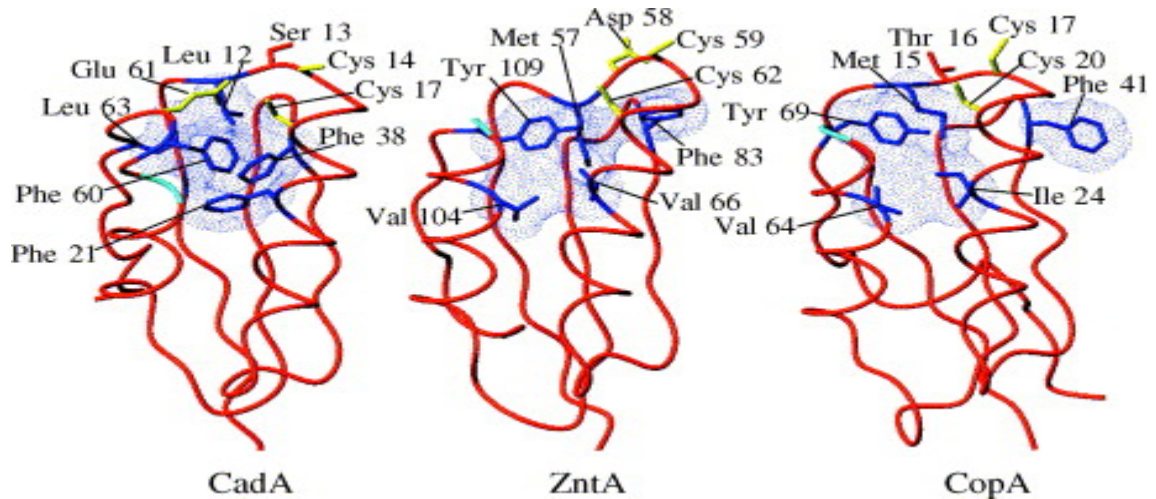


**Figure 1.7.** Solution structures of the N-terminal metal binding domains of *L.monocytogenes* CadA, *E.coli* ZntA and *B.subtilis* CopA. Metal ligands are in yellow, highly conserved residues in red, and the van der Waals contacts involving some hydrophobic residues are shown in blue (60).

### The Transmembrane region of ZntA

Unlike other groups of the P-type ATPase family, members of P<sub>1B</sub> group to which ZntA belongs have a smaller number of transmembrane helices and a smaller ATP binding loop. ZntA is a much simpler transporter when compared to the Ca<sup>2+</sup> ATPase or the Na<sup>+</sup>/K<sup>+</sup> ATPase where 2 metals are bound in the transmembrane region. ZntA has 8 transmembrane helices. The transmembrane region is essential for the activity of ZntA and one metal binding site is located here. Sequence analysis studies have shown that helices 6, 7 and 8 of ZntA have conserved residues which may be involved in metal binding and catalysis.

<i>M. tuberculosis</i>	RFIERFASIYTPVTGLAALTALIP-VLTGGD-PLTWIYRALVLLVISCPCALLISTPVA 289
<i>A. thaliana</i>	RLIDKCSQYYTPAIIILVSACVAIVP-VIMKVHNLKHWFHLALVVLVSGCPCGLILSTPVA 368
<i>S. aureus</i>	AFVDKFAKYYPPIIMVIAALVAVVP-PLFFGGSDTWVYQGLAVLVVGCPCALVISTPIS 382
<i>H. pylori</i>	KFITKFSRYYPVSVLFIALMIAVLPPLFSMG-SFDEWIYRGLVALMVSCPCALVISVPLG 355
<i>B. subtilis</i>	NFITKFAKYYPVAVVIAVLLAFVPPVLVSGAALSDWVYRALIFLVISCPCALVVISIPLG 368
<i>E. coli</i>	RFIDRFRIYTPAIMAVALLVTLVP-PLLFAASWQEWIYKGLTLLIGPCPCALVISTPAA 403

**Figure 1.8.** Alignments of H6 of ZntA and its close homologues.

<i>M. tuberculosis</i>	VNTGLTVAVKLSLAVLSVAGLVPLWAVAVGDMGLSLFVITNSLLLLARF----- 605
<i>A. thaliana</i>	ENVCLSIILKAGILALAFAGHPLIWA AVL V-DVGTCLLVIFNSMLLLREKKKIGNKKCYR 716
<i>S. aureus</i>	ANITFAIGIKIIALLLVIPGWLTLWIAILS-DMGATILVALNSLRMRVKDK----- 727
<i>H. pylori</i>	QNILFALGIKAVFIVLGLMGVAVSLWEAVFG-DVGVTLALANSMRAMRA----- 686
<i>B. subtilis</i>	QNIGFALGVKAIFLILGAFGIATMWEAVFS-DVGVTLAVANAMRVMRLKNK----- 702
<i>E. coli</i>	QNITIALGLKGIFLVTTLLGMTGLWLAFLA-DTGATVLVTANALRLLRRR----- 732

**Figure 1.9.** Alignment of H7 and H8 of ZntA and its close homologues.

Helix 6 in all P<sub>1B</sub> type ATPases has a conserved motif, [C/S/T] P[C/H] (X) 4[X/T] XP (figure 1.8). Sequence analysis studies suggest that transmembrane helices 6, 7 and 8 have conserved residues which may play a role in metal selectivity. For example, transporters selective for Cu<sup>+</sup>/Ag<sup>+</sup>, Zn<sup>2+</sup>, Pb<sup>2+</sup>, and Cd<sup>2+</sup> have a CPC motif in the sixth helix whereas other ATPases that are selective for Co<sup>2+</sup> or Cu<sup>2+</sup> have a conserved SPC and CPH motif (figure 1.4) (47, 55). Mutational studies on the cysteine residues in ZntA from *E. coli* and CopA from *A. fulgidus* have shown that when the cysteines were replaced by other amino acid residues this leads to complete loss in ATPase activity (47). Studies on the CPC motif in our laboratory have shown that mutations at each of the cysteines resulted in loss of ATPase activity and the mutants were unable to bind to metal ions (55). Mutational studies also indicated that the two Cysteines are essential

for  $Pb^{2+}$  binding. Serine and Histidine substitutions at these residues did not affect binding of  $Zn^{2+}$  and  $Cd^{2+}$  but the mutants were unable to confer resistance to toxic levels of  $Zn^{2+}$  and  $Cd^{2+}$  (55). ZntA and its close homologues that are selective for divalent metal ions have a conserved aspartate residue in helix 8 in addition to the CPC motif. None of the other subgroups of the  $P_{IB}$  family have a conserved acidic residue at this position (62). These studies indicate that metal selectivity is achieved by choosing metal ligands that result in high binding affinity and also optimal binding geometry.

In helices 7 and 8, there is a single conserved Asn residue at the cytoplasmic ends of these two helices (figure 1.9). However, sequence analysis of the P2 and P3 ATPases indicated the presence of a conserved Asp residue in helix 6, which corresponds to helix 8 in ZntA. Mutations of the Asp800 and Asp826 from  $Ca^{2+}$  ATPase SERCA1 (P2 ATPase) and  $Na^+/K^+$  ATPase lead to complete loss in activity (62).

$Ca^{2+}$ ATPase	EALIPVQLLWVNLVT	DGLPATALGFNPPDL	815
$Na^+/K^+$ ATPase	LPLGTITILCIDLGT	DMVPAISLAYEAAES	841
ZntA	TTLLGMTGLWLAVLA	DTGATVLVTANALRL	732

**Figure 1.10.** Alignments of H8 of ZntA compared to Helix 6 of  $Ca^{2+}$  ATPase and  $Na^+/K^+$  ATPase.

X-ray crystallographic studies on SERCA1 have shown that Asp acts as a bridging ligand to both the  $Ca^{2+}$  ions in the membrane. Studies on Asp714 in ZntA performed in our laboratory have shown that this residue in addition to the CPC motif is a ligand for metal ions, any substitution at this site leads to complete loss in enzyme activity (62). Biochemical studies indicate that lead

binding at the transmembrane site involves Asp, and the two Cys but it is slightly different from  $Zn^{2+}$  and  $Cd^{2+}$  (62). The transmembrane metal binding site like the N-terminal site binds to different metal ions ( $Cu^{2+}$ ,  $Ni^{2+}$ ,  $Co^{2+}$ ) with high affinity (63). These studies indicate that conserved residues in the transmembrane helices contribute to metal specificity and selectivity through correct metal coordination and geometry.

**Table 1.4.** Hard –Soft Acid - Base Classification of Metal Ions and Ligands (2).

Metals	Geometry	Ligands
$Zn^{2+}$ Intermediate	Tetrahedral, Square pyramidal	O-Carboxylate, Carbonyl, S-thiolate, Thioether N-imidazole
$Pb^{2+}$ soft	Trigonal, Square Planar, Octahedral	Sulfur ligands in RSH, $RS^-$ , $R_2S$ , S- Thiolate, Thioether, N-imidazole, O-Carboxylate
$Cd^{2+}$ soft	Tetrahedral, Octahedral	
$Ag^+$ soft	Linear, Planar, Tetrahedral	
$Cu^+$ soft	Linear, Trigonal, Tetrahedral, Octahedral	

### 1.11 Lead and Cadmium

Cadmium and lead are not essential for organisms. But these metals do enter the cells by unknown pathways. Studies have suggested that both cadmium and lead due to similarities with many of the physiologically relevant metals can compete with these and lead to harmful effects. Lead and cadmium both have a very high affinity for soft Lewis bases (2). There is a lot of literature on lead toxicity, unfortunately very little is known about the biochemical mechanisms or the lead efflux models. ZntA confers resistance and is activated by  $Pb^{2+} < Zn^{2+} < Cd^{2+}$ , however it does not confer any resistance to  $Ag^{+}$  and  $Hg^{2+}$  but these metals do activate the transporter (50). When the chemical properties of these metal ions are compared they have several differences.

Over the past several years all the research on ZntA point to a single fact that metal selectivity is not a function of metal affinity to the binding site rather the preferred geometry and coordination to the sites and also the change in conformation of the protein due to metal binding.

### 1.12 Aims of the thesis

The major goal of the research presented here has been to study the structural and biochemical aspects of ZntA which will give us an insight into the different mechanisms adopted by metal transporting proteins to achieve metal selectivity. Characterization of conserved cysteine residues in the cytoplasmic N-terminal domain of ZntA and the interaction of this domain with the core transporter has been presented in this thesis.

In the first part, research on conserved cysteine and aspartate residues in the N-terminal domain and their role in metal binding is presented. This cytoplasmic loop has two cysteine clusters –CCCDXXC- and -GMDCXXC-, previous studies in our lab have shown that both these cysteine motifs are required for  $Pb^{2+}$  binding but not  $Cd^{2+}$  and  $Zn^{2+}$  (56). ZntA has two metal binding sites, one in the membrane region and the other in the N-terminal region and both are involved in binding  $Pb^{2+}$ ,  $Cd^{2+}$ ,  $Zn^{2+}$ ,  $Cu^{2+}$ ,  $Co^{2+}$  and  $Ni^{2+}$  with similar affinity (56). These observations indicate that certain residues from both the motifs may be involved in contributing to metal selectivity and, in addition, these residues may also play a role in regulating metal binding geometry and coordination. In this study, the individual cysteine residues were altered to alanines and the individual aspartate residues were altered to alanine and asparagine in both the full length ZntA and in the N-terminal fragment. The effect of these mutations on the activity of the transporter and metal binding has been described in Chapter 2.

My research also focuses on elucidating the interaction between the N-terminal domain and the membrane domain. Earlier experiments showed that a mutant of ZntA which lacks the N-terminal domain,  $\Delta N$ -ZntA, was able to grow in the presence of  $Pb^{2+}$ ,  $Zn^{2+}$  and  $Cd^{2+}$  but the growth rate was slower than ZntA. This indicates that the presence of the N-terminal domain confers an in vivo growth advantage on ZntA (56).  $\Delta N$ -ZntA is active in vitro but the activity is 2-3 fold lower than the full length protein, indicating that the N-terminal portion is not essential for the in vitro activity of the protein but it does provide a kinetic advantage to the transporter (56). Studies on other  $P_{1B}$  type ATPases, such as

CopA from *E.coli* suggest the N-terminal domain may interact with metal chaperones or may be involved in copper regulated trafficking of copper pumps from intracellular compartments to the plasma membrane (49). Recent studies on CopA from *A.fulgius* have shown CopZ, a  $\text{Cu}^+$  chaperone, delivers  $\text{Cu}^+$  to the  $\text{Cu}^+$  ATPase transmembrane metal binding sites (64). The cytoplasmic metal binding domain of CopA does not perform this function of metal delivery but it plays a regulatory role (64). So far no zinc chaperone proteins have been found, so the important question is how does ZntA get its metal? Our theory, that the N-terminal domain binds to the metal ion from the cytoplasm and then passes it to the metal binding site in the transmembrane region, is supported by the results in the past from  $\Delta\text{N-ZntA}$ , and a site-directed double mutant, C59A/C62A-ZntA. In this section, the ATPase activity of the transporter was measured in the presence of N-terminal domain (N1-ZntA) bound to metal as the substrate in order to determine the catalytic rate at which N1-ZntA bound metal can activate the transporter. Metal transfer was also measured by transport assays. Fluorescence energy transfer measurements were performed to study the interaction between N1-ZntA and  $\Delta\text{N}$ . Chapter 3 of the thesis focuses on an ongoing project in the laboratory, which involves a characterizing a truncated form ZntA( $\Delta\text{E}231\text{-ZntA}$ ), which lacks the amino terminal domain and the first four transmembrane helices. This protein has the conserved CPC motif and Asp residue which are involved in metal binding. The in vivo resistance profile, ATPase activity of the transporter and the metal binding stoichiometry have been examined to investigate effect of loss of the first four transmembrane helices on

metal selectivity. The work presented in Chapter 4 is work in progress; the characterization of the truncated form of ZntA which lacks the first four transmembrane helices is described.

### **1.13 Significance of the thesis**

Transition metals play innumerable roles in biological systems. They are essential in several cellular reactions, they may be involved in catalysis by being a part of enzymes, and they also play an active role in stabilizing structures of proteins and nucleic acids, thus regulating several downstream biological pathways. But at the same time they and heavy metal ions can have toxic effects on cells because when these metal ions are in excess they can bind and react with several cellular components leading to undesirable consequences. To avoid these ill effects, organisms have evolved several mechanisms to regulate the homeostasis by uptake or elimination of essential ions such as iron, copper and zinc and nonessential ions such as cadmium, lead, mercury and silver (65-66). There has been an immense amount of research on iron and copper homeostasis systems for several years. Zinc is unique unlike iron and copper it does not display any redox activity. It is the second most abundant transition metal which is associated with several zinc binding proteins (4). There are several zinc transporters, ZIP family, CDF family (Zit's, ZnT's) and the ABC transporters in mammals. But not much is known of the metal binding, coordination, geometry and ion selectivity of these transporters. ZntA is a very good model protein to study the above roles as it is not only a zinc transporter but it also plays a role in the transport of heavy metals such as lead and



cadmium which are extremely toxic to cells. Results presented here are of significance because they give us an indication of the residues that contribute to ion selectivity and coordination geometry, and also describe the role of cytoplasmic N-terminal domain in kinetics, metal binding and transfer. These results can be used as a basis to explain mechanisms of transition and heavy metal binding and transport in several proteins involved in metal trafficking. These studies pave the way in understanding other metalloproteins; metal transport and trafficking are accomplished by proteins that display bioinorganic chemistry which is not similar to any of the other well documented metalloenzymes. The knowledge gained by elucidating the mechanism by which ZntA functions gives us an insight into how metal transporters work in many diseases such as Alzheimer's, Parkinson's, Acrodermatitis enteropathica, diabetes, asthma and certain kinds of cancers. Details of metal transporters in these diseases may provide insights for development of drugs against the above mentioned diseases.

#### 1.14 REFERENCES

1. Kaim, W., and Schwederski, B. (1994) *Bioinorganic Chemistry: Inorganic Elements in the Chemistry of Life*, John Wiley and Sons, England.
2. Roat-Malone, R. M. (2008) *Bioinorganic Chemistry: a short course*, 2nd ed., John Wiley and sons, USA.
3. Theil, T. C., and Raymond, K.N. (1994) Transition-Metal Storage, Transport, and Biomineralization, In *Bioinorganic Chemistry*

- (Bertini, I., Gray, H.B., Lippard, S., and Valentine, J., Ed.), University Science Books, California.
4. Frausto da Silva, J. J. R., and Williams, R.J.P. (2001) *The Biological Chemistry of Elements*, Oxford University Press.
  5. Banci, L., Bertini, I., Ciofi-Baffoni, S., Finney, L. A., Outten, C. E., and O'Halloran, T. V. (2002) A new zinc-protein coordination site in intracellular metal trafficking: solution structure of the Apo and Zn(II) forms of ZntA(46-118), *J Mol Biol* 323, 883-897.
  6. O'Halloran, T. V. (1993) Transition metals in control of gene expression, *Science* 261, 715-725.
  7. Lippard, S., and Berg, J.M. (1994) *Principles of Bioinorganic Chemistry*, University Science Books, CA.
  8. Arnesano, F., Banci, L., Bertini, I., Ciofi-Baffoni, S., Molteni, E., Huffman, D. L., and O'Halloran, T. V. (2002) Metallochaperones and metal-transporting ATPases: a comparative analysis of sequences and structures, *Genome Res* 12, 255-271.
  9. Finney, L. A., and O'Halloran, T. V. (2003) Transition metal speciation in the cell: insights from the chemistry of metal ion receptors, *Science* 300, 931-936.
  10. DiDonato, M., Narindrasorasak, S., Forbes, J. R., Cox, D. W., and Sarkar, B. (1997) Expression, purification, and metal binding properties of the N-terminal domain from the wilson disease putative copper-transporting ATPase (ATP7B), *J Biol Chem* 272, 33279-33282.

11. Kulkarni, P. P., She, Y. M., Smith, S. D., Roberts, E. A., and Sarkar, B. (2006) Proteomics of metal transport and metal-associated diseases, *Chemistry* 12, 2410-2422.
12. Rosenzweig, A. C. (2002) Metallochaperones: bind and deliver, *Chem Biol* 9, 673-677.
13. Shi, H., Bencze, K. Z., Stemmler, T. L., and Philpott, C. C. (2008) A cytosolic iron chaperone that delivers iron to ferritin, *Science* 320, 1207-1210.
14. Waldron, K. J., and Robinson, N. J. (2009) How do bacterial cells ensure that metalloproteins get the correct metal?, *Nat Rev Microbiol* 7, 25-35.
15. Waldron, K. J., Rutherford, J. C., Ford, D., and Robinson, N. J. (2009) Metalloproteins and metal sensing, *Nature* 460, 823-830.
16. Maret, W. (2009) Molecular aspects of human cellular zinc homeostasis: redox control of zinc potentials and zinc signals, *Biometals* 22, 149-157.
17. Rensing, C., and Mitra, B. (2007) Zinc, Cadmium, and Lead Resistance and Homeostasis, In *Molecular Microbiology of Heavy Metals*, pp 321-341, Springer Berlin/Heidelberg.
18. Blencowe, D. K., and Morby, A. P. (2006) Zn(II) metabolism in prokaryotes, *FEMS Microbiology Reviews* 27, 291-311.
19. Huffman, D. L., and O'Halloran, T. V. (2001) Function, structure, and mechanism of intracellular copper trafficking proteins, *Annu Rev Biochem* 70, 677-701.

20. DiDonato, M., and Sarkar, B. (1997) Copper transport and its alterations in Menkes and Wilson diseases, *Biochim Biophys Acta* 1360, 3-16.
21. Rolfs, A., and Hediger, A.M. (1999) Metal ion transporters in mammals: structure, function and pathological implications, *Journal of Physiology*, 1-12.
22. Andrews, N. C. (2008) Forging a field: the golden age of iron biology, *Blood* 112, 219-230.
23. Tottey, S., Waldron, K. J., Firbank, S. J., Reale, B., Bessant, C., Sato, K., Cheek, T. R., Gray, J., Banfield, M. J., Dennison, C., and Robinson, N. J. (2008) Protein-folding location can regulate manganese-binding versus copper- or zinc-binding, *Nature* 455, 1138-1142.
24. Smith, K. F., Bibb, L. A., Schmitt, M. P., and Oram, D. M. (2009) Regulation and activity of a zinc uptake regulator, Zur, in *Corynebacterium diphtheriae*, *J Bacteriol* 191, 1595-1603.
25. Nelson, N. (1999) Metal ion transporters and homeostasis, *EMBO J* 18, 4361-4371.
26. Eide, D. J. (2006) Zinc transporters and the cellular trafficking of zinc, *Biochim Biophys Acta* 1763, 711-722.
27. Outten, C. E., and O'Halloran, T. V. (2001) Femtomolar sensitivity of metalloregulatory proteins controlling zinc homeostasis, *Science* 292, 2488-2492.
28. Blencowe, D. K., and Morby, A. P. (2003) Zn(II) metabolism in prokaryotes, *FEMS Microbiol Rev* 27, 291-311.

29. Eide, D. J. (2005) The Zip Family of Zinc Transporters *Zinc Finger Proteins* 8, 261-264.
30. Jones, P. M., O'Mara, M. L., and George, A. M. (2009) ABC transporters: a riddle wrapped in a mystery inside an enigma, *Trends Biochem Sci* 34, 520-531.
31. Hantke, K. (2001) Bacterial zinc transporters and regulators, *Biometals* 14, 239-249.
32. Lichten, L. A., and Cousins, R. J. (2009) Mammalian zinc transporters: nutritional and physiologic regulation, *Annu Rev Nutr* 29, 153-176.
33. Grass G, W. M., Rosen BP, Smith RL, Rensing C. (2002) ZupT is a Zn(II) uptake system in *Escherichia coli*, *Journal of Bacteriology* 184, 864-866.
34. Grass, G., Franke, S., Taudte, N., Nies, D. H., Kucharski, L. M., Maguire, M. E., and Rensing, C. (2005) The metal permease ZupT from *Escherichia coli* is a transporter with a broad substrate spectrum, *J Bacteriol* 187, 1604-1611.
35. Jorgensen, P. L. (1975) Purification and characterization of (Na<sup>+</sup>,K<sup>+</sup>)-ATPase.V. Conformational changes in the enzyme Transitions between the Na-form and the K-form studied with tryptic digestion as a tool., *Biochim Biophys Acta* 401, 399-415.
36. Kuhlbrandt, W. (2004) Biology, Structure and Mechanism of P-type ATPases, *Nature* 5, 282-294.

37. Toyoshima, C., and Inesi, G. (2004) Structural basis of ion pumping by Ca<sup>2+</sup>-ATPase of the sarcoplasmic reticulum, *Annu Rev Biochem* 73, 269-292.
38. Lutsenko, S., and Kaplan, J.H.(1995). (1995) Organization of P-type ATPases:Significance of Structural Diversity, *Biochemistry* 34, 15607-15613.
39. Palmgren, M. G., Buch-Pedersen, M. J., and Moller, A. L. (2003) Mechanism of proton pumping by plant plasma membrane H<sup>+</sup>-ATPase: role of residues in transmembrane segments 5 and 6, *Ann N Y Acad Sci* 986, 188-197.
40. Toyoshima, C., Nomura, H., and Sugita, Y. (2003) Structural basis of ion pumping by Ca<sup>2+</sup>-ATPase of sarcoplasmic reticulum, *FEBS Lett* 555, 106-110.
41. Axelsen, K. B., and Palmgren, M. G. (1998) Evolution of substrate specificities in the P-type ATPase superfamily, *J Mol Evol* 46, 84-101.
42. Haupt, M., Bramkamp, M., Coles, M., Kessler, H., and Altendorf, K. (2005) Prokaryotic Kdp-ATPase: recent insights into the structure and function of KdpB, *J Mol Microbiol Biotechnol* 10, 120-131.
43. Bramkamp, M., and Altendorf, K. (2005) Single amino acid substitution in the putative transmembrane helix V in KdpB of the KdpFABC complex of *Escherichia coli* uncouples ATPase activity and ion transport, *Biochemistry* 44, 8260-8266.

44. Palmgren, M. G., and Axelsen, K. B. (1998) Evolution of P-type ATPases, *Biochim Biophys Acta* 1365, 37-45.
45. Arguello, J. M., Eren, E., and Gonzalez-Guerrero, M. (2007) The structure and function of heavy metal transport P1B-ATPases, *Biometals* 20, 233-248.
46. Silver, S., and Phung le, T. (2005) A bacterial view of the periodic table: genes and proteins for toxic inorganic ions, *J Ind Microbiol Biotechnol* 32, 587-605.
47. Arguello, J. M. (2003) Identification of ion-selectivity determinants in heavy-metal transport P1B-type ATPases, *J Membr Biol* 195, 93-108.
48. Rensing, C., Fan, B., Sharma, R., Mitra, B., and Rosen, B. P. (2000) CopA: An Escherichia coli Cu(I)-translocating P-type ATPase, *Proc Natl Acad Sci U S A* 97, 652-656.
49. Fan, B., and Rosen, B. P. (2002) Biochemical characterization of CopA, the Escherichia coli Cu(I)-translocating P-type ATPase, *J Biol Chem* 277, 46987-46992.
50. Sharma, R., Rensing, C., Rosen, B. P., and Mitra, B. (2000) The ATP hydrolytic activity of purified ZntA, a Pb(II)/Cd(II)/Zn(II)-translocating ATPase from Escherichia coli, *J Biol Chem* 275, 3873-3878.
51. Rensing, C., Mitra, B., and Rosen, B. P. (1998) A Zn(II)-translocating P-type ATPase from Proteus mirabilis, *Biochem Cell Biol* 76, 787-790.

52. Yoon, K. P., Misra, T. K., and Silver, S. (1991) Regulation of the cadA cadmium resistance determinant of *Staphylococcus aureus* plasmid pI258, *J Bacteriol* 173, 7643-7649.
53. Mana-Capelli, S., Mandal, A. K., and Arguello, J. M. (2003) Archaeoglobus fulgidus CopB is a thermophilic Cu<sup>2+</sup>-ATPase: functional role of its histidine-rich-N-terminal metal binding domain, *J Biol Chem* 278, 40534-40541.
54. Rensing, C., Sun, Y., Mitra, B., and Rosen, B. P. (1998) Pb(II)-translocating P-type ATPases, *J Biol Chem* 273, 32614-32617.
55. Dutta, S. J., Liu, J., Stemmler, A. J., and Mitra, B. (2007) Conservative and nonconservative mutations of the transmembrane CPC motif in ZntA: effect on metal selectivity and activity, *Biochemistry* 46, 3692-3703.
56. Liu, J., Stemmler, A. J., Fatima, J., and Mitra, B. (2005) Metal-binding characteristics of the amino-terminal domain of ZntA: binding of lead is different compared to cadmium and zinc, *Biochemistry* 44, 5159-5167.
57. Dutta, S. J., Liu, J., and Mitra, B. (2005) Kinetic analysis of metal binding to the amino-terminal domain of ZntA by monitoring metal-thiolate charge-transfer complexes, *Biochemistry* 44, 14268-14274.
58. Rosenzweig, A. C., Huffman, D. L., Hou, M. Y., Wernimont, A. K., Pufahl, R. A., and O'Halloran, T. V. (1999) Crystal structure of the Atx1 metallochaperone protein at 1.02 Å resolution, *Structure* 7, 605-617.
59. Rosenzweig, A. C., and O'Halloran, T. V. (2000) Structure and chemistry of the copper chaperone proteins, *Curr Opin Chem Biol* 4, 140-147.



60. Banci, L., Bertini, I., Ciofi-Baffoni, S., Su, X. C., Miras, R., Bal, N., Mintz, E., Catty, P., Shokes, J. E., and Scott, R. A. (2006) Structural basis for metal binding specificity: the N-terminal cadmium binding domain of the P1-type ATPase CadA, *J Mol Biol* 356, 638-650.
61. Arnesano, F., Banci, L., Bertini, I., Huffman, D. L., and O'Halloran, T. V. (2001) Solution structure of the Cu(I) and apo forms of the yeast metallochaperone, Atx1, *Biochemistry* 40, 1528-1539.
62. Dutta, S. J., Liu, J., Hou, Z., and Mitra, B. (2006) Conserved aspartic acid 714 in transmembrane segment 8 of the ZntA subgroup of P1B-type ATPases is a metal-binding residue, *Biochemistry* 45, 5923-5931.
63. Liu, J., Dutta, S. J., Stemmler, A. J., and Mitra, B. (2006) Metal-binding affinity of the transmembrane site in ZntA: implications for metal selectivity, *Biochemistry* 45, 763-772.
64. Gonzalez-Guerrero, M., and Arguello, J. M. (2008) Mechanism of Cu<sup>+</sup>-transporting ATPases: soluble Cu<sup>+</sup> chaperones directly transfer Cu<sup>+</sup> to transmembrane transport sites, *Proc Natl Acad Sci U S A* 105, 5992-5997.
65. Kramer, U., Talke, I. N., and Hanikenne, M. (2007) Transition metal transport, *FEBS Lett* 581, 2263-2272.
66. Ledwidge, R., Patel, B., Dong, A., Fiedler, D., Falkowski, M., Zelikova, J., Summers, A. O., Pai, E. F., and Miller, S. M. (2005) NmerA, the metal binding domain of mercuric ion reductase, removes Hg<sup>2+</sup> from proteins,

delivers it to the catalytic core, and protects cells under glutathione-depleted conditions, *Biochemistry* 44, 11402-11416.

## CHAPTER 2

**CONSERVED MOTIFS IN THE AMINO –TERMINAL DOMAIN OF ZNTA:  
THEIR ROLE IN METAL BINDING AND SELECTIVITY OF THE PUMP**

The N-terminal domain of ZntA (N1-ZntA) has residues which fall into two classes: those that are conserved in subgroups 1 and 2 of P<sub>IB</sub>-type ATPases and those that are only conserved in closely related homologues of ZntA. My goal has been to identify the role of these residues in metal binding and also in providing metal specificity.

**2.1 Introduction**

Transition metal ions are vital for cellular function and survival. Organisms have several proteins that maintain metal homeostasis, which are located in the cytosol, mitochondria and cell surface. One such class of proteins is the P<sub>IB</sub> ATPases; these are integral membrane proteins that transport heavy metals across cell membranes (36). This class of proteins is present in bacteria, yeasts, nematodes, and mammals. On the basis of sequence homology and substrate specificity this family has been classified in subgroups for example: P<sub>IB-1</sub> which is specific for monovalent metal ions like Cu<sup>+</sup> and Ag<sup>+</sup> and P<sub>IB-2</sub> which transport, divalent soft metal ions Zn<sup>2+</sup>, Cd<sup>2+</sup> and Pb<sup>2+</sup> (45). ZntA from *E.coli* and CadA from *S.aureus* are representative members of this second group. The reasons behind this metal selectivity and specificity in the P<sub>IB</sub> family of transporters are not well understood, though structural and biochemical studies have provided some details in this regard. The cytoplasmic N-terminal region of both P<sub>IB-1</sub> and P<sub>IB-2</sub> transporters have the conserved cysteine rich motif (CXXC) (47); this CXXC

motif is also present in some copper chaperone proteins and in the bacterial periplasmic mercury binding protein MerP. The Menkes protein ATP7B contains six copies of the CXXC motif, which are involved in binding copper and thus translocating it to the lumen. Proteins such as Atx1 and Ccc2, which play a role in copper delivery also have the CXXC motif (12). Structural studies of the Atx1, Ccc2, CopZ and MerP have shown that these proteins share a similar ferredoxin-like ( $\beta_1\text{-}\alpha_1\text{-}\beta_2\text{-}\beta_3\text{-}\alpha_2\text{-}\beta_4$ ) fold (8, 67). Solution structures of part of N1-ZntA (residues 46-118), comparing the apo and zinc bound forms have shown that it has a  $\beta\alpha\beta\beta\alpha\beta\beta$ -ferredoxin like fold which is very similar to that of copper chaperones and to the N-terminal soluble domains of  $\text{Cu}^+$  ATPases and MerP (5). Another NMR study has shown that in pumps that transport  $\text{Zn}^{2+}$  and  $\text{Cd}^{2+}$ , these metal ions are bound in tetrahedral co-ordination to two cysteine residues and the carboxylate oxygens of a conserved aspartic or glutamic acid residue. Sequence analysis of the  $P_{\text{IB}}$  pumps have shown that the conserved motif is DCXXC or CXXC with a conserved D/E suggesting that an acidic residue is necessary for conferring divalent metal ion selectivity (60). In addition to the DCXXC sequence, ZntA and its close homologues from *Salmonella typhi* and *Klebsiella pneumoniae* also have an upstream cysteine rich motif CCCDXXC in the N-terminal domain (56). Studies in our lab had suggested that this motif is required for binding lead at the N-terminal site in ZntA, and that this motif is present in pumps that are highly selective for lead (56). Data have shown that the membrane domain ( $\Delta\text{N-ZntA}$ ), which lacks the N-terminal domain, has 2-3 fold lower activity than wtZntA for  $\text{Pb}^{2+}$ ,  $\text{Cd}^{2+}$  and  $\text{Zn}^{2+}$  (56, 68). It has been

suggested that the N1-ZntA is not necessary for the overall activity of the protein but it provides a kinetic advantage to the protein (68). Stoichiometry measurements by ICP-MS have shown that the isolated domain, N1-ZntA, binds to lead, zinc, cadmium, copper, nickel and cobalt with a stoichiometry of 1. Additionally another construct N2-ZntA, where the first 46 residues were deleted was constructed. N2-ZntA bound to zinc and cadmium with similar stoichiometry as N1-ZntA but N2-ZntA was unable to bind to lead (56).

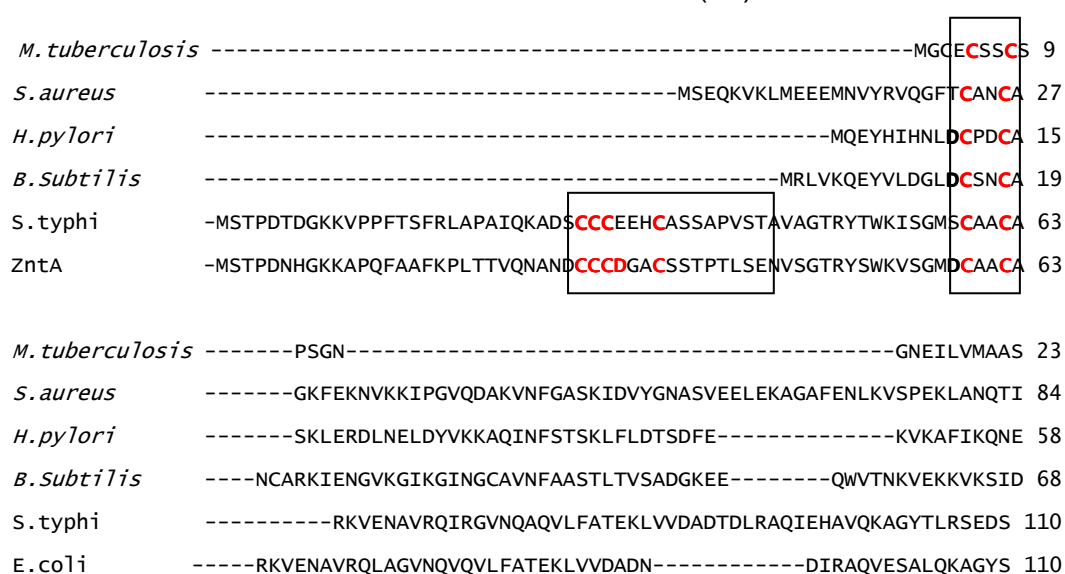


**Figure 2.1.** Alignments of the N-terminal domain of members of P<sub>1B-2</sub> group.

In this study, the importance of each individual cysteine residue, as well as the aspartate residues, in the two cysteine-rich motifs in metal ion binding and conferring metal selectivity was examined. The effect of alanine and/or asparagine substitutions on metal binding and in vivo and in vitro activity was evaluated. Individual alanine mutations at Cys31, Asp32, Cys35, Asp58, Cys59 and Cys62 had reduced ATPase activities and they also lost the ability to bind lead and cadmium ions. The profile of these mutants for zinc was interesting; none of the substitutions bound to zinc ion, additionally these mutants exhibited

lower in vivo and in vitro activity when compared to wtZntA. To understand the co-ordination environment of lead, zinc and cadmium, and obtain details regarding ligand environment and geometry, the technique of X-ray Absorption Spectroscopy (XAS) was used. The XAS experiment and analysis were performed in collaboration with Dr. James Penner Hahn at University of Michigan.

## 2.2 Materials

Plasmid pBAD/mycHis-C and *E.coli* strain LMG194 were obtained from Invitrogen; plasmid pET16B was obtained from Novagen. Chemicals for the ATPase activity assay and standard metal solutions were purchased from Sigma. Metal standards used for inductively coupled plasma mass spectrometry (ICP-MS) were from VWR.

## 2.3 Experimental Methods

### 2.3.1 Construction of N1-ZntA with carboxyl - terminal strep tag

N1-ZntA (residues 1-111 of ZntA followed by an eight residue strep tag) was created by PCR using the plasmid pZntA as template and the oligonucleotides 5'-CTA CTG TTT CTC CAT ACC C 3' as forward primer and 5' GCG CTC GAG TTA TTT TTC GAA CTG CGG GTG GCT CCA CAG GGA ATA GCC TGC 3' as the reverse primer. The amplified PCR product was cloned into pET16b using Nco1 and Xho1 sites; this was then transformed into *E.coli* strains TG1 and BI21.

### 2.3.2 Construction of C29A, C30A, C31A, D32A, D32N, C35A, D58A, D58N, C59A, C62A

In order, to identify the residues involved in metal binding sites, several point mutations were created. All these mutants were created in ZntA using the

quick change site directed mutagenesis kit and the following nucleotides were used: **C29A** - 5' AAC GCC AAC GAC **GCA** TGC TGC GAC GGC 3' and 5' GCC GTC GCA GCA **TGC** GTC GTT GGC GTT C 3'; **C30A** - 5' AAC GCC AAC GAC TGC **GCA** TGC GAC GGC GC 3' and 5' GCG CCG TCG CAT **GCG** CAG TCG TTG GCG TTC 3'; **C31A** - 5' AAC GAC TGT TGC **GCT** GAC GGC GCC TGT TCC 3' and 5' GGA ACA GGC GCC GTC **AGC** GCA ACA GTC GTT 3'; **D32A** – 5' AAC GAC TGT TGC TGC **GCC** GGC GCA TGT TCC 3' and 5' GGA ACA TGC GCC **GCC** GCA ACA GTC GTT 3'; **D32N** - 5' AAC GAC TGT TGC **AAC** GGC GCC TGT TCC -3' and 5' GGA ACA GGC GCC **GTT** GCA GCA ACA GTC GTT-3'; **C35A** – 5' TGC GAC GGC **GCA** GCT AGC AGC ACG CCA AC 3' and 5' AGT TGG CGT GCT GCT AGC **TGC** GCC GTC GC 3' ; **D58A** – 5' GTC AGC GGC ATG **GCA** TGC GCC GCC TGT GC 3' and 5' GCA CAG GCG GCG CAT **GCC** ATG CCG CTG AC 3'; **D58N** – 5' GTC AGC GGC ATG **AAT** TGC GCA GCC TGT GCG 3' and 5' CGC ACA GGC TGC GCA **ATT** CAT GCC GCT GAC 3', **C59A** – 5' GTC AGC GGC ATG GAC **GCC** GCG GCC TGT GCG CGC 3' and 5' GCG CGC ACA GGC CGC **GCC** GTC CAT GCC GCT GAC 3' ; **C62A** – 5' GGC ATG GAC TGC GCC GCG **GCT** GCG CGC AAG GTA G 3' and 5' CTA CCT TGC GCG **CAG** **CCG** CGG CGC AGT CCA TGC C 3'. The altered bases for the mutations are indicated in red. The QuikChange mutagenesis is a 4 step procedure, where the oligonucleotide primers, each complementary to the opposite strands of the vector, are extended during temperature cycling by Pfu \Turbo DNA polymerase. Following temperature cycling the amplified DNA is then treated with Dpn1 which digests the parental DNA template. The amplified

and Dpn digested DNA is then transformed into XL1-Blue supercompetant cells. Colonies were picked and plasmids purified and checked by digestion with the corresponding restriction enzyme. The plasmids were also verified by automated DNA sequencing (WSU). The mutant genes were cloned in pBAD-mycHis C vector from Invitrogen and expressed in strain LMG194 (zntA::cat), this strain is a zntA knock out strain. All these mutants were created in the full length construct with a C-terminal His tag (50).

These mutants were also created in the N1-ZntA fragment. The mutant ZntA plasmid was used as template and the pBAD-75 (5'-ATA AGA TTA GCG GAT CCT-3') and ZntA-N1strepreverse (5'-GCG CTC GAG TTA TTT TTC GAA CTG CGG GTG GCT CCA CAG GGC ATA GCC TGC-3') as the oligonucleotides for PCR. The PCR product and pET16B were digested using Nco1 and Xho1. Following restriction digestion the pET16B and the amplified DNA were ligated together to generate the plasmid N1-ZntA with the mutation. The N1-ZntA was inframe with strep tag at the C-terminus. The sequence was verified by automated DNA sequencing at WSU.

### **2.3.3 Protein expression and Purification of the ZntA mutants**

The His-tagged full length ZntA mutants were expressed by growing LMG194 (zntA::cat) cells transformed with the appropriate plasmid at 37°C overnight for about 15 hrs in ZY medium (supplemented with 0.5% glycerol, 0.05% glucose, 0.2% alpha lactose, 1mM MgSO<sub>4</sub>) followed by induction with 0.2% arabinose. Cells were harvested after 15 hrs of growth, washed with ice-cold buffer containing 25mM Tris, pH 7.0 and 100mM KCl, and cell pellets were



stored at  $-20^{\circ}\text{C}$ . Protein purification procedures were all performed at  $4^{\circ}\text{C}$ . Frozen cells were thawed and resuspended in buffer A (25 mM Tris, pH 7.0, 100 mM sucrose, 1 mM PMSF, 1 mM EDTA and 1 mM  $\beta$ -mercaptoethanol (BME)) at 0.2g/ml. The cells were broken at 20,000 p.s.i using a French press; the lysed cells were then incubated with DNase 1 (0.02mg/ml) and 2mM  $\text{MgCl}_2$  for 30 min. The lysed cells were then centrifuged at 8000 rpm for 30min. The supernatant was then centrifuged at 40,000 rpm for 1 h to separate the membranes from the soluble fraction of cells. The pellet from this centrifugation was resuspended in buffer B (1 mM Tris pH 7.0, 100 mM sucrose, 1 mM EDTA, 1 mM PMSF, and 1 mM BME), stirred for 1 h at  $4^{\circ}\text{C}$ , and then it was centrifuged at 40,000 rpm for 1 h. The membrane was then resuspended in buffer C (25 mM Tris pH 7.0, 100 mM sucrose, 500 mM NaCl, 1 mM PMSF and 1 mM BME). Triton-X-100 was added to a final concentration of 1% and the suspension was stirred for 1 h at  $4^{\circ}\text{C}$ . The solubilized membranes were then centrifuged at 40,000 rpm for 1 h to remove the insoluble fraction. The supernatant was then loaded on a charged  $\text{Ni}^{2+}$ -pro-bond column. The column was washed successively with buffer C, buffer C + 50 mM imidazole, and buffer C + 100 mM imidazole. Finally the protein was eluted using 30 ml of buffer C with 300 mM imidazole. 1 ml fractions were collected and analyzed for protein. Protein containing fractions were pooled and loaded on 40 ml Sephadex G-25 columns to remove imidazole. Protein fractions were collected and concentrated using YM-100 centricons. The protein was stored at  $-80^{\circ}\text{C}$  with 10 % glycerol as a cryoprotectant.

### 2.3.4 Protein expression and purification of N1-ZntA and N1-ZntA mutants

The strep tagged N1-ZntA was expressed by growing the N1-ZntA transformed BL21DE3*plysS* strain at 37°C in Luria Bertani medium supplemented with 100µg/ml ampicillin until the absorbance at 600 nm was 0.8. This was followed by induction with 0.1 mM IPTG and then the temperature was lowered to 30°C. Cells were harvested 4 h after induction, washed with ice-cold buffer containing 25 mM Tris, pH 7.0 and 100 mM KCl, and cell pellets were stored at -20°C. The strep tag is a short peptide (8 amino acids, WSHPQFEK), which binds with high selectivity to Streptactin, an engineered streptavidin. The frozen cell pellets were thawed and resuspended in buffer A (100 mM Tris pH 7.0, 150 mM NaCl, and 1 mM EDTA). The cells were broken at 20,000 p.s.i, the lysed cells were then incubated with DNase 1 (0.02mg/ml) and 2mM MgCl<sub>2</sub> for 30 min. The lysed cells were then centrifuged at 8000 rpm for 30 min. The supernatant was then centrifuged at 40,000 rpm for 1 h to separate the membranes from the soluble fraction of cells. The supernatant was loaded onto a 5ml streptactin Sepharose column (IBA Technologies). The column was washed with 5 bed volumes of buffer A, and then the protein was eluted using 6 times 0.5 column volume buffer A + 2.5 mM desthiobiotin. 1ml fractions were collected and analyzed for protein. Protein containing fractions were pooled and loaded on 40 ml Sephadex G-25 columns which were pre-equilibrated with buffer B (10 mM Bis Tris pH 7.0 and 150 mM KCl) to remove desthiobiotin and EDTA. Protein fractions were collected and concentrated using YM-3 centricons. The protein was stored at -80°C with 10 % glycerol as a cryoprotectant.

### 2.3.5 Determination of Protein Concentration

Protein concentrations were determined by Bichinchonic acid assay, using bovine serum albumin as standard. In this assay the proteins reduce  $\text{Cu}^{2+}$  to  $\text{Cu}^{+}$  in a concentration dependent manner. Bichinchonic acid forms a purple complex with  $\text{Cu}^{+}$ , which has an absorbance maximum at 562 nm. This absorbance is proportional to the protein concentration. BSA is used to generate a standard curve.

### 2.3.6 ATPase Activity Measurements

The activity of ZntA and the ZntA mutants was measured by a coupled spectroscopic assay, involving pyruvate kinase and lactate dehydrogenase. The regeneration of ATP is coupled to the oxidation of NADH, which is monitored at 340 nm (50). The buffer for the reaction was 0.05 M Bis tris, 0.1 M acetic acid, and 0.05 M triethanolamine at pH 7.0. The reaction mixture (1ml) also contained 0.1% asolectin, 0.2% Triton-X-100, 10% glycerol, 5 mM ATP, 0.25 mM NADH, 1.25 mM phosphoenolpyruvate, 7 units of pyruvate kinase, and 10 units of lactate dehydrogenase, with or without metal ion ( $\text{Zn}^{2+}$ ,  $\text{Pb}^{2+}$ ,  $\text{Cd}^{2+}$ ). The proteins were reduced by incubation with 2 mM DTT for 1 h prior to the reaction. About 0.5-2mg/ml protein was used per assay. The reaction mixture was incubated for 5 min at 37°C before initiating the reaction with 5 mM  $\text{MgCl}_2$ .

Thiolates in the assay buffer are known to increase the ATPase activity (50). The activities of the mutants were also investigated in the presence of thiolates. Along with the other assay ingredients, thiolates were also added. The concentration of the thiolate form of cysteine required to generate a constant

metal ion: thiolate ion ratio was calculated using the Henderson-Hasselbach equation, using a pKa of 8.33 for cysteine and a pH of 7.0. The data obtained was fit to the Michaelis-Menten equation,

$$v = V_{\max} \times S / (K_M + S)$$

where,  $V_{\max}$  equals the maximum velocity,  $S$  is the concentration of metal,  $K_M$  is the Michaelis constant for the substrate metal ion (50).

### 2.3.7 Measurement of Metal Binding Affinity of the N1-ZntA mutants

The purified N1-ZntA and N1-ZntA mutants were incubated with 1mM Tris (2-carboxy-ethyl) phosphine hydrochloride (TCEP) for 1 h on ice. The buffer (10mM Bis-tris, pH 7.0) and metal solutions were deoxygenated and equilibrated with argon. The TCEP was removed by passing the protein on a 10 ml Sephadex G-25 column under partially anaerobic conditions. For the fluorescence titration, the reduced protein was titrated with increasing concentration of different metal solutions ( $Zn^{2+}$ ,  $Pb^{2+}$ , and  $Cd^{2+}$ ). The metal solutions were added to the reduced protein using gas tight Hamilton syringe in a sealed cuvette. After each addition the solution was mixed well, and the fluorescence spectrum collected. The protein was excited at 290nm and an emission spectrum between 300-500nm was measured.

### 2.3.8 Preparation of Metal bound N1 and N1-mutants

To measure the stoichiometry of metals bound to N1-ZntA and the site-specific mutants, the protein was reduced with 1 mM TCEP for 1 h at 4 ° C. The reduced protein was then incubated with metal salts for 1 h at 4 ° C, the excess metal was removed by passing through a Sephadex G–25 column (56).

### **2.3.9 Measurement of Metal Binding Stoichiometry of the N1-ZntA mutants by ICP-MS**

The metal content was measured by a PE Sciex Elan 9000 ICP-MS (inductively coupled mass spectrometry) with a cross-flow nebulizer and Scott type spray chamber. The RF power was 1000 W, and the argon flow was optimized at 0.92 L/min. The optimum lens voltage was centered on rhodium sensitivity. The data were collected as counts per second. Lead, Cadmium and Zinc standards were obtained from VWR. Standard calibration curves were determined from samples diluted from stock solutions of 1000 ppm standard solutions. The samples and standards solutions were all diluted in 2% HNO<sub>3</sub>.

### **2.3.10 Sensitivity to metal salts**

The sensitivity of *E.coli* strains LMG194, LMG194 (zntA::cat) and LMG194 (zntA::cat) transformed with pZntA, or the site specific mutants, to lead, cadmium and zinc was measured. The cells were grown in low phosphate media, pH 7.5. Cells were grown overnight and then diluted 100 fold in the same media in the presence of lead acetate, zinc chloride, and cadmium chloride. Cell growth at 37 °C was monitored at 600 nm over a period of 24 hours (56, 69).

### **2.3.11 X-Ray Absorption Spectroscopy (XAS)**

XAS was used to study the coordination geometry and ligand environment of metal bound to wild type N1-ZntA. This experiment was performed in collaboration with Dr. Jim Penner-Hahn's laboratory at University of Michigan. XAS samples of different metals bound to N1-ZntA were prepared as follows. The purified proteins were reduced with 1mM TCEP for an hour. The protein was

then passed through a 10ml Sephadex G-25 column pre-equilibrated with 10mM Bis-Tris to remove the reducing agent, under anaerobic conditions. The reduced apo-proteins (~1 mM) were incubated with 0.9 equivalents of metal salt solutions for 1 h on ice. The protein was then passed through a 10 ml Sephadex G-25 column pre-equilibrated with 10 mM Bis-Tris to remove any unbound metal. Protein concentrations of the fractions collected were checked by the Bichinchonic acid assay. The protein fractions were pooled and concentrated to about ~50 $\mu$ l, 30% glycerol was mixed with the protein for uniform glass formation. The final protein concentration was determined by BCA and the final metal content of the protein was determined by ICP-MS. Then the samples were loaded in Lucite cells, with Kapton tape window and immediately frozen in liquid nitrogen. XAS data for all the N1-ZntA samples were collected at the Stanford Synchrotron Radiation Laboratory (SSRL) beamline 9-3. Harmonic rejection was achieved by using a pair of Rh-coated mirrors. For Co, Cu, Zn, Cd: K-edge fluorescence excitation spectra, and for Pb:L<sub>3</sub>-edge fluorescence excitation spectra, were collected using a Canberra 30-element Germanium solid-state detector array equipped with a filter and Soller slits focused on the sample. During data collection, the sample temperature was maintained between 10-14 K using the Oxford Instruments continuous-flow liquid-helium cryostat. Three nitrogen filled ion chambers were used to measure the X-ray intensity at different points along the photon path. The first ion-chamber was placed in front of the sample to measure the incident intensity ( $I_0$ ), the second ion-chamber was placed just after the sample to measure the transmitted intensity ( $I_1$ ) and there

was a third ion-chamber ( $I_2$ ) that was placed after  $I_1$ . The X-ray energies were calibrated by collecting the absorption spectra of the reference metal foils simultaneously with those of the proteins (e.g. Co foil with the Co-N1 sample). The spectra were measured using 5 eV steps in the pre-edge region, 0.3 eV steps in the edge and  $0.05 \text{ \AA}^{-1}$  increments in the extended X-ray absorption fine structure (EXAFS) region with integration times ranging from 1 to 25 s in a  $k^3$ -weighted manner giving a total scan time of 25 to 40 minutes (total scan time was different for different metals) per scan. Six to twelve scans were collected for each protein sample depending on the metal concentration and each metal-bound sample was prepared in duplicates to check reproducibility. Each channel for each scan was checked for spectral anomalies and all the channels with significant glitches (2–3 channels per scan) were discarded before averaging. In order to test for possible radiation damage, the first and the last scan for each sample were compared. No change was observed for any metal-bound samples.

The data were calibrated, reduced and averaged using the EXAFSPAK suite of programs (George, G.N. Stanford Synchrotron Radiation Laboratory, Menlo Park, CA, 1990.). The first inflection points of different metal foils were assigned at certain values for calibration of the data. The averaged data were background subtracted and normalized to give the final spectra (70). The data were then converted to  $k$ -space using the equation  $k = \sqrt{2m_e(E - E_0)/\hbar^2}$  where  $E$  is the incident photon energy and  $E_0$  is the threshold (binding) energy of the core electron. In our calculation  $E_0$  was 7725 eV for Co, 9000 eV for Cu, 9680 eV for

Zn, 13055 eV for Pb and 26730 eV for Cd. The EXAFS data can be described by

$$\text{the equation: } \chi(k) = \sum_s \frac{N_s A_s(k) S_{AS}(k)}{k R_{AS}^2} \exp(-2k^2 \sigma_{AS}^2) \sin(2k R_{AS} + \phi_{AS}(k))$$

where  $N_s$  is the number of scatterers at a distance  $R_{AS}$ ,  $A_s(k)$  is the effective backscattering amplitude,  $S_{AS}$  is a scale factor,  $\sigma_{AS}^2$  is the Debye-Waller factor i.e. the mean-square disorder,  $\phi_{AS}(k)$  is the total phase shift experienced by the photoelectron and the sum is taken over all shells of scattering interactions. The Fourier transforms were calculated using  $k^3$ -weighted data over a  $k$  range from 2–12  $\text{\AA}^{-1}$  to 2–15  $\text{\AA}^{-1}$  for different metals. Experimental data were fit with theoretical EXAFS amplitude and phase functions calculated using FEFF 7.02. Single scattering parameters were calculated for M–O, M–S and M–M using appropriate bond lengths taken from the Cambridge Structural Database (CSD) for each metal.  $R_{AS}$  and  $\sigma_{AS}$  were varied,  $N_s$  was held fixed at reasonable integer values.

## 2.4 Results

### 2.4.1 The in vivo resistance activity of N1-ZntA mutants to $\text{Pb}^{2+}$ , $\text{Zn}^{2+}$ and $\text{Cd}^{2+}$ in the growth medium

The *zntA* deleted *E.coli* strain, LMG194 (*zntA::cat*) is sensitive to toxic levels of  $\text{Pb}^{2+}$ ,  $\text{Zn}^{2+}$  and  $\text{Cd}^{2+}$ ; it is unable to grow even after 24-30 h and this sensitivity can be complemented by *wzntA*. The cysteine (C29A, C30A, C31A, C35A, C59A and C62A) and the aspartate (D32A, D32N, D58A, D58N) mutants were tested for their ability to confer resistance to  $\text{Pb}^{2+}$ ,  $\text{Zn}^{2+}$  and  $\text{Cd}^{2+}$ . For comparison, the  $\Delta$ N-ZntA mutant, in which the N-terminal domain is deleted, was



also tested. All the site-specific mutants were able to confer resistance to  $Pb^{2+}$ ,  $Zn^{2+}$  and  $Cd^{2+}$ , better than the  $\Delta N$ -ZntA mutant. In the presence of zinc, a slight lag was observed for some mutants compared to ZntA itself.

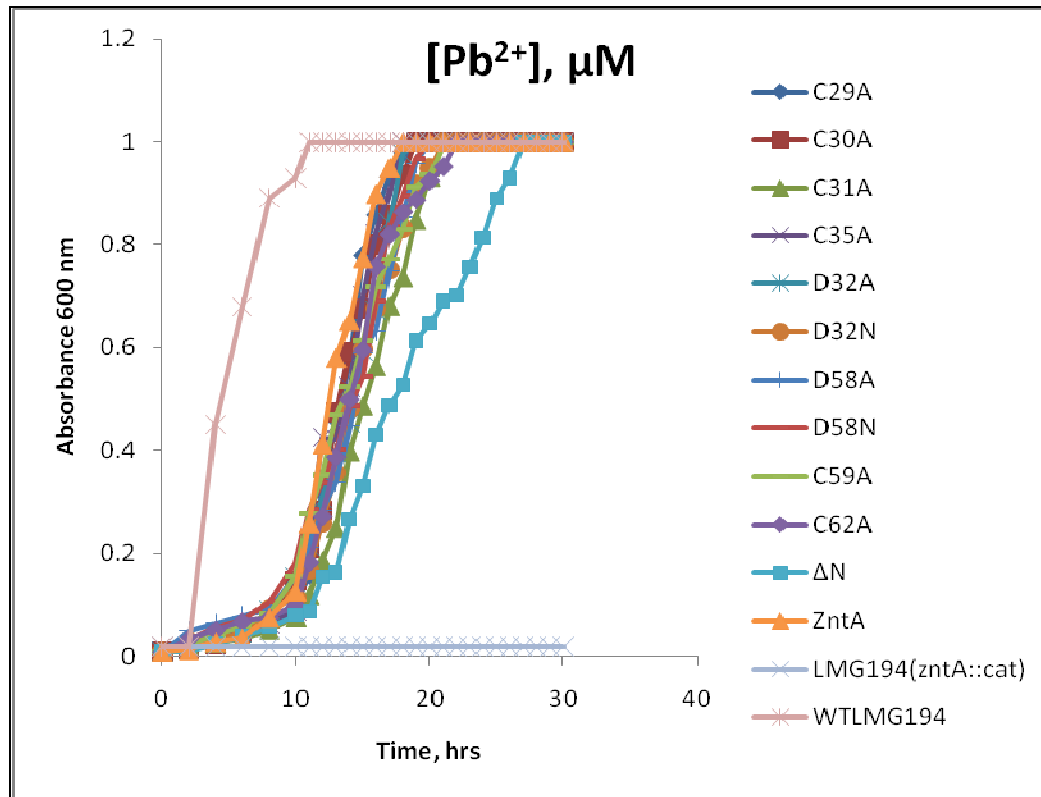


**Figure 2.2.** Resistance to Lead, Zinc and Cadmium salts by the wild type strain LMG194, the *zntA*-deleted strain LMG194(*zntA::cat*), and the deleted strain transformed with the plasmids containing *wtzntA*,  $\Delta N$ -ZntA and the site-specific mutants in the N-terminal domain.

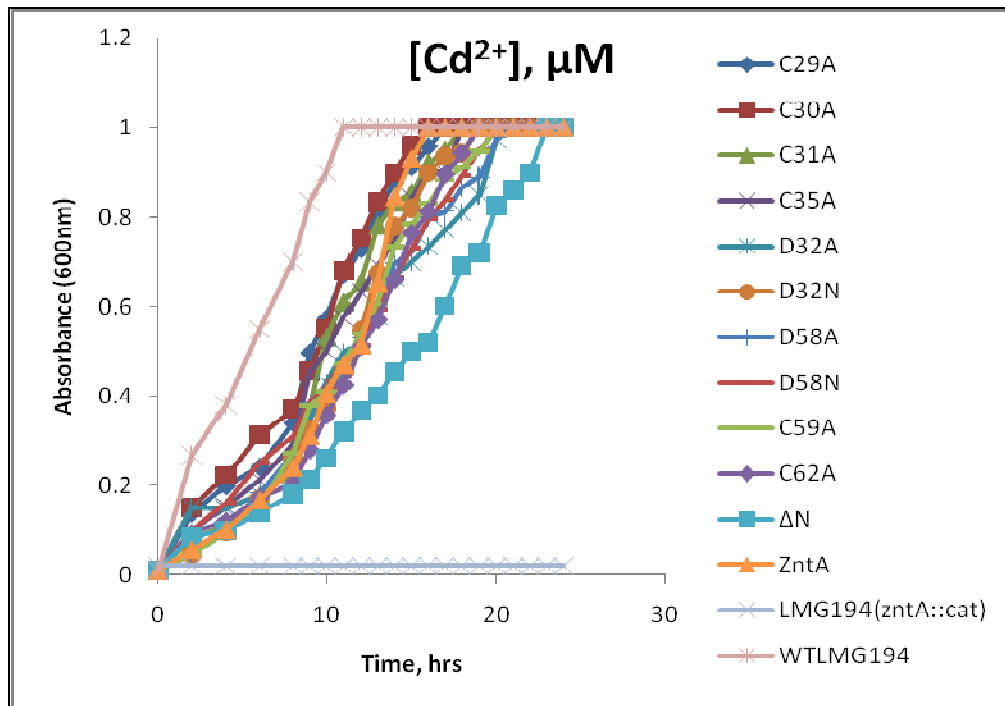
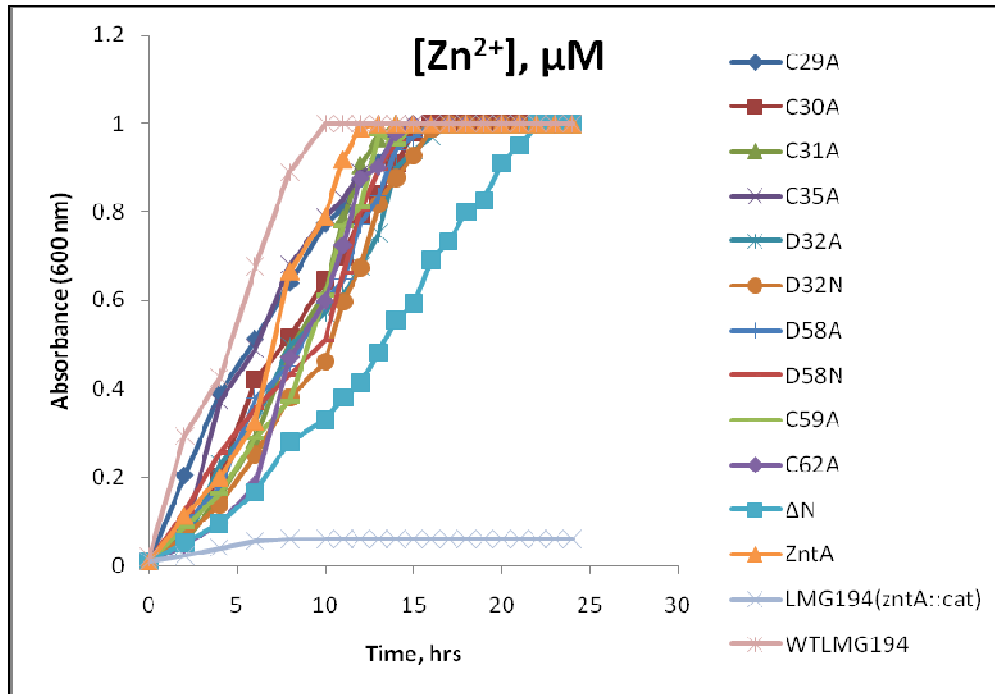


**Figure 2.2.** Resistance to Lead, Zinc and Cadmium salts by the wild type strain LMG194, the *zntA*-deleted strain LMG194(*zntA::cat*), and the deleted strain transformed with the plasmids containing wt*zntA*,  $\Delta$ N-ZntA and the site-specific mutants in the N-terminal domain.

### 2.4.2 Activity of the Purified N1-ZntA mutants

The ATPase activity of  $\Delta$ N-ZntA, ZntA and the site specific mutants at the N-terminal domain were measured for the metal ions  $Pb^{2+}$ ,  $Zn^{2+}$  and  $Cd^{2+}$ . Previous studies showed that the metals ions stimulate the ATP hydrolysis activity of wtZntA, with  $Pb^{2+}$  exhibiting the highest activity (Table 2.1) (50). Previous studies in the lab have also shown that there is a 4-8 fold increase in the ATPase activity of ZntA in the presence of thiolate forms of cysteine or glutathione in the assay medium. This is perhaps because the metal thiolate complex is a better substrate; within the cell metal ions are expected to be present as complexes of small molecule chelators such as cysteine or glutathione (50). The activities obtained for wtZntA in the presence of metal ions and thiolate form of cysteine in the ratio 1:1 for  $Pb^{2+}$ ,  $Zn^{2+}$  and  $Cd^{2+}$  were ~2500, ~ 800 and 1000 nmol/(mg.min), respectively (Tables 2.1,2.2,2.3). All the mutants showed higher activities in the presence of the thiolate form of cysteine.

For the alanine substitutions at Cys29, Cys30, and Cys35, the lead and cadmium stimulated activity was similar to that of ZntA (Table 2.1). The mutants C31A, D32A, D32N D58A, D58N, C59A, and C62A showed a 2-3 fold decrease in activity for  $Pb^{2+}$  (Table 2.1). All the mutants showed higher activities in the presence of the thiolate form of cysteine. However, mutations at C31, D32, D58, C59 and C62 showed lower activities in comparison to wtZntA, when the lead: thiolate complex was provided as the substrate.

**Table 2.1.** Kinetic Parameters obtained for ZntA,  $\Delta$ N and the mutants for  $Pb^{2+}$  in the absence and presence of the thiolate form of cysteine present at a concentration equal to the  $Pb^{2+}$  concentration.

	$Pb^{2+}$		$Pb^{2+}$ + Thiolate	
	$V_{max}$ nmoles/mg/min	$K_M$ $\mu$ M	$V_{max}$ nmoles/mg/min	$K_M$ $\mu$ M
<b>ZntA</b>	584 $\pm$ 30	5 $\pm$ 0.9	2500 $\pm$ 70	166 $\pm$ 16
<b><math>\Delta</math>N-ZntA</b>	320 $\pm$ 6	11.6 $\pm$ 0.8	1095 $\pm$ 67	55 $\pm$ 11
<b>C29A</b>	574 $\pm$ 9.5	2.8 $\pm$ 0.2	2194 $\pm$ 34	89 $\pm$ 4.3
<b>C30A</b>	557 $\pm$ 15	5.7 $\pm$ 0.85	2066 $\pm$ 51	66 $\pm$ 5.6
<b>C31A</b>	264 $\pm$ 8	10 $\pm$ 1	1756 $\pm$ 56	115 $\pm$ 10
<b>D32A</b>	284 $\pm$ 8	8.4 $\pm$ 0.8	1422 $\pm$ 28	37 $\pm$ 3
<b>D32N</b>	317 $\pm$ 22	6.7 $\pm$ 2.3	817 $\pm$ 30	70 $\pm$ 8
<b>C35A</b>	611 $\pm$ 30	14 $\pm$ 2	2361 $\pm$ 54	249 $\pm$ 13
<b>D58A</b>	201 $\pm$ 3.4	3 $\pm$ 0.27	954 $\pm$ 26	26 $\pm$ 3.2
<b>D58N</b>	325 $\pm$ 20	11 $\pm$ 2	1145 $\pm$ 69	268 $\pm$ 37
<b>C59A</b>	263 $\pm$ 5	7.7 $\pm$ 0.53	1198 $\pm$ 27	236 $\pm$ 12
<b>C62A</b>	132 $\pm$ 3.8	3.2 $\pm$ 0.46	1045 $\pm$ 16	47 $\pm$ 2.7

All the alanine substitutions and the asparagine substitutions at the conserved cysteine and aspartate residues displayed 2-3 fold lower activities in the presence of  $Zn^{2+}$  (Table2.2). Zinc:thiolate induced activities of the mutants is

higher. However, substitutions at C31, D32, D58, C59 and C62 showed lower activities in comparison to wtZntA, when zinc: thiolate complex was provided as the substrate.

**Table 2.2** Kinetic Parameters obtained for ZntA,  $\Delta N$  and the mutants for  $Zn^{2+}$  in the absence and presence of the thiolate form of cysteine present at a concentration equal to the  $Zn^{2+}$  concentration.

	$Zn^{2+}$		$Zn^{2+} + \text{Thiolate}$	
	$V_{max}$ nmoles/mg/min	$K_M$ $\mu M$	$V_{max}$ nmoles/mg/min	$K_M$ $\mu M$
<b>ZntA</b>	250 $\pm$ 13	10 $\pm$ 2	710 $\pm$ 28	96 $\pm$ 11
<b><math>\Delta N</math>-ZntA</b>	81 $\pm$ 7	9.3 $\pm$ 1.2	372 $\pm$ 6	42 $\pm$ 3
<b>C29A</b>	86 $\pm$ 5.5	7 $\pm$ 1.6	1096 $\pm$ 28	36 $\pm$ 3.8
<b>C30A</b>	92 $\pm$ 3.25	3 $\pm$ 0.87	1005 $\pm$ 30	148 $\pm$ 13.4
<b>C31A</b>	61 $\pm$ 1.48	2.24 $\pm$ 0.31	786 $\pm$ 16.2	105 $\pm$ 6.5
<b>D32A</b>	85 $\pm$ 3	3.2 $\pm$ 0.6	748 $\pm$ 10	71 $\pm$ 3.1
<b>D32N</b>	127 $\pm$ 13	15 $\pm$ 4.8	753 $\pm$ 11.8	94 $\pm$ 9.7
<b>C35A</b>	75 $\pm$ 1.8	4.7 $\pm$ 0.47	697 $\pm$ 19	154 $\pm$ 11
<b>D58A</b>	82 $\pm$ 3	3.8 $\pm$ 0.65	587 $\pm$ 7.4	75 $\pm$ 3
<b>D58N</b>	100 $\pm$ 9.7	16 $\pm$ 4	730 $\pm$ 19	74 $\pm$ 5.4
<b>C59A</b>	60 $\pm$ 2	3.22 $\pm$ 0.5	568 $\pm$ 21	127 $\pm$ 13.7
<b>C62A</b>	51 $\pm$ 1	4.7 $\pm$ 0.4	526 $\pm$ 15	70 $\pm$ 7.2

The cadmium stimulated activity for the alanine substitutions at Cys29, Cys30, and Cys35, was similar to that of ZntA (Table2.3). C31A, D32A, C59A and C62A showed slightly lower activities in the presence of Cd<sup>2+</sup>.

**Table 2.3.** Kinetic Parameters obtained for ZntA,  $\Delta$ N and the mutants for Cd<sup>2+</sup> in the absence and presence of the thiolate form of cysteine present at a concentration equal to the Cd<sup>2+</sup> concentration.

	Cd <sup>2+</sup>		Cd <sup>2+</sup> + Thiolate	
	V <sub>max</sub> nmoles/mg/min	K <sub>M</sub> μM	V <sub>max</sub> nmoles/mg/min	K <sub>M</sub> μM
<b>ZntA</b>	250 ± 13	10 ± 2	710 ± 28	96 ± 11
<b>ΔN-ZntA</b>	81 ± 7	9.3 ± 1.2	372 ± 6	42 ± 3
<b>C29A</b>	59 ± 1.3	2.2 ± 0.28	1103 ± 19.7	118 ± 6.11
<b>C30A</b>	84 ± 3	4.6 ± 1.2	1309 ± 95	226 ± 39
<b>C31A</b>	15 ± 1.8	7.3 ± 2.5	818 ± 16	23 ± 2.1
<b>D32A</b>	22 ± 2.4	3 ± 1.3	744 ± 13	69 ± 4.2
<b>D32N</b>	56 ± 4	0.3 ± 1.3	566 ± 13	14 ± 1.7
<b>C35A</b>	97 ± 6.66	6.9 ± 1.4	1041 ± 31	250 ± 17
<b>D58A</b>	76 ± 2	3.3 ± 0.35	703 ± 17	27 ± 3
<b>D58N</b>	57 ± 4	2.5 ± 0.8	552 ± 48	42 ± 14
<b>C59A</b>	52 ± 3	2.27 ± 0.6	635 ± 6.4	129 ± 3.7
<b>C62A</b>	26 ± 3.7	6 ± 1.12	872 ± 16	28 ± 2.2

### 2.4.3 Stoichiometry of Metal Binding to N1-ZntA mutants using ICP-MS

To understand the importance of the cysteine and aspartate residues in the CCCDXXC and the DCXXC in binding metal ions, we determined the metal binding stoichiometries of the mutants in the isolated fragment N1-ZntA, purified with a strep – tag (Table 2.4). Wild-type N1-ZntA can bind to one metal ion with high affinity (56). Binding stoichiometry for C29A, C30A, and C35A was 1 for  $Pb^{2+}$  and  $Cd^{2+}$ . The results indicate that the alanine and asparagine substitutions at C31, D32, D58, C59, and C62, disrupted the binding of  $Pb^{2+}$  and  $Cd^{2+}$  while residues C29, C30 and C35 appear not to be important in binding these two metal ions. Surprisingly, it was observed that any mutations in the upstream CCCDXXC and downstream DCXXC motifs affected zinc binding completely, though earlier studies showed that  $Zn^{2+}$  binding was unaffected when the upstream motif was deleted in a  $\Delta 46$ -ZntA mutant, which lacks the first 45 residues (5, 56).

**Table 2.4.** Stoichiometry of Metal bound to N1-ZntA and N1-ZntA mutants using Inductively Coupled Plasma Mass Spectrometry (ICP-MS); x = No Binding.

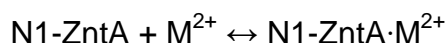
	<b>Lead</b>	<b>Zinc</b>	<b>Cadmium</b>
<b>N1-ZntA</b>	1 ± 0.0	1 ± 0.1	1 ± 0.0
<b>C29A-N1ZntA</b>	1 ± 0.0	x	1 ± 0.0
<b>C30A-N1ZntA</b>	1 ± 0.0	x	1.1 ± 0.0
<b>C31A-N1ZntA</b>	x	x	x
<b>D32A-N1ZntA</b>	x	x	x
<b>D32N-N1ZntA</b>	x	x	x
<b>C35A-N1ZntA</b>	1 ± 0.0	x	0.8 ± 0.0
<b>D58A-N1ZntA</b>	x	x	x
<b>D58N-N1ZntA</b>	x	x	x
<b>C59A-N1ZntA</b>	x	x	x
<b>C62A-N1ZntA</b>	x	x	x

#### 2.4.4 Affinity of $Pb^{2+}$ , $Zn^{2+}$ and $Cd^{2+}$ for the amino terminal metal binding site mutants using direct fluorescence quenching

The N-terminal domain has one tryptophan residue. The fluorescence emission of the tryptophan residue is quenched when this isolated domain binds metal ions. This tryptophan fluorescence quenching is a useful method to measure the affinity of different divalent metal ions. A titration of N1-ZntA with increasing concentrations of  $Pb^{2+}$  is shown in Figure 2.3; similar decreases in



fluorescence were observed for  $\text{Cd}^{2+}$  and  $\text{Zn}^{2+}$  also. The change in fluorescence intensity at 340 nm was plotted vs. the metal ion concentration in Figure 2.4. The data were fit to the following equation (using Kaleidagraph) that assumes a 1:1 binding model for the protein.



$$K_E = [\text{E} \cdot \text{M}^{2+}] / [\text{E}][\text{M}^{2+}] \quad \text{Equation(2)}$$

where  $K_E$  is the association constant of the metal and protein,  $[\text{E}]$ ,  $[\text{M}^{2+}]$  and  $[\text{E} \cdot \text{M}^{2+}]$  are the concentrations of initial enzyme, initial metal and metal complex with enzyme. The association constants calculated from the titration data are summarized in Table 2.5. The affinity of the buffer, Bis-Tris was taken into account when fitting the data. Mutants C31A, D32A, D32N, D58A, D58N, C59A, and C62A did not show any fluorescence quenching, suggesting they were unable to bind lead, in agreement with the results from ICP-MS.

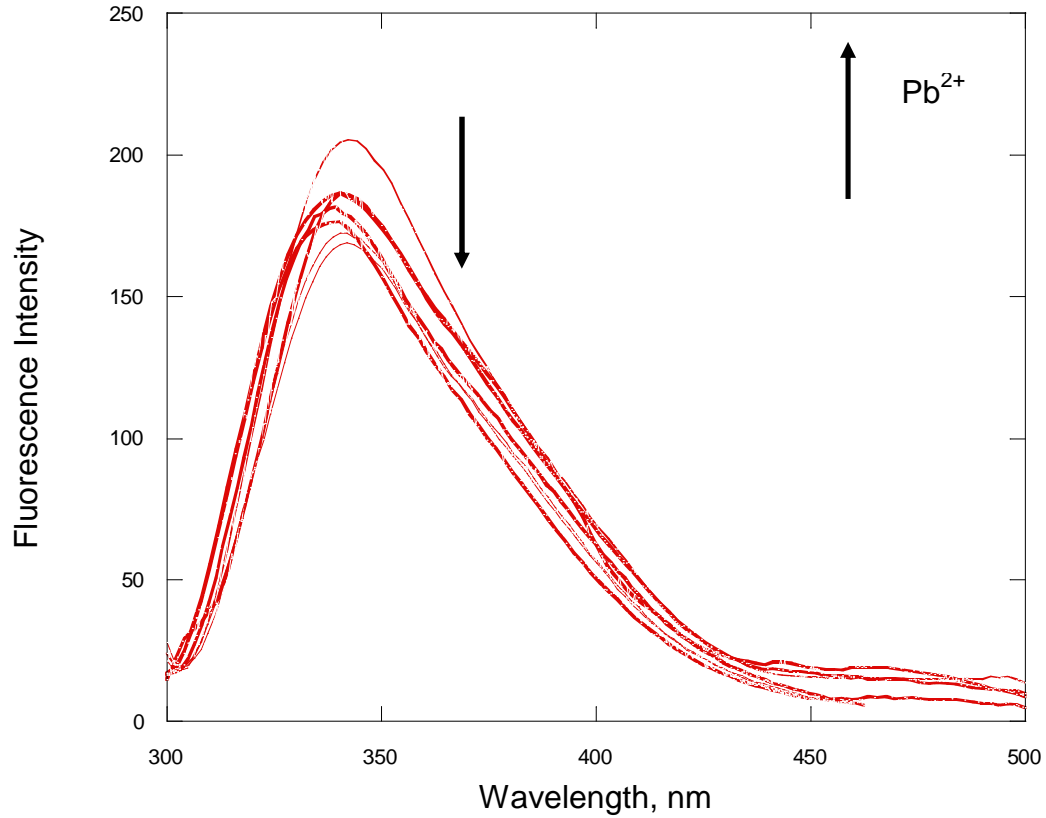


**Figure 2.3.** Representative spectra obtained during titration of 10  $\mu\text{M}$  N1-ZntA with increasing concentrations of  $\text{Pb}^{2+}$  (0-15  $\mu\text{M}$ ) in 10 mM Bis-Tris, pH 7.0 at 20°C. The arrow denotes the decrease in fluorescence as increasing amounts of  $\text{Pb}^{2+}$  are added.

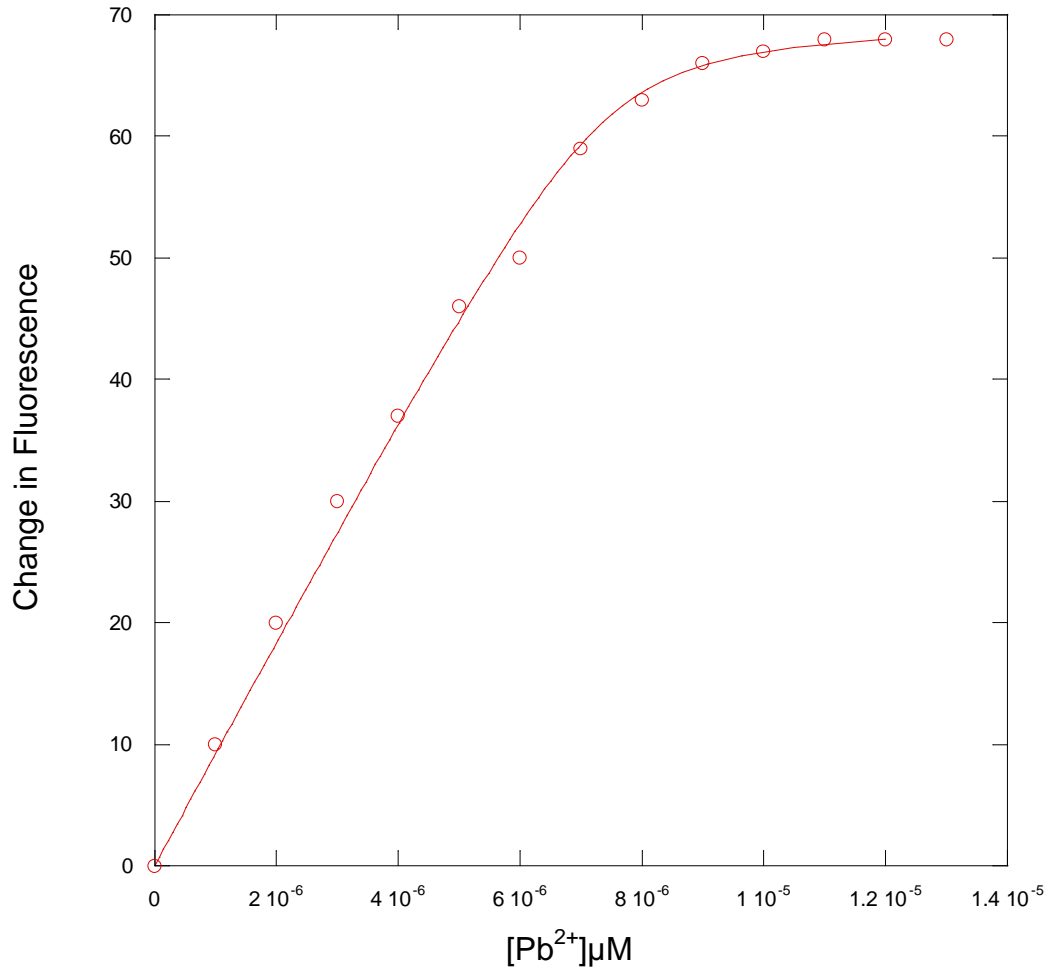


**Figure 2.4.** Plot of change in fluorescence emission at 340 nm from Figure 2.5 above as a function of the added lead salt concentration. The data were fitted to equation 2.

**Table 2.5.** Association constants for the binding of lead, zinc and cadmium to the N1-ZntA mutants.

	Lead $M^{-1}$	Zinc $M^{-1}$	Cadmium $M^{-1}$
N1-ZntA	$(1.8 \pm 0.8) \times 10^9$	$(4.9 \pm 2) \times 10^7$	$(3.6 \pm 0.9) \times 10^7$
C29A	$(8.1 \pm 4.5) \times 10^9$	x	$(5.24 \pm 2) \times 10^7$
C30A	$(4.6 \pm 2.5) \times 10^9$	x	$(1.13 \pm 0.5) \times 10^7$
C35A	$(2.35 \pm 0.9) \times 10^9$	x	$(6.2 \pm 2.2) \times 10^7$

#### 2.4.5 Analysis of Lead, Zinc, Cadmium, Cobalt and Copper binding by X-ray absorption spectroscopy

Although structural information of a portion of N1-ZntA bound to zinc has been solved, details regarding the co-ordination environment of lead and cadmium bound to N1-ZntA are not available. Here, XAS has been used to study the structure of lead, zinc, cadmium ions bound to N1-ZntA, thus providing detailed information with respect to ligand environment and geometry. The co-ordination environment of cobalt and copper bound to N1-ZntA was also examined, because our metal stoichiometry experiments suggested that cobalt binding to N1-ZntA is sub stoichiometric unlike the other metal ions, and in the case of copper, to test whether N1-ZntA can bind to  $Cu^{2+}$ , since it has the CXXC motif, observed in  $Cu^+$ -transporting pumps.

### ***N1-ZntA-Lead***

The N1-ZntA-Pb complex is best simulated with 3 sulfur ligands at a distance of 2.66 Å. Normalized L3-edge spectra of N1-ZntA-Pb sample is presented in Figure 2.5a. The EXAFS data were extracted using the value of  $E_0 = 13055$  eV. The EXAFS data and the Fourier Transform of the EXAFS (k range of 1-14 Å<sup>-1</sup>) are plotted in Figure 2.5b. The data are in blue and fits are in red dotted lines. The best fit results are presented in Table 2.6. No significant second shell interaction was found for any of them.

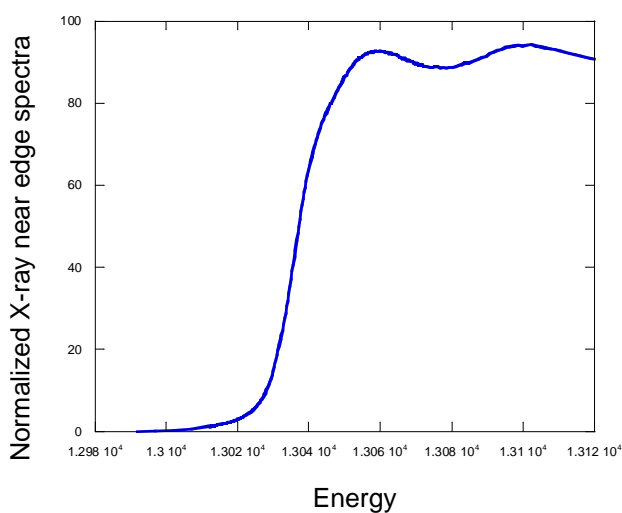


**Figure 2.5a.** Normalized edge spectra of Pb L3-edge for the N1-ZntA-Pb sample.

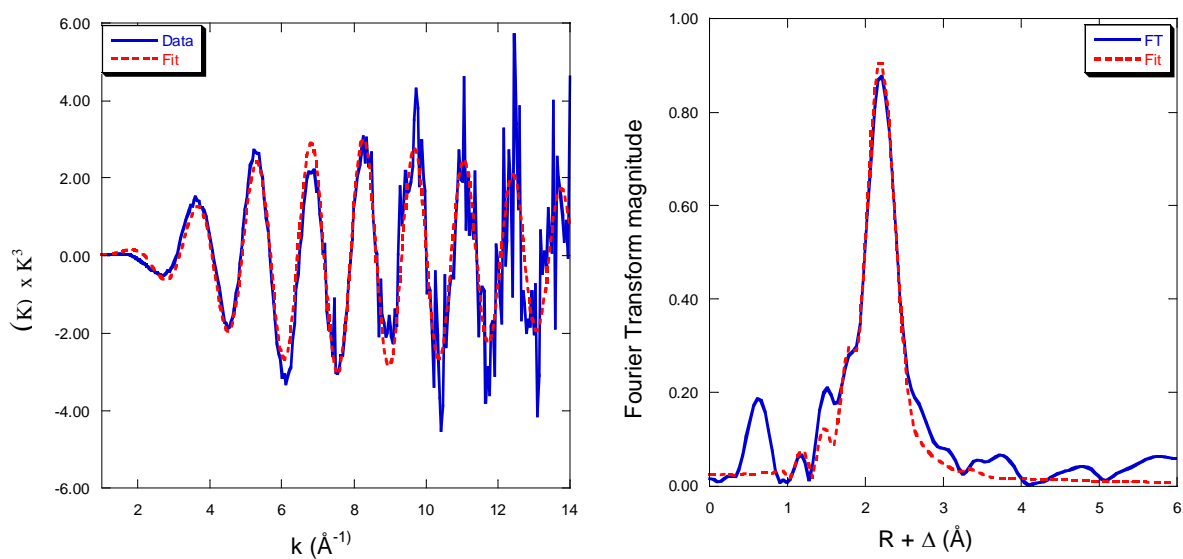


**Figure 2.5b.** EXAFS data and fit for the N1-ZntA-Pb sample.

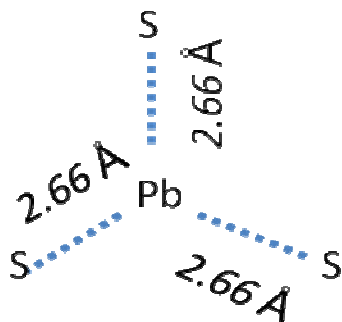


**Figure 2.5c.** Graphical representation of approximate lead coordination geometry.

### **N1-ZntA-Zinc**

The N1-ZntA-Zn sample was best modeled to two oxygen and two sulfur atoms. The normalized K-edge spectra of Zinc are presented in Figure 2.6a. The EXAFS data were extracted using the value of  $E_0 = 13055$  eV. The EXAFS data and the Fourier Transform of the EXAFS ( $k$  range of  $1-14 \text{ \AA}^{-1}$ ) are plotted in

Figures 2.6b. The data are in blue and fits are in red dotted lines. The best fit results are presented in Table 2.6.

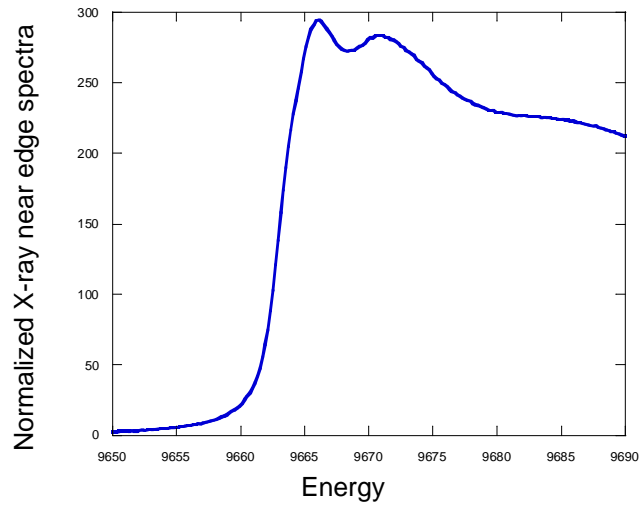


**Figure 2.6a.** Normalized K-edge spectra of N1-ZntA-Zn sample.

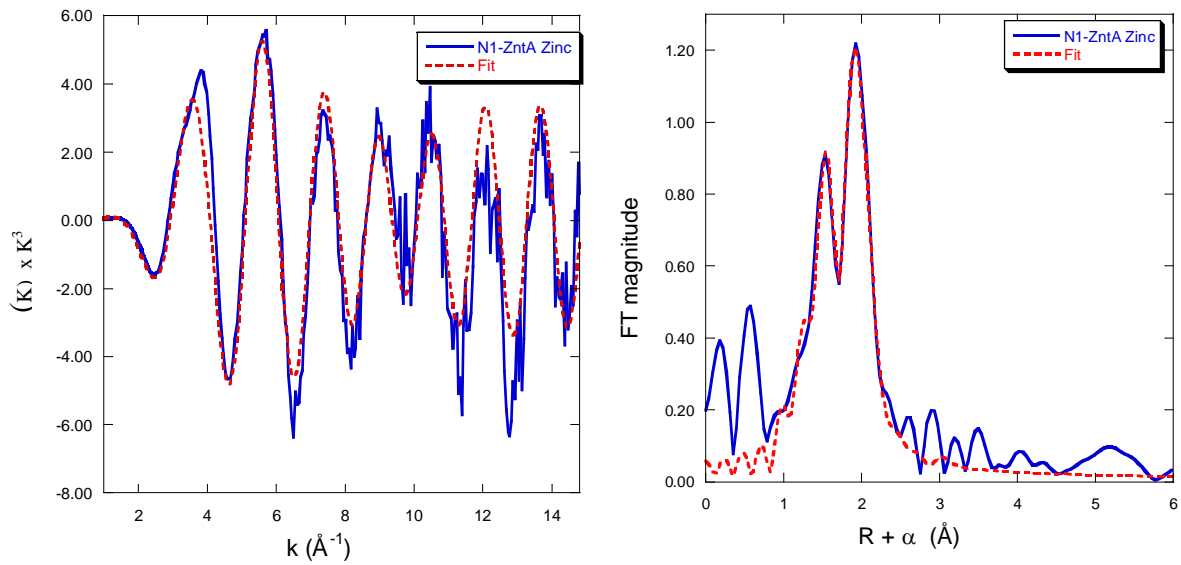


**Figure 2.6b.** EXAFS data and fit for N1-ZntA-Zn sample.

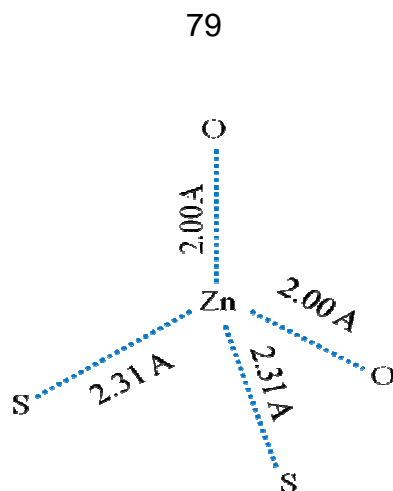


**Figure 2.6c.** Graphical representation of approximate zinc coordination geometry.

### ***N1-ZntA-Copper***

Cu k-edge spectrum of the N1-ZntA-Cu sample is normalized and presented in Figure 2.7a. From the energy of the edge jump it is evident that the oxidation state of the metal is  $\text{Cu}^+$ , though the sample was prepared by incubating the reduced N1-ZntA with  $\text{Cu}^{2+}$  in the absence of any reductant. The XANES feature at the energy of 8983.5 eV is consistent with the  $1s \rightarrow 4p$  transition of the  $\text{Cu}^+$  center and also similar with those of the trigonal  $\text{Cu}^+$  model complexes (71). The EXAFS data were extracted using the value of  $E_0 = 9000$  eV. The EXAFS data and the Fourier Transform of the EXAFS (k range of 1-12.7 Å are plotted in Figs 2.7b and 2.7c. The data are in blue and fits are in red dotted lines. The best fit results are presented in Table 2.6. The first shell interaction for  $\text{Cu}^+$  can be best modeled by 3S ligands at a distance of 2.26 Å. This Cu-S distance is in agreement with the trigonal geometry and is longer than the linear Cu-S distance (~2.17 Å). The second shell interaction can only be modeled by a Cu-Cu interaction pointing towards the formation of a binuclear Cu complex in



solution, which is in agreement with the XAS studies of ATP7B Wilson disease protein (72).

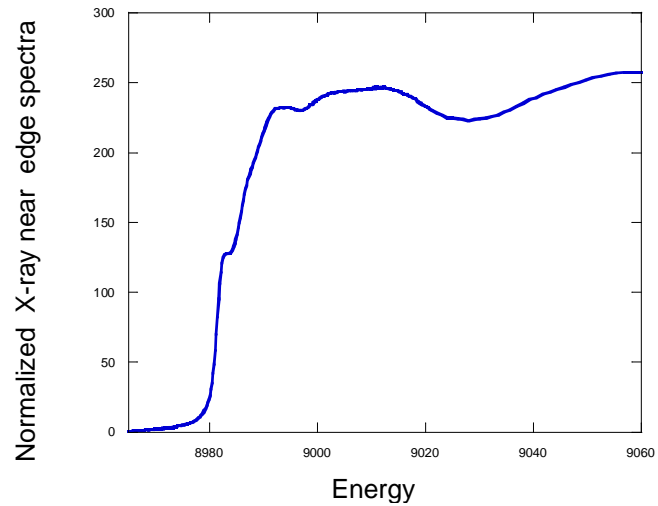


**Figure 2.7a.** Normalized K-edge spectra of N1-ZntA-Cu sample.

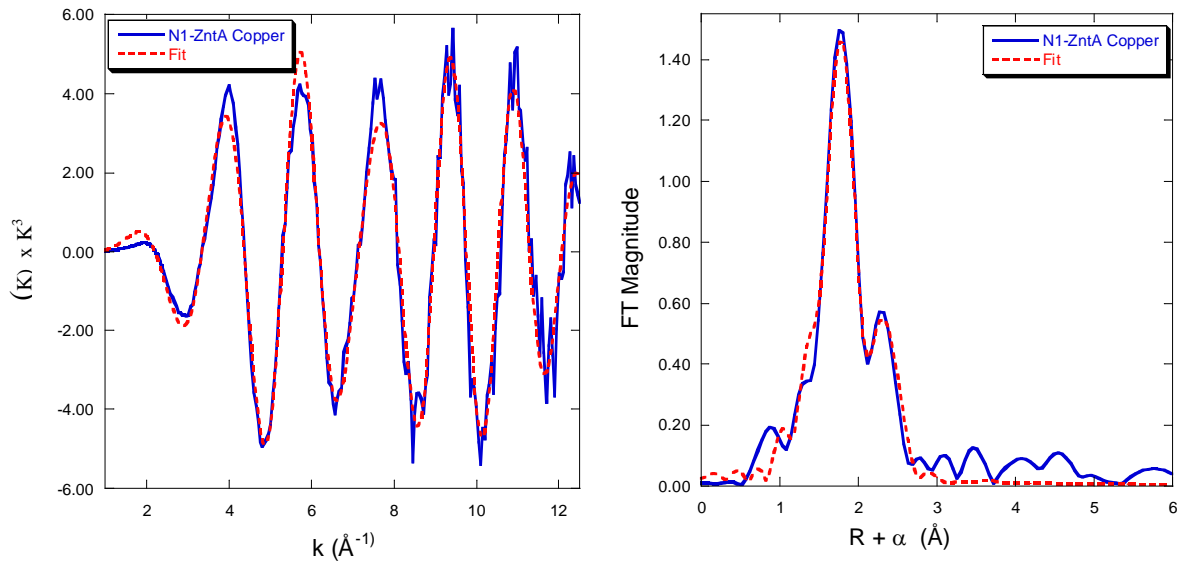


**Figure 2.7b.** EXAFS data and fit for N1-ZntA-Cu sample.

### ***N1-ZntA-Cobalt***

From the edge spectra (Figure 2.8a) we can conclude that the Co is in the +2 oxidation state with a weak pre-edge peak at around 7709 eV. The EXAFS data were extracted with  $E_0 = 7725$  eV. The  $k^3$  weighted EXAFS data and Fourier Transform ( $k = 1-15 \text{ \AA}^{-1}$ ) are presented in Figures 2.8b. The data is plotted in blue and the fit is in red dotted line. The best fit parameters are presented in table 2.6. From the fitting results  $\text{Co}^{2+}$  appears to be in a distorted tetrahedral geometry. The first shell peaks can be best modeled with a mixture of both O/N and S interactions with 1 O/N and 3S around the  $\text{Co}^{2+}$  center. Our previous results have shown that binding of  $\text{Co}^{2+}$  to N1-ZntA was sub stoichiometric, suggesting that one  $\text{Co}^{2+}$  bridges two protein molecules.

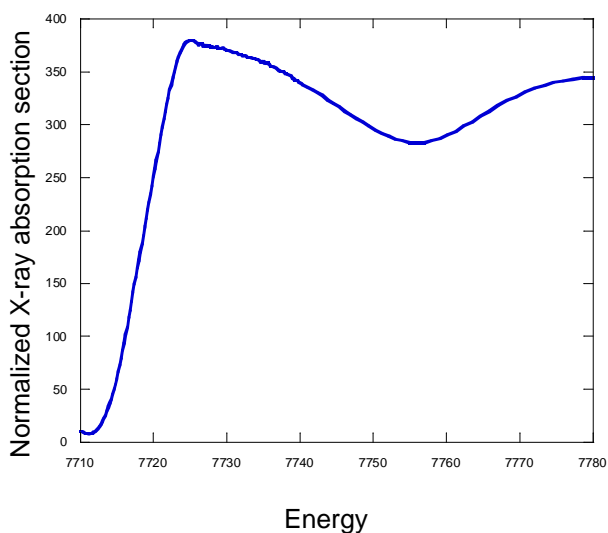


**Figure 2.8a.** Normalized Co (II) k-edge absorption spectrum in N1-ZntA-Co sample.

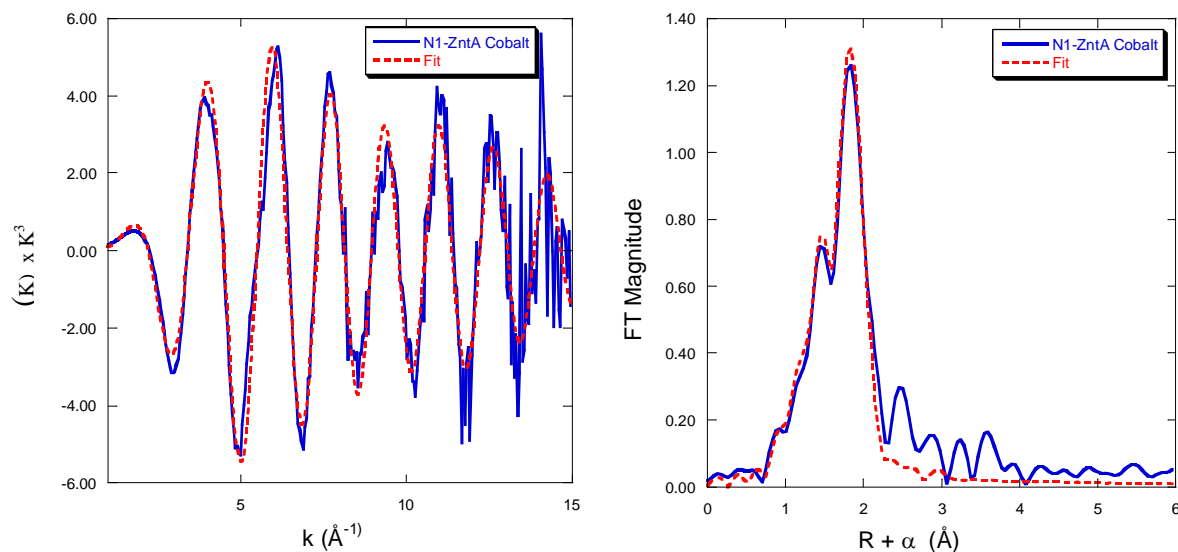


**Figure 2.8b.** EXAFS and Fit for the N1-ZntA-Co sample.

### ***N1-ZntA-Cadmium***

Cd k-edge spectrum of the Cd-Znta sample is normalized and presented in Figure 2.9a. The EXAFS data were extracted using the value of  $E_0 = 26730$  eV. The EXAFS data and the Fourier Transform of the EXAFS ( $k$  range of 1-15  $\text{\AA}^{-1}$ ) are plotted in Figures 2.9b & 2.9c. The data are in blue and fits are in red dotted lines. The best fit results are presented in Table 2.6. From the best fit results it is difficult to predict whether the Cd is present in a 5 or 6 coordinate environment. The first shell interaction for Cd can be best modeled by either 3O/N and 2S or 3O/N and 3S ligands. The low  $z$  ligands O/N are present at a distance of 2.35  $\text{\AA}$  and the S ligands are present at a distance of 2.57  $\text{\AA}$ . Though the goodness of fit value is better for the 5-coordinate fit, the Debye-Waller factors for both O/N and S are very low. The second shell interaction can be modeled by a Cd-Cd interaction pointing towards the formation of a binuclear Cd complex in solution.

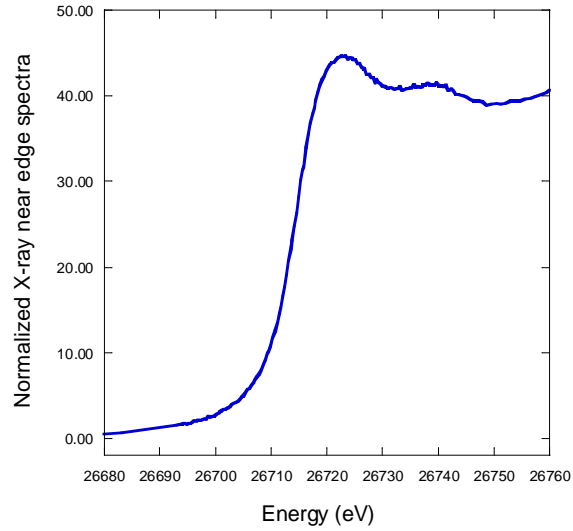


**Figure 2.9a.** Normalized Cd (II) k-edge absorption spectrum in N1-ZntA-Cd sample.

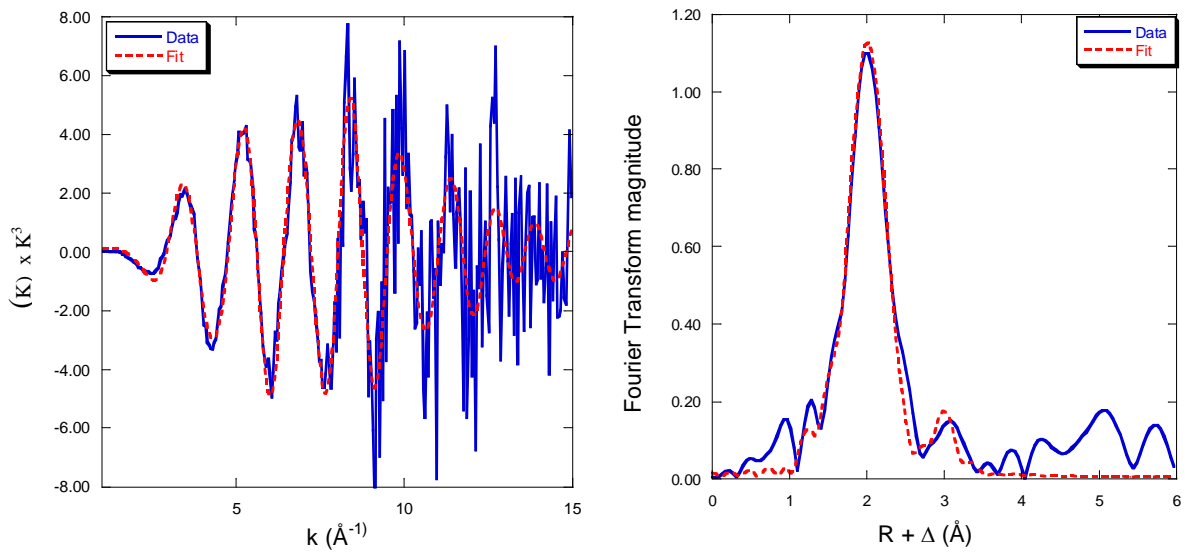


**Figure 2.9b.** EXAFS and 5 co-ordinate fit for the N1-ZntA-Cd sample.

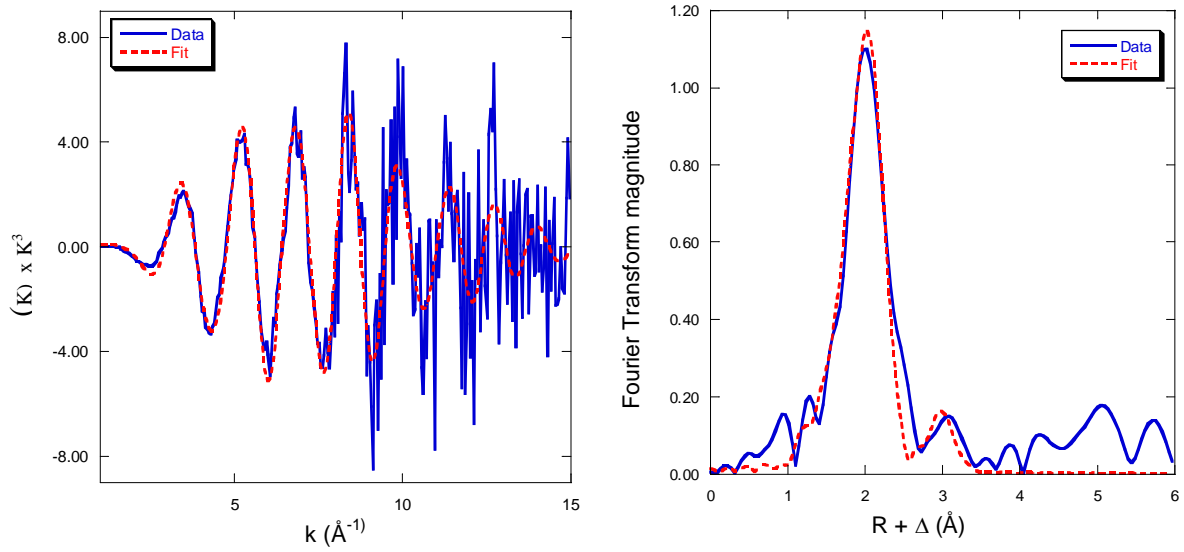


**Figure 2.9c.** EXAFS and 6 co-ordinate fit for the N1-ZntA-Cd sample.

**Table 2.6.** EXAFS Fitting results for Lead, Zinc, Cadmium, Copper and Cobalt.

Sample	Ligand <sup>a</sup>	CN <sup>b</sup>	R (Å) <sup>c</sup>	$\sigma^2 \times 10^3$ (Å <sup>2</sup> ) <sup>d</sup>	$\Delta E_0$	F $\times 10^{-3}$ <sup>e</sup>
Lead	S	3	2.66	2.81	-16.6	0.2083
Zinc	O	2	2.0	3.90	-13.4	0.3545
	S	2	2.31	1.73		
Cadmium	S	2	2.58	1.00	-4.83	0.8174
	Cd	1	3.29	8.36		
	O	3	2.35	1.08		
	S	3	2.57	3.23	-6.42	0.8453
	Cd	1	3.28	3.28		
	O	3	2.35	2.35		
Copper	S	3	2.26	5.04	-14.4	0.1598
	Cu	1	2.70	9.53		
Cobalt	S	3	2.26	3.38	-12.006	0.8785
	Co	1	1.90	2.09		

a = Scattering atoms, b = Average metal-ligand coordination number,

c = Average metal – ligand bond length, d = Average Debye Waller factor,

e = number for degrees of freedom weighted mean square deviation between data and fit

## 2.5 Discussion

The amino terminal domain of P<sub>IB</sub> type ATPases has been studied, but very little is known about the molecular basis of metal selectivity and specificity of this family of proteins. Sequence analysis has shown that the CXXC motif is present in copper and lead/zinc/cadmium transporting ATPases; it is also present in some other proteins including copper chaperones and mercury binding proteins. Studies of the Cu<sup>+</sup> ATPases, which can have multiple copies of CXXC motif, and CadA, a Cd<sup>2+</sup>-ATPase, have demonstrated that the cysteines in this motif are metal binding ligand sites (8). ZntA not only has the CXXC motif but also a CCCDCXXC motif in its amino terminal domain. ICP-MS measurements have shown that N1-ZntA binds to a wide variety of metal ions with a stoichiometry of one, with the exception of cobalt. The N-terminal domain of the Cu<sup>+</sup> ATPase also binds to different metal ions: Cu<sup>+</sup>, which is a substrate, and to zinc and cadmium which are not substrates, through different geometry (10, 61). Some P<sub>IB</sub> ATPases like the Cu<sup>2+</sup> ATPases have a histidine rich amino terminal domain which may be specialized for binding to divalent copper, some others like the cobalt transporters do not have the amino terminal domain (47). Thus it is observed that P<sub>IB</sub> ATPases have different conserved metal binding motifs in the N-terminal domains that maybe involved in conferring metal selectivity. Previous results in the lab have suggested that the extra cysteines located upstream of the CXXC motif play a role in lead binding (56). To investigate further the residues involved in conferring selectivity in ZntA, we constructed individual alanine mutants and additionally the Asp32 and Asp58

were mutated to asparagines. The residues were replaced by alanine to avoid any possibility of side chains acting as metal ligand. In D32N and D58N, the carboxylate oxygens of aspartate side chain were replaced by the amide of asparagine to examine if a charged residue at this position is essential for the activity and the metal binding. In vivo, all the mutants display similar resistance profile as wtzntA for lead and cadmium, but Cys31, Cys59, Cys62, Asp32, Asp58, Asn32 and Asn58 all show a slight lag in the presence of zinc (Figure 2.2). The individual alanine substitutions at Cys31, Cys59, Cys62, Asp32, Asp58 and the asparagine substitutions at Asp32 and Asp58 showed 2 fold lower ATPase activity with lead and 2-3 fold lower activity for zinc and cadmium when compared to wtzntA (Tables 2.1, 2.2, 2.3). In vivo, metals are bound to different chelators such as citrates, histidines or thiolates. When the metal is provided as a metal thiolate complex in the assay medium, a 4-8 fold increase in the ATPase activities of ZntA for lead, zinc and cadmium is observed. When metal thiolate complex was provided as the substrate, the thiolates increased the ATPase activity of the mutants with lead, cadmium and zinc. The lead: thiolate complex induced activity of Cys31, Cys59, Cys62, Asp32, Asp58, Asn32, and Asn58 showed a 5-6 fold increase, and the cadmium, zinc thiolate activities for the mutants were similar to that of wtzntA (Table 2.1, 2.2, 2.3). This may be because the thiolates may compensate for the replaced cysteine and aspartate, thus increasing the activities of the mutants.

Previous metal binding studies, both by ICP-MS and by metal titration, show that N1-ZntA has a single high affinity metal binding site; it binds to a single



lead, zinc and cadmium ion. The mutants in N1-ZntA: - C29A, C30A, C35A are able to bind to lead and cadmium with a stoichiometry of 1 with high affinity, this was expected since they showed in vitro activities comparable to wtzntA (Table 2.4). Values of lead and cadmium binding affinity obtained for C29A, C30A and C35A were similar to those obtained for N1-ZntA (Table 2.5). Thus, C29, C30 and C35 are not involved in binding lead or cadmium. However the mutants at C31, D32, D58, C59 and C62 were unable to bind lead and cadmium, suggesting that these residues played a role in binding these two metal ions. Surprisingly none of the N1-ZntA mutants were able to bind zinc. Zinc has a very small ionic radius ( $0.88\text{\AA}$ ), and it is much smaller than lead and cadmium (4). Structural studies of a portion of the N-terminal domain of ZntA (residues 46-118) has been solved; from this it was observed that zinc binds with a tetrahedral coordination to the two cysteine and the aspartate residue of the GMDCXXC motif and has no contribution from the upstream motif (5). Our results suggest that the upstream cysteines together with the Asp32 form a structure that precludes any kind of interaction of the upstream site with the downstream zinc binding site, leaving the DCXXC site free to bind zinc. To probe the local structural environment of zinc, lead and cadmium metal bound to N1-ZntA metal binding site, X-ray absorption spectroscopy was used. The binding of lead, cadmium and zinc at the amino terminal site is different for each of these metal ions. Lead binds with a trigonal geometry to the two cysteines of the CXXC and Cys31 of the upstream motif, this coordination environment is similar to  $\text{Pb}^{2+}$  binding in some proteins in thiol rich environments (Figure 2.5, Table 2.6) (63).

Similar to the solution structure of the  $Zn^{2+}$  bound form of N2-ZntA, zinc bound to N1-ZntA with 4 co-ordinate geometry to two sulfurs (Cys59 and Cys62) and two oxygens; one of the oxygens is from the Asp58 and the other may be from water or the upstream Asp32 (Figure 2.6, Table 2.6)(7).

In CadA, a  $Cd^{2+}$  ATPase from *Listeria monocytogenes*,  $Cd^{2+}$  is bound with a tetrahedral geometry at the N-terminus by two Cys and two oxygen atoms of a conserved acidic residue located at a distance (60). Sequence alignments of the N-termini of CadA, ZntA and CopA like proteins have shown that all these proteins have a conserved CXXC motif. CadA like sequences have a conserved acidic residue Glu61 located in loop 5 which is spatially positioned near the CXXC motif, but in the case of ZntA homologues there is a conserved Asp in loop1; solution structure has demonstrated that it is involved in zinc binding. However, in Cu (I)-ATPases this acidic residue is absent. This indicates that the presence of the acidic residue provides an appropriate coordination sphere for divalent metal ions such as zinc and cadmium. In N1-ZntA, since the carboxylate ligand is located adjacent to the metal cysteine ligands, the metal binding site is better fit for zinc which is a smaller ion than cadmium.

Unlike CadA, EXAFS data suggest that cadmium bound to N1-ZntA displays 5 or 6 coordinate geometry. Structural studies on CadA have also shown that it forms a homodimer containing one cadmium atom per monomer. In the case of N1-ZntA also, Cd-Cd interaction was observed. It is possible that the two cadmium atoms share two thiolate ligands; additionally they may bind to another S atom and 3 oxygen atoms (Figure 2.9, Table 2.6).

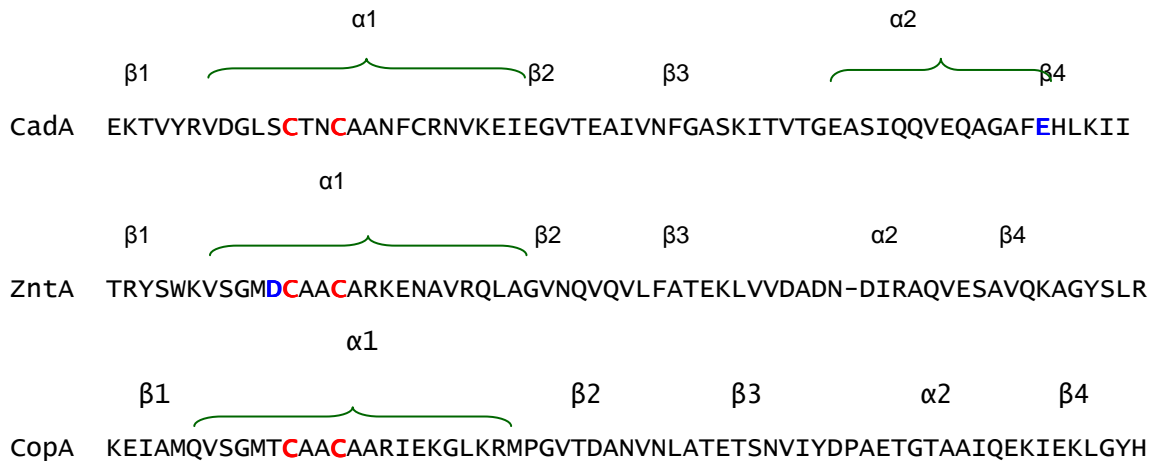


**Figure 2.10** Sequence alignments of the N-terminal domain of P<sub>IB</sub> ATPases.

N1-ZntA binds to cobalt and copper in addition to lead, cadmium and zinc. The cobalt and copper structural environment was also examined. Co<sup>2+</sup> binds to 3 sulfurs and a oxygen (Figure 2.8), our metal stoichiometry results have shown that binding of Co<sup>2+</sup> to N1-ZntA is sub stoichiometric, suggesting that one Co<sup>2+</sup> bridges two protein molecules such that it cannot be displaced by other metal ions (56). Co<sup>2+</sup> ATPases lack the N-terminal domain; this may be because the CXXC motif is not ideal for Co<sup>2+</sup> binding and subsequent transfer to the transport site in the membrane.

Studies on the Wilson's disease protein (ATP7B) have shown that not only is the bound copper in the +1 oxidation state, but also Cu<sup>2+</sup> atoms get reduced to Cu<sup>+</sup> upon binding to the domain. Simulations of the copper EXAFS of for N1-ZntA, with three sulfurs and one copper are best fit with a ligand environment of 3.0 Cu-S atoms at 2.26 and one Cu-O at 1.98 Å (Figure 2.7, Table 2.6), suggesting that Cu<sup>+</sup> displays a tetrahedral geometry. The

cysteine-rich motif in N1-ZntA is not ideal for binding  $\text{Cu}^{2+}$ , since it is reduced to  $\text{Cu}^+$ . This may explain why  $\text{Cu}^{2+}$ -ATPases have a histidine rich motif.

Over the past several years studies of many metalloproteins have all pointed towards the fact that metal selectivity is not a result of thermodynamic parameters like binding affinity. Selectivity is achieved through specific coordination geometry which leads to the correct changes in protein conformation. ZntA is a transporter that has to detoxify *E.coli* against three different divalent metal ions of very different sizes. The DCXXC motif is a specialized zinc binding motif. In order to accommodate the much larger  $\text{Pb}^{2+}$  ion, an additional cysteine from the upstream motif has been conserved. Thus the N-terminal domain of ZntA has been evolved to bind both lead and zinc efficiently. Unfortunately, cadmium, which has similar coordination preferences as zinc, but falls in the middle of the other two in ionic radii, is not bound optimally by N1-ZntA. This results in  $\text{Cd}^{2+}$  being the least efficient substrate for ZntA. The transporter compensates for the lower activity with  $\text{Cd}^{2+}$  by producing more of the protein when its regulator, ZntR is induced by  $\text{Cd}^{2+}$  (26). In conclusion, this study on N1-ZntA has shown that Cys31 from the CCCDXXC motif, as well as the GMDCXXC conserved motif play important roles in metal selectivity to two metal ions of highly different sizes.

## 2.6 REFERENCES

1. Kuhlbrandt, W. (2004) Biology, Structure and Mechanism of P-type ATPases, *Nature* 5, 282-294.

2. Arguello, J. M., Eren, E., and Gonzalez-Guerrero, M. (2007) The structure and function of heavy metal transport P1B-ATPases, *Biometals* 20, 233-248.
3. Arguello, J. M. (2003) Identification of ion-selectivity determinants in heavy-metal transport P1B-type ATPases, *J Membr Biol* 195, 93-108.
4. Rosenzweig, A. C. (2002) Metallochaperones: bind and deliver, *Chem Biol* 9, 673-677.
5. Arnesano, F., Banci, L., Bertini, I., Ciofi-Baffoni, S., Molteni, E., Huffman, D. L., and O'Halloran, T. V. (2002) Metallochaperones and metal-transporting ATPases: a comparative analysis of sequences and structures, *Genome Res* 12, 255-271.
6. Banci, L., Bertini, I., Ciofi-Baffoni, S., Huffman, D. L., and O'Halloran, T. V. (2001) Solution structure of the yeast copper transporter domain Ccc2a in the apo and Cu(I)-loaded states, *J Biol Chem* 276, 8415-8426.
7. Banci, L., Bertini, I., Ciofi-Baffoni, S., Finney, L. A., Outten, C. E., and O'Halloran, T. V. (2002) A new zinc-protein coordination site in intracellular metal trafficking: solution structure of the Apo and Zn(II) forms of ZntA(46-118), *J Mol Biol* 323, 883-897.
8. Banci, L., Bertini, I., Ciofi-Baffoni, S., Su, X. C., Miras, R., Bal, N., Mintz, E., Catty, P., Shokes, J. E., and Scott, R. A. (2006) Structural basis for metal binding specificity: the N-terminal cadmium binding domain of the P1-type ATPase CadA, *J Mol Biol* 356, 638-650.

9. Liu, J., Stemmler, A. J., Fatima, J., and Mitra, B. (2005) Metal-binding characteristics of the amino-terminal domain of ZntA: binding of lead is different compared to cadmium and zinc, *Biochemistry* 44, 5159-5167.
10. Mitra, B., and Sharma, R. (2001) The cysteine-rich amino-terminal domain of ZntA, a Pb(II)/Zn(II)/Cd(II)-translocating ATPase from Escherichia coli, is not essential for its function, *Biochemistry* 40, 7694-7699.
11. Sharma, R., Rensing, C., Rosen, B. P., and Mitra, B. (2000) The ATP hydrolytic activity of purified ZntA, a Pb(II)/Cd(II)/Zn(II)-translocating ATPase from Escherichia coli, *J Biol Chem* 275, 3873-3878.
12. Poole, R. K., Williams, H. D., Downie, J. A., and Gibson, F. (1989) Mutations affecting the cytochrome d-containing oxidase complex of Escherichia coli K12: identification and mapping of a fourth locus, *cydD*, *J Gen Microbiol* 135, 1865-1874.
13. Weng, T. C., Waldo, G. S., and Penner-Hahn, J. E. (2005) A method for normalization of X-ray absorption spectra, *Journal of Synchrotron Radiation* 12, 506-510.
14. DiDonato, M., Hsu, H. F., Narindrasorasak, S., Que, L., Jr., and Sarkar, B. (2000) Copper-induced conformational changes in the N-terminal domain of the Wilson disease copper-transporting ATPase, *Biochemistry* 39, 1890-1896.
15. Ralle, M., Lutsenko, S., and Blackburn, N. J. (2004) Copper transfer to the N-terminal domain of the Wilson disease protein (ATP7B): X-ray absorption spectroscopy of reconstituted and chaperone-loaded metal

- binding domains and their interaction with exogenous ligands, *J Inorg Biochem* 98, 765-774.
16. DiDonato, M., Narindrasorasak, S., Forbes, J. R., Cox, D. W., and Sarkar, B. (1997) Expression, purification, and metal binding properties of the N-terminal domain from the wilson disease putative copper-transporting ATPase (ATP7B), *J Biol Chem* 272, 33279-33282.
  17. Arnesano, F., Banci, L., Bertini, I., Huffman, D. L., and O'Halloran, T. V. (2001) Solution structure of the Cu(I) and apo forms of the yeast metallochaperone, Atx1, *Biochemistry* 40, 1528-1539.
  18. Frausto da Silva, J. J. R., and Williams, R.J.P. (2001) *The Biological Chemistry of Elements*, Oxford University Press.
  19. Liu, J., Dutta, S. J., Stemmler, A. J., and Mitra, B. (2006) Metal-binding affinity of the transmembrane site in ZntA: implications for metal selectivity, *Biochemistry* 45, 763-772.
  20. Eide, D. J. (2006) Zinc transporters and the cellular trafficking of zinc, *Biochim Biophys Acta* 1763, 711-722.

## CHAPTER 3

**THE N-TERMINAL DOMAIN OF ZNTA: IT'S ROLE AS AN ATTACHED METAL CHAPERONE TO THE TRANSPORTER**

Evidence is presented in this chapter that the role of the N-terminal domain of ZntA is to act as a metal chaperone to the core transporter domain.

**3.1 Introduction**

Inside the cell, several regulatory proteins are in place to control the intracellular concentration of essential metal ions and as well as toxic metal ions. An example is metallothionein, which is a metal sequestering protein. It binds to copper and zinc, serving as a reservoir for these metal ions, and additionally it also binds to cadmium and helps in the detoxification of this ion (1). In addition to the metal sequestering proteins, we also have metallochaperones, which bind to metal ions and transfer them to target proteins. Copper chaperones (Atx1, CopZ, CCS) (2) are the best studied ones; some other examples of chaperone proteins are UreE which is a nickel chaperone that delivers  $\text{Ni}^{2+}$  to urease (14), frataxin and human poly(rc) binding protein 1(PCBP1) are iron chaperones that deliver iron to iron sulfur clusters and ferritin (4). But, so far no metallochaperone proteins are known for zinc. Therefore, how do zinc ions exist in organisms? It is likely that zinc ions are chelated to small molecule chaperones – such as cysteines, glutathione, citrate, inside the cell, as well as stored in organelles or bound to storage proteins such as metallothionein.

Zinc is an essential transition metal required for many biological reactions, but at the same time any increase or decrease in the cellular zinc concentration can have adverse effects. ZntA is a member of the  $\text{P}_{1\text{B}2}$  ATPase family which is



one of the components involved in zinc homeostasis in *E.coli* (5). ZntA consists of 8 transmembrane helices and a hydrophilic metal-binding N-terminal region.

For all P-type ATPases, binding of metal ions at the transmembrane region is a crucial step in the reaction mechanism. How does the transmembrane region get the metal ion? In the case of  $\text{Cu}^+$ -ATPases, the metal ion is acquired directly from the cytoplasmic pool by several copper chaperones that deliver the metal specifically to the  $\text{Cu}^+$  transporters (6). This metal delivery has been extensively studied in  $\text{Cu}^+$ -ATPases.

ZntA has two metal binding sites, one in the N-terminal domain and the other in the membrane domain (7). The N-terminal domain is about ~110 residues long and it has a characteristic CXXC metal binding sequence which is conserved in many  $\text{P}_{\text{IB}}$  ATPases (CopA, CopB, CadA),  $\text{Cu}^+$  chaperones like Atox1, Atx1 and CopZ, metallothioneins, and MerA which is a mercury binding protein (8, 66). Studies in some of the bacterial  $\text{Cu}^+$  transporters have shown that the N-terminal metal binding domain binds to  $\text{Cu}^+$  with high affinity; the deletion of this domain does not prevent the activation of the copper transporter but it does reduce the activity of the transporter (10, 11). Recently it was shown that *Archaeoglobus fulgidus*  $\text{Cu}^+$  chaperone CopZ interacted and delivered  $\text{Cu}^+$  to CopA (64). Another enzyme, mercuric ion reductase (MerA), which is involved in  $\text{Hg}^{2+}$  acquisition and reduction in the cytoplasm of bacterial cells, also has the characteristic CXXC sequence (66). Early studies indicated that the presence of NmerA is dispensable to the cells; however it was later prove that the N-terminal domain of NmerA binds to  $\text{Hg}^{2+}$  ion and delivers it to the catalytic domain of

MerA at kinetically efficient rates (66). Studies in our lab have shown that a mutant lacking the N-terminal domain had 2-3 fold lower activity than the full length protein, suggesting that the presence of the N-terminus increases the catalytic activity.

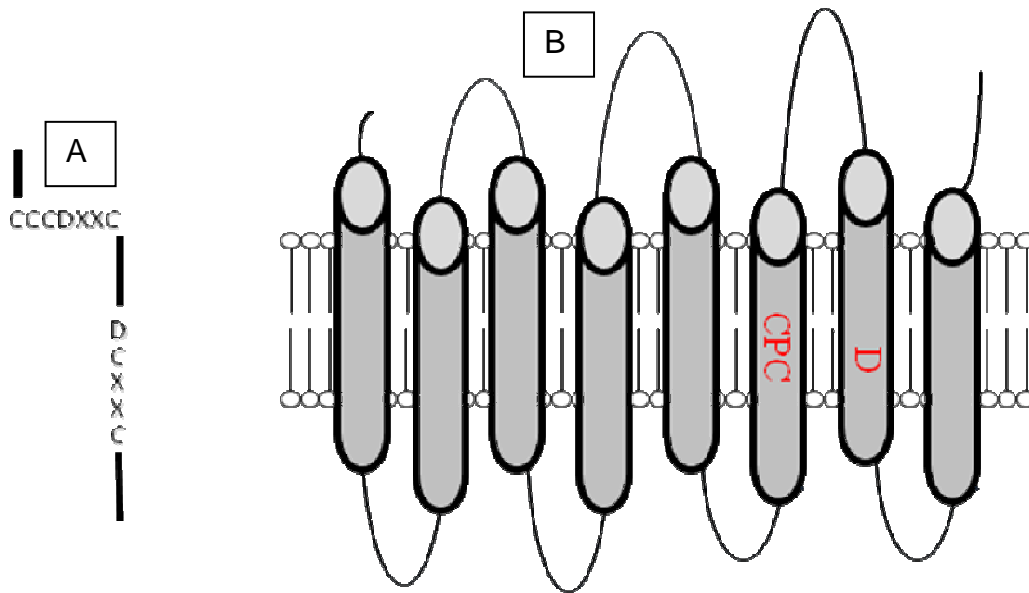


**Figure 3.1.** The two metal binding sites in ZntA, one in N-terminal fragment(A) and the second site in the membrane domain(B).

Both the metal binding domains bind to lead, zinc and cadmium with a stoichiometry of 1; the binding affinity for the above mentioned metal ions at the two sites are similar ( $Pb^{2+} \sim 10^9 M^{-1}$ ,  $Zn^{2+}$  and  $Cd^{2+} \sim 10^8 M^{-1}$ ) (56, 63). These results point toward the fact that metal ion exchange between the two sites is feasible. Since no protein chaperones have been identified for zinc in *E.coli*, we wondered if the N-terminal domain acts to acquire zinc ions efficiently from small molecule chelators in the cytosol and then deliver it to the transmembrane metal-binding site. In the present work, our goal was to investigate the function of the

N-terminal domain of ZntA (N1-ZntA) as an attached metal chaperone to the transporter. Our theory is that the N-terminal metal binding domain being solvent exposed, binds to metal ions more efficiently than the membrane site and then directly delivers the metal to the transmembrane site. To examine this theory, the activity of  $\Delta N$  and ZntA using metal bound N1-ZntA as the substrate was measured. In the presence of metal bound N1-ZntA everted membrane vesicles of  $\Delta N$ -ZntA and ZntA displayed ATP dependent lead, zinc, cadmium accumulation. Double cysteine mutants in a truncated construct of ZntA ( $\Delta 46$ -ZntA) labeled with pyrene maleimide displayed excimer formation, indicating that the two metal binding regions are located in close proximity. The interaction between N1-ZntA and  $\Delta N$  was shown by a fluorescence resonance energy transfer (FRET) experiment where the energy transfer between pyrene maleimide labeled  $\Delta N$ -ZntA and coumarin maleimide labeled N1-ZntA was observed. These studies demonstrate that the metal-binding site in N1-ZntA is spatially close to the metal-binding site in the transmembrane region, and it is feasible for the two sites to exchange metal ions. Thus, we believe that N1-ZntA performs the role of an attached metal chaperone that binds to metal ions from small molecule chelators in the cytosol and comes in close proximity of the membrane domain to facilitate direct metal delivery to the transmembrane site.

### 3.2 Materials

Plasmid pBAD/mycHis-C and *E.coli* strain LMG194 were obtained from Invitrogen; plasmid pET16B was obtained from Novagen. Chemicals for the ATPase activity assay and standard metal solutions were purchased from

Sigma. The fluorophores pyrene maleimide, dibromobimane, and coumarine maleimide were purchased from Molecular Probes. Metal standards used for inductively coupled plasma mass spectrometry (ICP-MS) were from VWR.

### 3.3 Methods

#### 3.3.1 Construction of ZntA and $\Delta$ N-ZntA with a carboxyl – terminal strep tag

ZntA and  $\Delta$ N-ZntA were cloned into the expression vector pBAD/Myc-HisC by polymerase chain reaction (PCR). A Nco1 site was generated at the initiation codon, and an EcoR1 site was created downstream of the termination site using the following oligonucleotides, 5'- ATA AGA TTA GCG GAT CCT-3' and 5'- GCG GAA TTC TTA TTT TTC GAA CTG CGG GTG GCT CCA TCT CCT GCG CAA C-3'. The PCR product and the vector were digested with Nco1 and EcoR1, after which the amplified DNA fragment and the vector were ligated together to generate ZntA. The gene for  $\Delta$ N-ZntA was created with residues 2-106 being deleted by PCR, using the oligonucleotide, 5'- CGT GCC ATG GCA GGC TAT TCC CTG CGC -3' and the same reverse primer used for making the ZntA-strep. The resulting PCR product and the vector, following digestion with Nco1 and EcoR1, were ligated together to create p $\Delta$ N-ZntA. The sequence of both ZntA and  $\Delta$ N-ZntA was confirmed using DNA sequencing analysis; both the genes were in frame with the strep tag at the carboxyl terminus.

#### 3.3.2 Construction N1-ZntA with carboxyl - terminal strep tag

N1-ZntA(1-111 amino acids) was created by PCR using the plasmid pZntA as template and the oligonucleotides 5'-CTA CTG TTT CTC CAT ACC C 3' as forward primer and 5' GCG CTC GAG TTA TTT TTC GAA CTG CGG GTG

GCT CCA CAG GGA ATA GCC TGC 3' as the reverse primer. The amplified PCR product was cloned into pET16b using Nco1 and Xho1 sites; this was then transformed into *E.coli* strains TG1 and BI21.

### **3.3.3 Construction of Co-expression vector containing both $\Delta$ N-ZntA (membrane domain) and N1-ZntA (N-terminal domain) in pBADmycHisP**

N1-ZntA and  $\Delta$ N-ZntA were cloned into pBADmycP (commercially available pBADmycHisC modified with a built in Precision Protease cleavage site to enable the His tag to be cleaved off) by polymerase chain reaction. The forward and reverse primers used for  $\Delta$ N-ZntA were 5'- GCG TGC CAT GGC AGG CTA TTC 3' and 5' GAT CTC GAG TCA TCT CCT GCG CAA CAA 3' respectively. Then following digestion with Nco1 and Xho1 the PCR product and pBADmycP were ligated and cloned into *E.coli* strain TG1. N1-ZntA polymerase chain reaction was set up using 5' TAA GAA TTC AGG AGG AAT TAA CCA TGG CG 3' as the forward primer and 5' CCG AAG CTT TCA TTT TTG CAG CGC AGA 3' as the reverse primer. The PCR product and pBADmycP were subjected to double digestion with EcoR1 and HindIII; the fragments were then ligated and transformed to *E.coli* strain TG1. Both pBAD-N and pBAD- $\Delta$ N were digested with EcoR1 and HindIII, the small fragment from pBAD-N was ligated to the large fragment of pBAD- $\Delta$ N digest and then cloned into *E.coli* strains TG1 and deletion LMG194 (zntA::cat). The sequence was confirmed by DNA sequencing analysis; both N1-ZntA and  $\Delta$ N-ZntA were in frame.

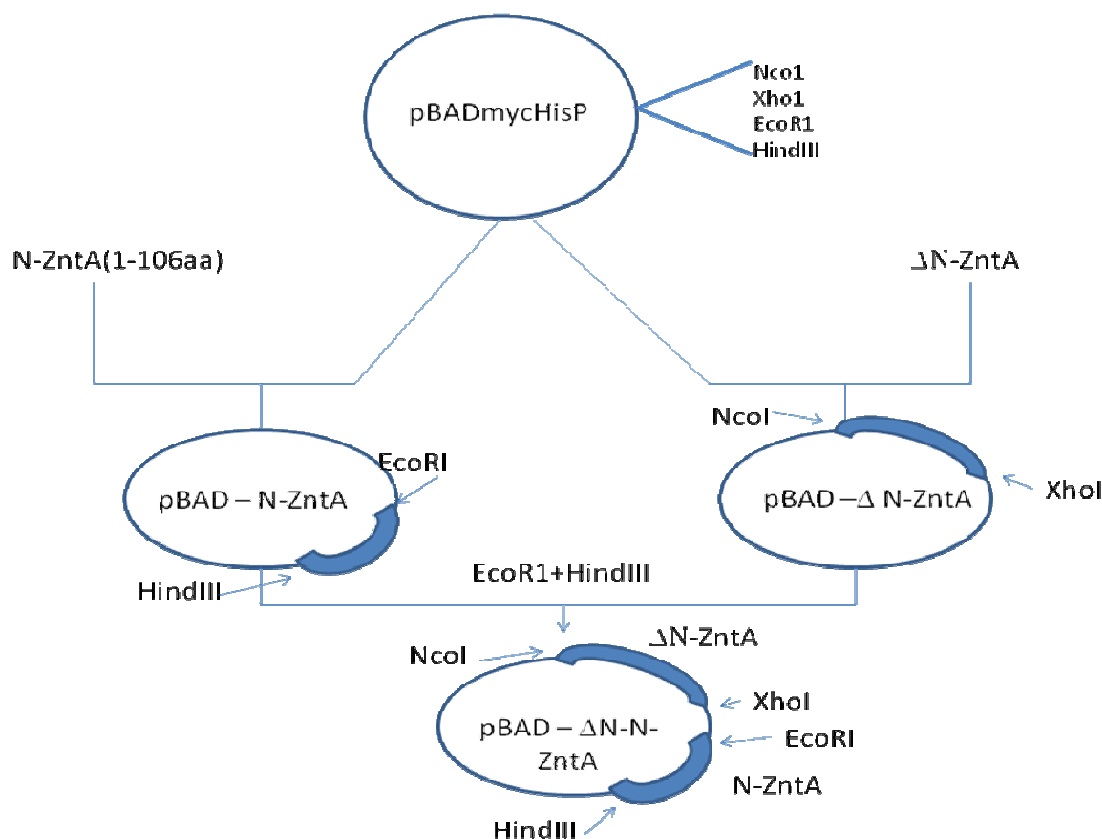


**Figure 3.2.** Scheme for construction of Co-expression vector.

### 3.3.4 Construction of double and single cysteine mutants in $\Delta 46$ -ZntA

$\Delta 46$ -ZntA was chosen instead of ZntA since this fragment of ZntA contained cysteine residues from the two metal binding sites and the upstream cysteine 4 residues in the first 45-residue fragment were absent. Thus,  $\Delta 46$ -ZntA only has five remaining cysteines in total, C59 and C62 from the N-terminal CXXC motif, C392 and C394 from the transmembrane metal binding site, and the non-conserved C518. The main purpose of creating these mutations was to generate proteins with two Cys residues, one in each of the 2 metal binding sites. C59A/ZntA, C62A/ZntA, C392A/C518A/ZntA and C394A/C518A/ZntA plasmids were transformed into DAM methylase<sup>+</sup> strains. Bcl1 digestion of DNA

is inhibited by the *dam* gene product of *E.coli*, which methylates the 6N position of adenine within the sequence GATC. Therefore Bcl1 digestion of DNA isolated from *E.coli dam* cells is inhibited in methylated TG\*ATCA and DAM methylase<sup>□</sup> strain was used. The plasmids were digested with Bcl1 and EcoR1, the small fragment from C59A/ZntA and C62A/ZntA were ligated with the large fragment from C392A/C518/ZntA and C394A/C518A and transformed into *E.coli* strain TG1. The sequences were verified by DNA sequencing to check for presence of triple mutations in ZntA. The plasmids containing the triple mutants were amplified by PCR using forward primer 5' TCT GAA CAT ATG TCC GGC ACC CGC 3' and reverse primer 5' GAC GGC GCT ATT CAG ATC CTC 3', this lead to the deletion of first 46 residues of ZntA. Following digestion, the PCR product and pBADmycHisC were ligated and cloned into *E.coli* strain TG1 and deletion LMG194 (*zntA::cat*). The  $\Delta$ 46-ZntA single mutants were created using Quick change site directed mutagenesis kit from Stratagene. For  $\Delta$ 46-C59A/C392A/C394A/C518A/ZntA the forward and reverse primers used were 5' CTG ATT GGC GCC CCG GCT GCG TTA GTG ATA TCA ACG CCT G 3' and 5'-CAG GCG TTG ATA TCA CTA ACG CAG CCG GGG CGC CAA TCA G 3' respectively. The  $\Delta$ 46-C59A/C62A/C392A/C394C/C518A/ZntA was amplified by PCR using 5'- GTC AGC GGC ATG GAC GCC GCG GCC GCT GCG CGC AAG GTA G-3' as the forward primer and 5'-CTA CCT TGC GCG CAG CGG CCG CGG CGT CCA TGC CGC TGA C-3' as the reverse primer. The clones were transformed into *E.coli* strains TG1 and deletion LMG194 (*zntA::cat*). All the genes were in frame with the hexa histidyl tag at the carboxyl terminal end.

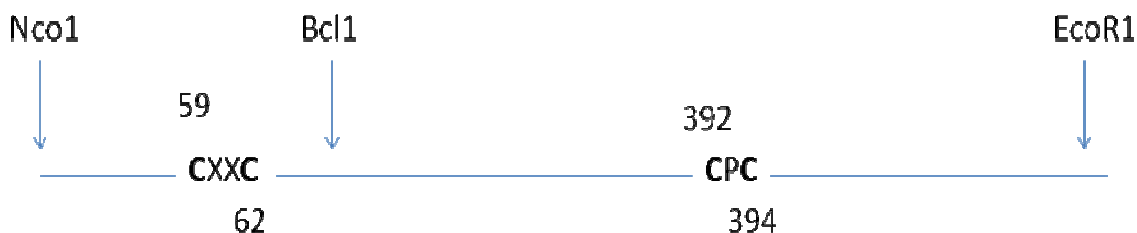


**Figure 3.3.** The location of restriction enzymes and the position of cysteine residues that are mutated.

### 3.3.5 Expression and purification of the N terminal domain of ZntA (N1-ZntA)

BL21 (DE3) pLysS cells, transformed with N1-ZntA were grown at 37° C until the O.D<sub>600</sub> was 1 and then induced with 0.1mM IPTG. Following induction the cells were grown for ~4 hours at 30° C. Harvested cells were resuspended in Buffer A (100 mM Tris, pH 8.0, 150 mM NaCl, 1mM EDTA) and stored at -20° C until further use. The frozen cell suspension was thawed and then disrupted at 20,000 p.s.i. The cell lysate was incubated (~20ml) with DNase I (0.02mg/ml) and 2 mM MgCl<sub>2</sub> and then centrifuged at 8000 rpm for 30 min, after which the supernatant was then centrifuged at 40,000 rpm for 1 h. Following centrifugation the supernatant was loaded onto a 5ml Strep-Tactin column that was pre-equilibrated with 2 column volumes of Buffer A. The flow through was collected and reloaded on the column. After the cell extract completely entered the column, the column was washed 5 times with 1 column volume of Buffer A. The protein was eluted with Buffer B (Buffer A + 2.5 mM desthiobiotin, which is a reversible binding specific competitor). Fractions were collected and analyzed for



protein. Protein containing fractions were pooled and concentrated using 3K Amicon cut off concentrators.

### 3.3.6 Expression and Purification of ZntA and $\Delta$ N- ZntA

Both ZntA and  $\Delta$ N-ZntA were expressed by growing the ZntA and  $\Delta$ N-ZntA transformed LMG194 (*zntA::cat*) cells at 37° C in Luria-Bertani medium supplemented with 100 $\mu$ g/ml ampicillin to mid-log phase and then induced with 0.02% arabinose. Cells were harvested 4 h after induction, washed with ice-cold buffer containing 25 mM Tris, pH 7 and 100 mM KCl, and stored at -20 °C until further use (50). The entire purification procedure was performed at 4°C. The frozen cells were thawed and resuspended in buffer A (25 mM Tris, pH 7.0 with 100 mM sucrose, 1 mM EDTA and 1 mM phenylmethylsulfonyl fluoride (PMSF)) at 0.2 g/ml and disrupted at 20,000 p.s.i. The cell lysate was incubated with DNase I (0.02mg/ml) and 2 mM MgCl<sub>2</sub> for 30 min. The cell lysate was then centrifuged at 8000 rpm for 30 min. The supernatant was centrifuged at 40,000 rpm for 1 h to separate the membrane from the soluble cellular fraction. The pellet from the ultracentrifugation was resuspended in a low ionic strength buffer containing 2 mM Tris pH 7.0 with 100 mM sucrose and 1 mM EDTA, 1 mM PMSF. This removed the F1-ATPase from the membranes, which reduced the background ATPase activity that was not stimulated by soft metal ions. After the low ionic strength wash, the membranes were ultracentrifuged once again. The membranes were stored at 4°C overnight. The membranes were then resuspended into Buffer C ( 25 mM Tris, pH 7.0, 100 mM sucrose, 500 mM NaCl) until O.D<sub>280</sub> = 1. Triton-X-100 was added dropwise to a final concentration

of 1% and the suspension was stirred at 4°C for 1 h. The suspension was then centrifuged at 40,000 rpm for 1 h to separate the insoluble membranes. The Triton-X-100 solubilized fraction was then loaded on a strep-tactin column that was pre-equilibrated with buffer D (buffer C + 0.2% Triton-X-100). The resin was subsequently washed with 25 ml of Buffer D. The protein was finally eluted with 20 ml of buffer D containing 2.5 mM desthiobiotin. 1 ml fractions were collected and analyzed for protein. Protein containing fractions were pooled and loaded on a 40 ml Sephadex G-25 column pre-equilibrated with Buffer E (25 mM Tris pH 7.0, 100 mM sucrose, 50 mM KCl, 0.2% Triton-X-100) to remove the desthiobiotin. 1 ml fractions were collected and assayed for protein. The protein containing fractions were pooled and concentrated using Centricon concentrators. The concentrated protein was then stored at -70°C using glycerol as the cryoprotectant.

### **3.3.7 Protein concentration determination**

Protein concentrations were determined using the bichinchonic acid reagent with bovine serum albumin as standard.

### **3.3.8 Metal bound sample preparation for ATPase activity measurements and transport assays**

In assays where the N1-ZntA metal complex was used as the metal source, N1-ZntA protein was reduced with 1mM TCEP for 1 hour at 4 ° C. The reduced protein was then incubated with metal salts for 1 hour at 4° C; the excess metal was removed by passing through a Sephadex G– 25 column (56).

### 3.3.9 Measurement of Metal Concentration by ICP-MS

The metal content was measured by a PE Sciex Elan 9000 ICP-MS (inductively coupled mass spectrometry) with a cross-flow nebulizer and Scott type spray chamber. The RF power was 1000 W, and the argon flow was optimized at 0.92 L/min. The optimum lens voltage was centered on rhodium sensitivity. The data were collected as counts per second. Lead, Cadmium and Zinc standards were obtained from VWR. Standard calibration curves were determined from samples diluted from stock solutions of 1000 ppm standard solutions. The samples and standards solutions were all diluted in 2% HNO<sub>3</sub>.

### 3.3.10 ATPase activity assay

The metal dependant ATPase activity of the purified proteins (ZntA,  $\Delta$ N-ZntA) was assayed by the pyruvate kinase and lactate dehydrogenase coupled spectroscopic assay (50). In this assay, the ATP regeneration from ADP is coupled to the oxidation of NADH. The reaction was monitored at 340 nm for 20 min. Prior to the assay the purified ZntA/ $\Delta$ N-ZntA was incubated with 2 mM dithiothrethiol (DTT) at 4°C for 1 h. The assay buffer was made up of 0.1 M acetic acid, 0.05 M Bis Tris, and 0.05 M triethanolamine, pH 7.0. The reaction mixture also contained 0.1% purified asolectin, 0.1% Triton-X-100, 10% glycerol, 5.0 mM each ATP and Mg(II), 0.25 mM NADH, 1.25 mM phosphoenolpyruvate, 14 units of pyruvate kinase, and 20 units of lactate dehydrogenase, with or without lead, cadmium and zinc ions. To check the metal transfer from the N-terminal region of ZntA (N1-ZntA) to the membrane region of ZntA, metal bound

N1-ZntA was used as a substrate for measuring the ATPase activity. Data were fitted to Michaelis-Menten equation.

$$v = V_{\max} \times S / (K_M + S)$$

where,  $V_{\max}$  equals the maximum velocity,  $S$  is the concentration of metal/N1-ZntA bound metal,  $K_M$  is the Michaelis constant for the substrate.

### 3.3.11 Transport Assays in everted membrane vesicles

ZntA and  $\Delta N$  cells were resuspended in Buffer A (25mM Tris, pH 7.0 with 100mM sucrose, 1 mM EDTA and 1mM phenylmethylsulfonyl fluoride (PMSF)) at 0.2 g/ml and disrupted at 20,000 p.s.i. The cell lysate was incubated with DNase I (0.02 mg/ml) and 2 mM  $MgCl_2$  for 30 mins. Unbroken cells were removed by centrifugation at 8000 x g for 30 min. Membrane vesicles were pelleted by centrifugation at 40,000 x g for 60 min, washed and then resuspended in buffer containing 25 mM Bis-Tris pH 7.0, 250 mM sucrose and 500 mM NaCl. The resuspended pellets were frozen in aliquots and stored at  $-70^\circ C$  with glycerol as the cryoprotectant. The transport assays were performed at room temperature. The assay mixture contained 900  $\mu l$  of 25 mM Bis-Tris, pH 7.0, 200 mM KCl, 250 mM sucrose, 1–2 mg of membrane protein, 5 mM ATP or ADP, 10  $\mu M$  lead/cadmium/zinc salts or metal bound N1-ZntA. The reaction was initiated by addition of 5 mM  $MgSO_4$ . At intervals, 100  $\mu l$  sample was withdrawn, filtered through pre-washed and blocked (blocked by washing with 1 ml of buffer containing 25 mM Bis-Tris, pH 7.0, 200 mM KCl, 250 mM sucrose and 10 mM  $MgSO_4$ ) 0.22  $\mu m$  nitrocellulose filters. After the sample was filtered, the filters were washed with 5 ml of the above buffer and then dried. In order to measure

the metal content, the filters were completely digested in 300  $\mu\text{l}$  of 70% concentrated  $\text{HNO}_3$  at  $70^\circ\text{C}$  for 20 min. The samples were then diluted with HPLC grade water, and the total metal content was determined by ICP-MS.

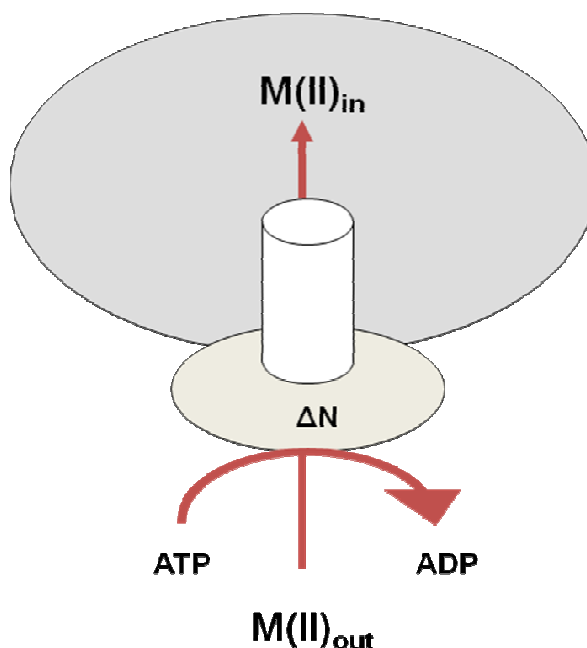


**Figure 3.4.** Transport Assay in everted membrane vesicles.

### 3.3.12 Fluorescence Studies to monitor intermolecular crosslinking

Energy transfer experiments were performed using N1-ZntA labeled with coumarin maleimide and  $\Delta\text{N}$ -ZntA labeled with pyrene maleimide. The proteins were reduced with 1 mM TCEP for 1 hour at  $4^\circ\text{C}$  and then incubated with  $\sim 2$  fold excess fluorescent probes. The labeled proteins were then passed through Sephadex G-25 columns to remove the excess fluorophore. Labeling stoichiometries for each probe were calculated using the extinction coefficient of  $40,000 \text{ cm}^{-1} \text{ M}^{-1}$  for pyrene maleimide at 338 nm, and  $33,000 \text{ cm}^{-1} \text{ M}^{-1}$  for coumarin maleimide at 384 nm (73). The fluorescence measurements were performed using a Photon Technology International spectrofluorimeter. Energy

transfer between  $\Delta$ N-ZntA bound pyrene maleimide and N1-ZntA bound coumarin maleimide was followed in this experiment using the pyrene maleimide excitation wavelength of 340 nm and monitoring its emission in the absence and presence of labeled N1-ZntA.

### 3.3.13 Fluorescence studies to monitor intramolecular crosslinking

Single and double cysteine mutants that were purified with 0.05 mM dodecyl maltoside (DDM) instead of Triton-X-100 were reduced with 1mM TCEP and then incubated with 100-fold excess pyrene maleimide at room temperature. The excess pyrene was removed by passage through gel filtration Sephadex G-25 columns pre-equilibrated with buffer containing 25 mM Tris, pH 7.0, 100 mM sucrose, 50 mM KCl and 0.05 mM dodecyl maltoside (DDM). Fractions were checked for protein by performing crude bichinchonic acid assays. The concentration of protein bound pyrene maleimide in the pooled fractions was measured using an extinction coefficient of  $40,000 \text{ cm}^{-1} \text{ M}^{-1}$  at 340 nm. Fluorescence measurements were performed using Photon Technology International spectrofluorimeter. The samples were excited at 340 nm, and the emission spectrum recorded in the range 350-600 nm. Pyrene maleimide shows emission peaks at 376 nm and 396 nm (74-75). Pyrene also shows a characteristic excimer emission at  $\sim$ 470 nm when two pyrene molecules are within 4-6 Å of each other. The formation of this excimer was monitored (75).

### 3.3.14 Competition Survival Assay

The *E.coli* strains LMG194 (*zntA::cat*) transformed with pZntA and p $\Delta$ N-ZntA were grown overnight at 37°C in low-phosphate medium with either ampicillin

(100 µg/ml) or chloramphenicol (25 µg/ml). The overnight cultures were mixed in a 1:1 ratio, and diluted 1:100 in fresh low-phosphate medium containing 100 µg ampicillin and 50 µM zinc chloride, and grown at 37°C overnight. Each morning, for 6 consecutive days, the overnight cultures were diluted 1:100 into fresh media and grown. Plasmids were extracted from the mixed culture, and equal amounts of DNA were analyzed by digestion with Nco1 and EcoR1. The digested DNA fragments were run on a 0.7% agarose gel containing 0.5 µg/ml ethidium bromide and observed at 302 nm.

### 3.3.15 Sensitivity to metal salts

The sensitivity of *E.coli* strains LMG194 and LMG194 (zntA::cat) and LMG194 (zntA::cat) transformed with pZntA, pΔN-ZntA, pΔN-N1 to lead, cadmium and zinc was measured. The cells were grown in low phosphate media, pH 7.5. Cells were grown overnight and then diluted 100 fold in the same media in the presence of lead acetate, zinc chloride, and cadmium chloride. Cell growth at 37 °C was monitored at 600 nm over a period of 24 hours.

## 3.4 Results

### 3.4.1 N1-ZntA confers a Competitive Advantage to ZntA

From previous studies in the lab, it was observed that ΔN-ZntA is active in vivo but it grows more slowly compared to ZntA (56). To understand the importance of the N-terminal domain of ZntA in providing a survival advantage to ZntA, a competition survival experiment was performed (76). The *E.coli* strain LMG (zntA::cat), in which the ZntA gene had been deleted were used. These had either a plasmid with ZntA or ΔN-ZntA in the same vector. Equal amounts of

the two types of cells were mixed together and grown in the presence of 50  $\mu$ M zinc in low phosphate medium. Each day the mixed culture was diluted 100 fold, and the amount of  $\Delta$ N-ZntA and ZntA plasmids was analyzed by restriction enzyme digestion with Nco1 and EcoR1. Digestion of both plasmids produced a 4.2 kbp fragment and a 2 kbp fragment for ZntA, and 1.8 kbp fragment for  $\Delta$ N-ZntA. After day 3,  $\Delta$ N-ZntA completely disappeared (Figure 3.5). Thus, the presence of the N-terminal domain in the ZntA gene allowed it to competitively survive compared to a transporter lacking this domain.



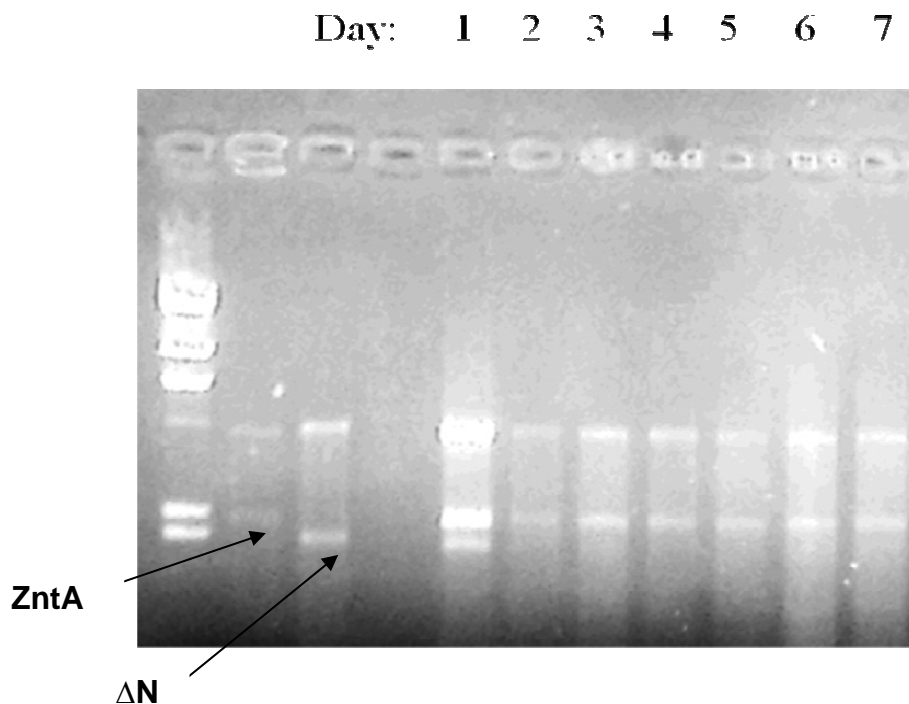


**Figure 3.5.** Molecular competition between ZntA and  $\Delta$ N-ZntA.

Cells of *E.coli* strain LMG194(*zntA::cat*) with either ZntA or  $\Delta$ N-ZntA were grown in mixed culture for 9 days with daily dilutions into fresh ZAB medium in the presence of 50 $\mu$ M Zn. Equal amounts of DNA were separated by electrophoresis on a 0.7% agarose gel. The plasmids on Nco1 and EcoR1 digestion produced a 4.1-kbp fragment of vector DNA, and a 2 kbp fragment of ZntA and 1.8 kbp fragment of  $\Delta$ N. The restriction digestion fragments, of ZntA before growth (Lane 2),  $\Delta$ N (Lane 3), after day 1 (Lane 4), after day2 (lane 5), after day 3 (lane 6), after day 4 (lane 7), after day 5 (lane 8), after day 6 (lane 9), after day 7 (lane 8).

### 3.4.2 The resistance profile of a co-expression vector in the presence of $Pb^{2+}$ , $Cd^{2+}$ , and $Zn^{2+}$

With the observation that N1-ZntA provides a survival advantage to ZntA, we wanted to verify if it also provides a growth advantage when expressed as a separate domain. We constructed a co-expression plasmid which had both  $\Delta$ N-

ZntA and N1-ZntA ( $\Delta N.N1$ ). This was then cloned into an *E.coli* strain from which the entire *zntA* gene was deleted. The time courses of growth of wild type *E.coli* strain, LMG194, the *zntA*-deleted strain, LMG194(*zntA::cat*), and the deleted strain transformed with plasmids containing either a copy of the *wzntA* gene,  $\Delta N$ , or  $\Delta N.N1$  are shown in Figure 3.6. All the strains were able to grow in the presence of  $10\mu\text{M Pb}^{2+}$ ,  $50\mu\text{M Zn}^{2+}$ , and  $5\mu\text{M Cd}^{2+}$ . When compared to the growth of ZntA, both  $\Delta N$ -ZntA and  $\Delta N.N1$  grew slowly. The profile of  $\Delta N.N1$  was identical to that of  $\Delta N$ -ZntA with respect to lead, cadmium and zinc. This may be because the N1-ZntA is not directly attached to  $\Delta N$ -ZntA and therefore it does not provide an additional support to  $\Delta N$ -ZntA for growth.

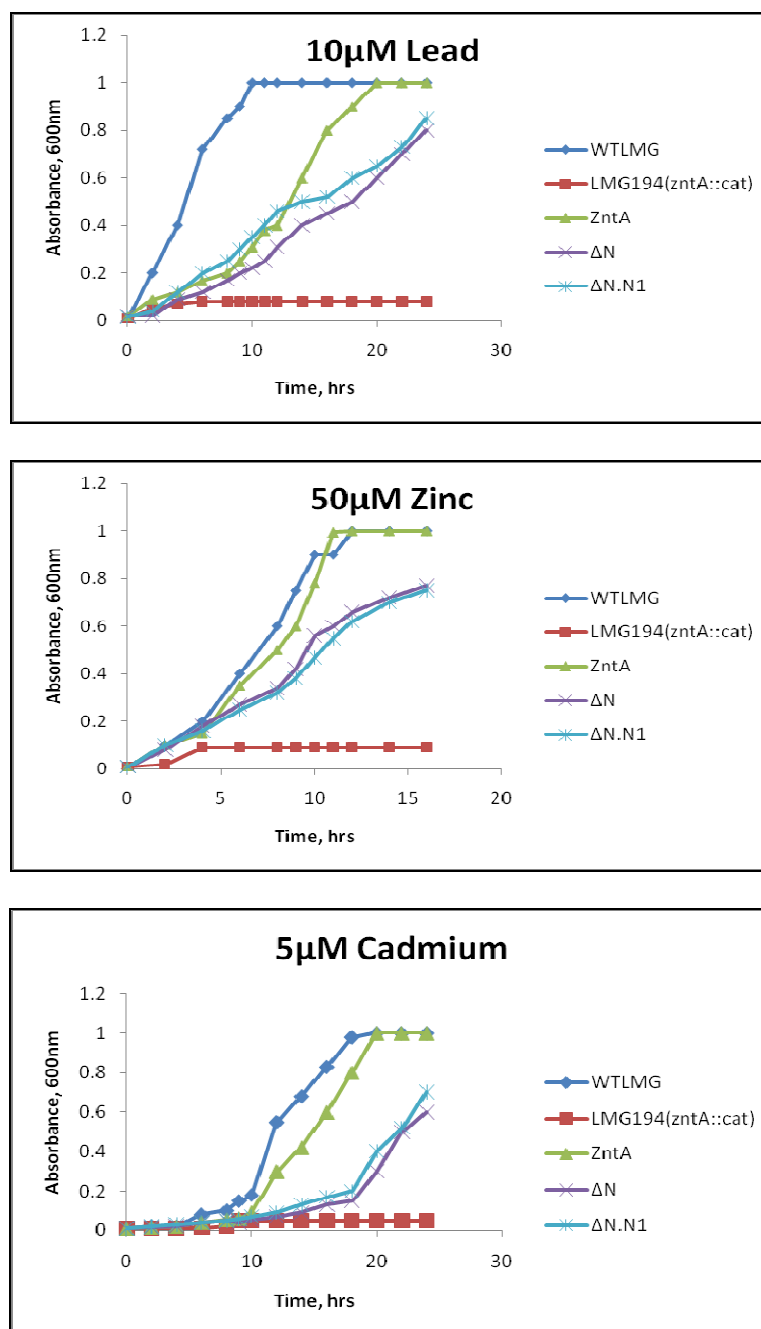


**Figure 3.6.** Resistance to lead, zinc, and cadmium salts by the wild type strains, LMG194 (◆), LMG194 (zntA::cat) (■), and the zntA deleted strain transformed with plasmids ZntA (▲), ΔN-ZntA(x), and ΔN.N1 (\*). The cells were grown in low phosphate medium in the presence of 10 µM lead acetate, 50 µM zinc chloride,

and 5  $\mu\text{M}$  cadmium chloride at 37°C, and the cell growth was monitored at the mentioned time points by measuring the absorbance at 600 nm.

### **3.4.3 ZntA and $\Delta\text{N-ZntA}$ membrane vesicles supplied with N1-ZntA-bound metal as the substrate, can catalyze ATP- dependent transport of lead, zinc and cadmium**

In this experiment we tested the ability of ZntA and  $\Delta\text{N-ZntA}$  membrane vesicles to catalyze ATP dependent metal transport when the metal source was supplied as N1-ZntA bound form. Everted membrane vesicles were prepared from cells of  $\Delta\text{N-ZntA}$  and ZntA. The metal source provided was in the form of metal bound N1-ZntA. In the absence or presence of an energy source (ATP) and metal bound N1-ZntA supplied as the substrate, uptake of zinc/lead/cadmium by the everted membrane vesicles of both ZntA and  $\Delta\text{N-ZntA}$  was observed, only when ATP was present (Figure3.7).

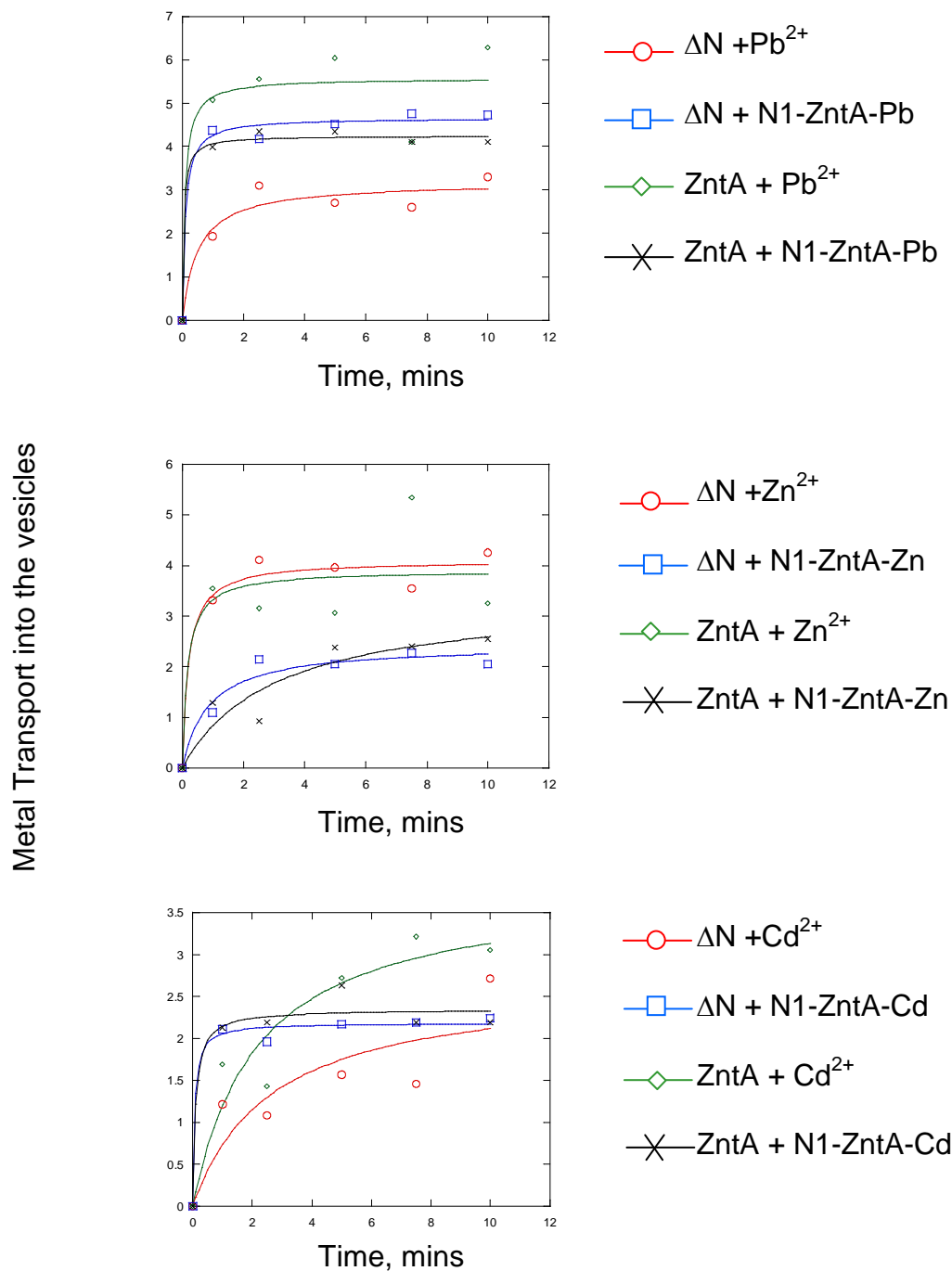


**Figure 3.7.** ATP dependent metal uptake by everted membrane vesicles (Refer to Methods section 3.3.11 for detailed reaction conditions). In the absence of ATP no metal uptake was observed.

### 3.4.4 The transmembrane domain of ZntA and $\Delta$ N-ZntA, can catalyze ATP hydrolysis activity when the substrate is metal bound to the N-terminal domain

Our hypothesis is that the cytosolic N-terminal domain binds to metal and transfers it directly to the transmembrane metal binding site. Lead, zinc, and cadmium stimulate ATP hydrolysis for both ZntA and  $\Delta$ N-ZntA (50). To assess if the metal bound N-terminal domain can deliver metal ion to the catalytic pump and in turn activate the pump, the activity of the transporter was measured using metal bound N1-ZntA as the substrate. As shown in Figure 3.7, metal bound N1-ZntA was a very good substrate for the membrane domain ( $\Delta$ N-ZntA). We wanted to measure and compare the kinetic parameters of ZntA and  $\Delta$ N-ZntA using metal bound N1-ZntA as substrate. Earlier results, comparing the ATPase activity for ZntA and  $\Delta$ N-ZntA showed that the activity of  $\Delta$ N-ZntA was 2-3 fold lower than ZntA (56). Table 3.1 summarizes the kinetic parameters for  $\Delta$ N-ZntA and ZntA for metal stimulated ATPase activity in the presence of 5mM MgCl<sub>2</sub> and ATP at pH 7.0 and 37°C. Interestingly, when metal bound N1-ZntA was used as substrate, the activity of  $\Delta$ N-ZntA was higher than when the substrates were free metal ions in buffer (Table 3.1). Also, the V<sub>max</sub> values were lower for ZntA than for  $\Delta$ N-ZntA, a reversal of what is observed when free metal ions are used in the assay buffer. The lower values may be because ZntA already has an N-terminal domain, and addition of metal bound N1-ZntA as substrate leads to the two metal binding sites (the transmembrane metal binding site and the cytosolic metal binding site) competing for the metal ion.

**Table 3.1.** Kinetic parameters obtained for  $\Delta$ N-ZntA and ZntA for  $Pb^{2+}$ ,  $Cd^{2+}$  and  $Zn^{2+}$  as free species in buffer and in the N1-ZntA bound form.

	$\Delta$ N-ZntA		ZntA	
	$V_{max}$ (nmol.mg <sup>1</sup> .min <sup>-1</sup> ) 1)	app $K_M$ ( $\mu$ M)	$V_{max}$ (nmol.mg <sup>1</sup> .min <sup>-1</sup> )	app $K_M$ ( $\mu$ M)
Pb(II)	320 $\pm$ 6	11.6 $\pm$ 0.8	560 $\pm$ 13	5.6 $\pm$ 0.6
N1-ZntAPb(II)	404 $\pm$ 11	0.8 $\pm$ 0.07	250 $\pm$ 8.3	0.3 $\pm$ 0.04
Cd(II)	66 $\pm$ 3	4.1 $\pm$ 0.6	60 $\pm$ 3	5.5 $\pm$ 1.2
N1-ZntACd(II)	300 $\pm$ 7.5	0.25 $\pm$ 0.022	147 $\pm$ 8.6	0.36 $\pm$ 0.064
Zn(II)	81 $\pm$ 7	9.3 $\pm$ 1.2	250 $\pm$ 13	10.3 $\pm$ 2
N1-ZntAZn(II)	270 $\pm$ 14	0.47 $\pm$ 0.06	166 $\pm$ 7.2	0.3 $\pm$ 0.035

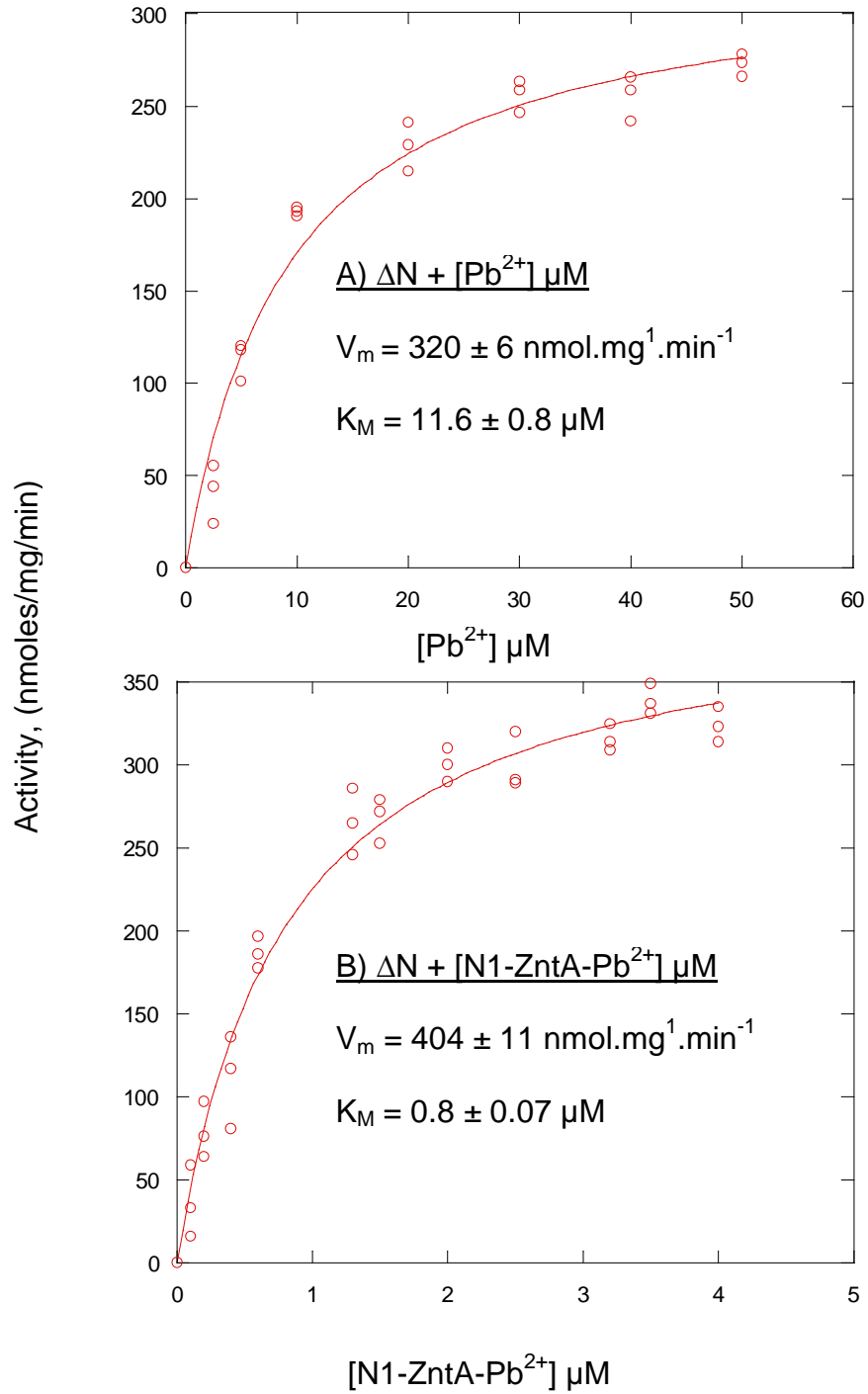


**Figure 3.8.**  $\Delta N$ -ZntA ATPase Activity in the presence of  $Pb^{2+}$  (A) and N1-ZntA bound  $Pb^{2+}$  (B).



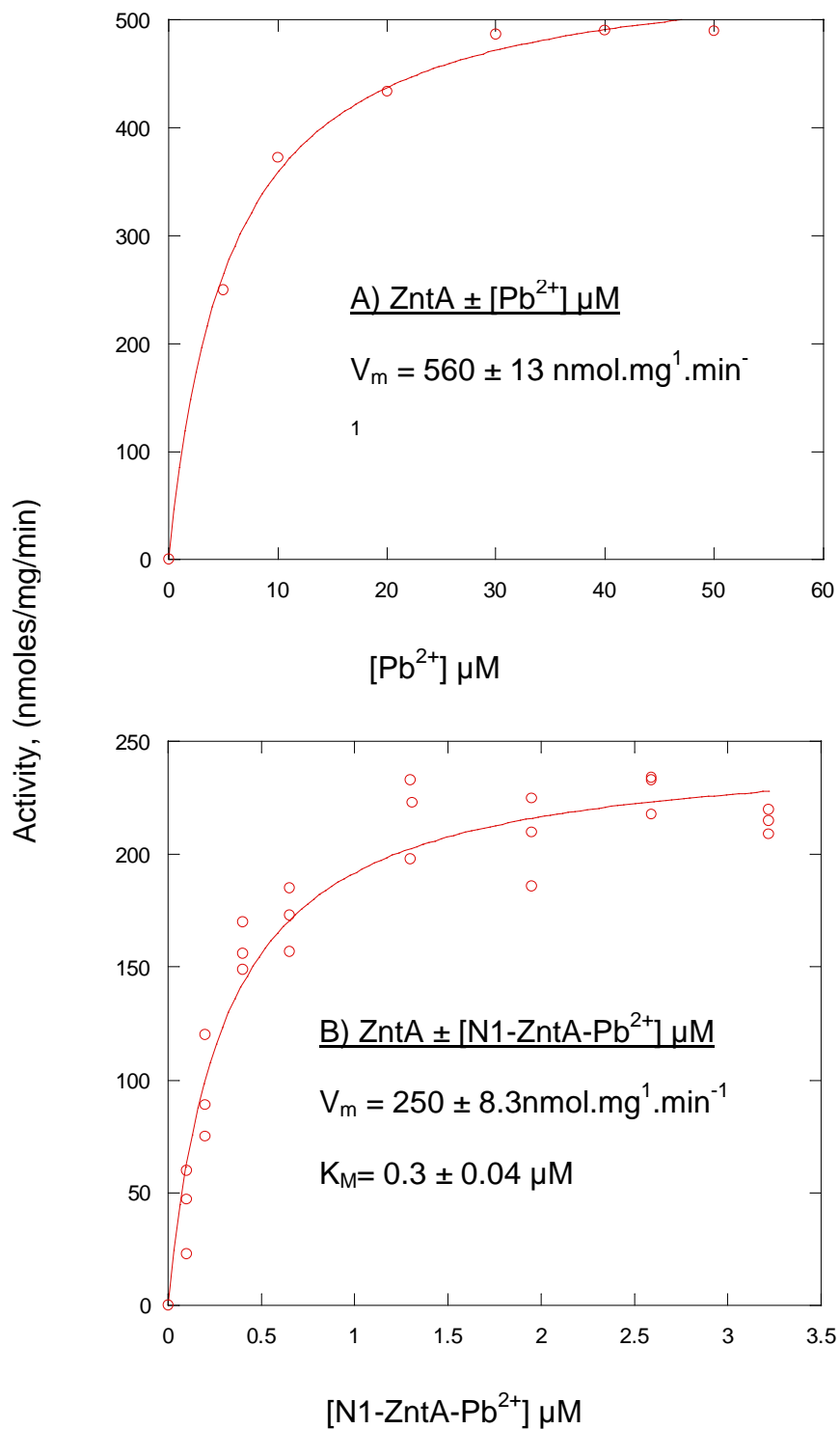
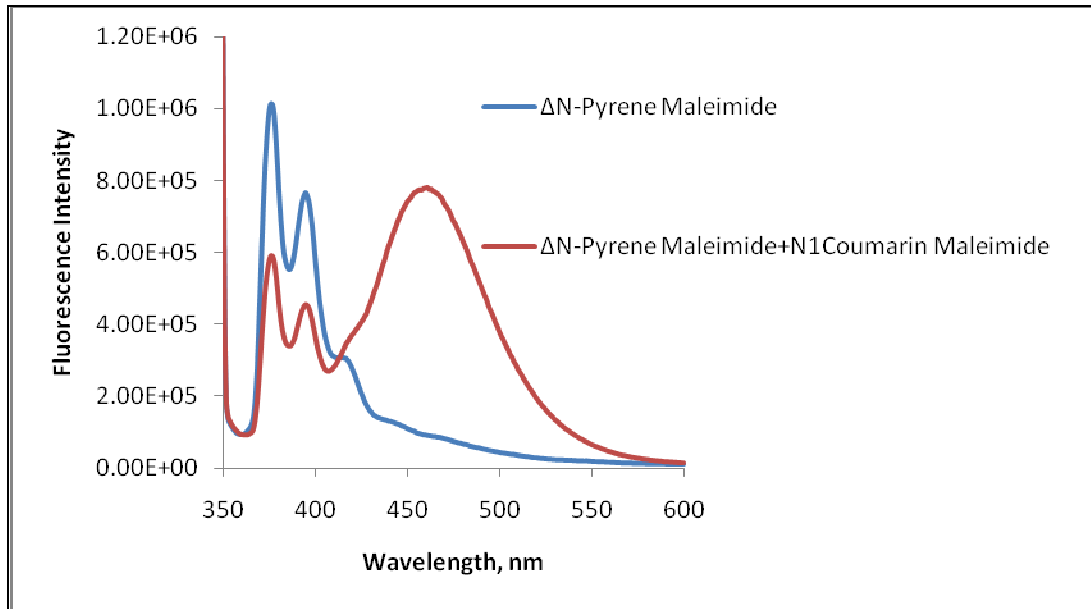


Figure 3.9. ZntA ATPase Activity in the presence of Pb<sup>2+</sup> (A) and N1-ZntA bound Pb<sup>2+</sup>.

### 3.4.5 Interaction of N1-ZntA with $\Delta$ N-ZntA

Whether a direct interaction between the two metal binding sites in N1-ZntA and  $\Delta$ N-ZntA is feasible or not was examined by an energy transfer experiment. Both sites contain cysteine residues. Therefore, the cysteines in N1-ZntA were labeled with coumarin maleimide and that in  $\Delta$ N-ZntA was labeled with pyrene maleimide. Both are cysteine specific reagents and are essentially non-fluorescent until they react with thiols. Coumarin maleimide has an emission maximum at 469 nm when excited at 384 nm (73). The absorption maximum for pyrene is around 340 nm. Its emission maximum is usually a doublet peak at about 376 and 396 nm. When two pyrene molecules are spatially close, they can form an excimer, with a broad emission spectrum centered at about 470 nm. In this experiment, the fluorescence resonance energy transfer between the coumarin maleimide labeled N1-ZntA and pyrene maleimide labeled  $\Delta$ N-ZntA was observed, in which the emission energy from pyrene was transferred to coumarin. The mixture of coumarin maleimide labeled N1-ZntA and pyrene labeled  $\Delta$ N-ZntA was excited at 340 nm (excitation emission peak of pyrene); a characteristic coumarin emission peak at 470 nm was observed (Figure 3.10). Therefore, coumarin could be excited by transfer of emission energy from the pyrene emission spectrum, which overlaps with the coumarin excitation spectrum. This indicates that the two domains, N1-ZntA and  $\Delta$ N-ZntA can come close to each other for this energy transfer to occur.



**Figure 3.10.** Fluorescence resonance energy transfer from Pyrene maleimide labeled  $\Delta$ N-ZntA (peak at 370 and 390 nm) to coumarin maleimide labeled N1-ZntA (peak at ~ 470 nm) using an excitation wavelength of 340 nm.

### 3.4.6 Proximity of the two metal binding domains binding sites

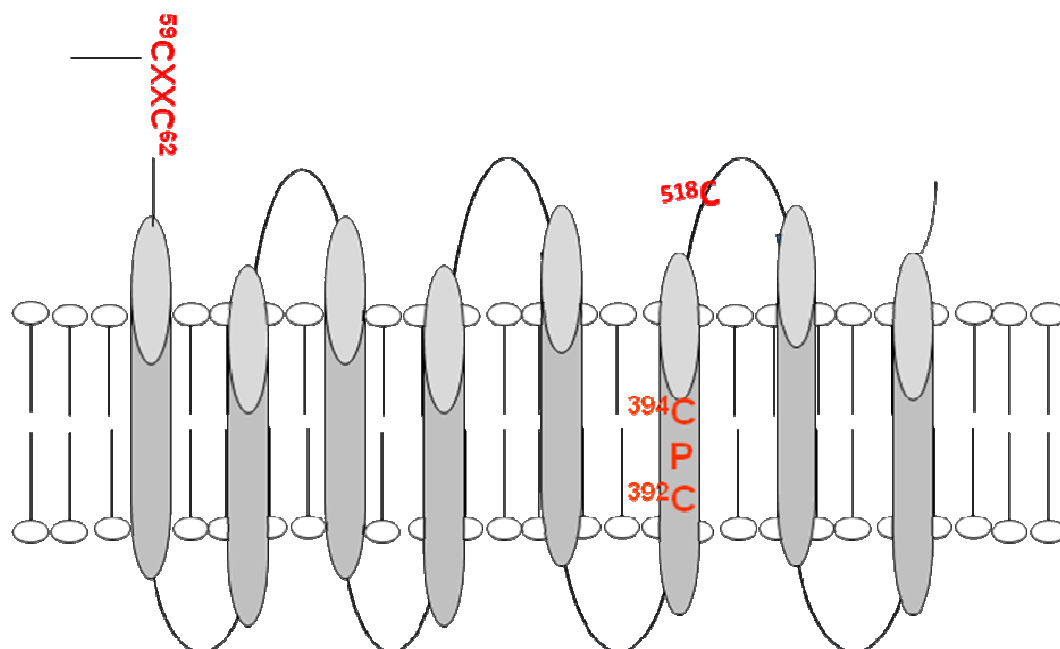


**Figure 3.11.** Model showing cysteine residues in  $\Delta 46$ -ZntA.

As mentioned earlier, ZntA has two metal binding sites; one in the transmembrane region and the other in the cytosolic N-terminal domain. Both the metal binding sites have conserved cysteine residues (CPC and CXXC). Since the results of the ATPase activity assay and transport assay have shown that metal bound to N1-ZntA can be transferred to the membrane site, our hypothesis is that the cysteine residues of the two metal-binding sites come close to each other for metal transfer to occur. To examine the proximity of the cysteine residues in the two domains we used the property of pyrene to form excimer with a characteristic fluorescence emission spectrum. We constructed mutants in a truncated form of ZntA called  $\Delta 46$ -ZntA (the first 46 residues of ZntA were deleted); this construct was used because the two cysteine containing metal

binding sites were intact and the four upstream cysteine residues were absent. This helped in generation of mutants in which either one or two cysteines were present in the entire protein. The double mutants were  $\Delta 46$ -C59A/C62/C392A/C394/ZntA,  $\Delta 46$ -C59A/C62/C392/C394A/ZntA,  $\Delta 46$ -C59/C62A/C392A/C394/ZntA,  $\Delta 46$ -C59/C62A/C392/C394A/ZntA. Single mutants were created for controls; these were  $\Delta 46$ -C59A/C62/C392A/C394A/C518A/ZntA and  $\Delta 46$ -C59A/C62A/C392A/C394/C518A/ZntA. Each of these mutant proteins was labeled with pyrene maleimide at room temperature. The labeling ratios for each of the double mutants are  $\sim 2$  and each of the single mutants is  $\sim 1$ . This was determined using the known extinction coefficient for pyrene maleimide. The maximum absorbance peak for these mutants was around  $\sim 340$  nm. When the emission spectra for these mutants were measured, the characteristic pyrene peaks at 375 nm and 390 nm were observed; additionally a small, broad peak centered at  $\sim 480$  nm was observed for double cysteine mutants. This emission peak is indicative of a pyrene excimer which is formed only when the two pyrene molecules interact within a distance of 6-10 Å. As a control, the single cysteine containing proteins when subjected to similar reaction conditions, did not display the characteristic pyrene excimer. This control experiment indicates that the excimer formation is not due to dimerization of the mutant proteins. The excimer formation indicates that the cysteines in the two metal binding sites in ZntA can approach within 6-10 Å of each other.

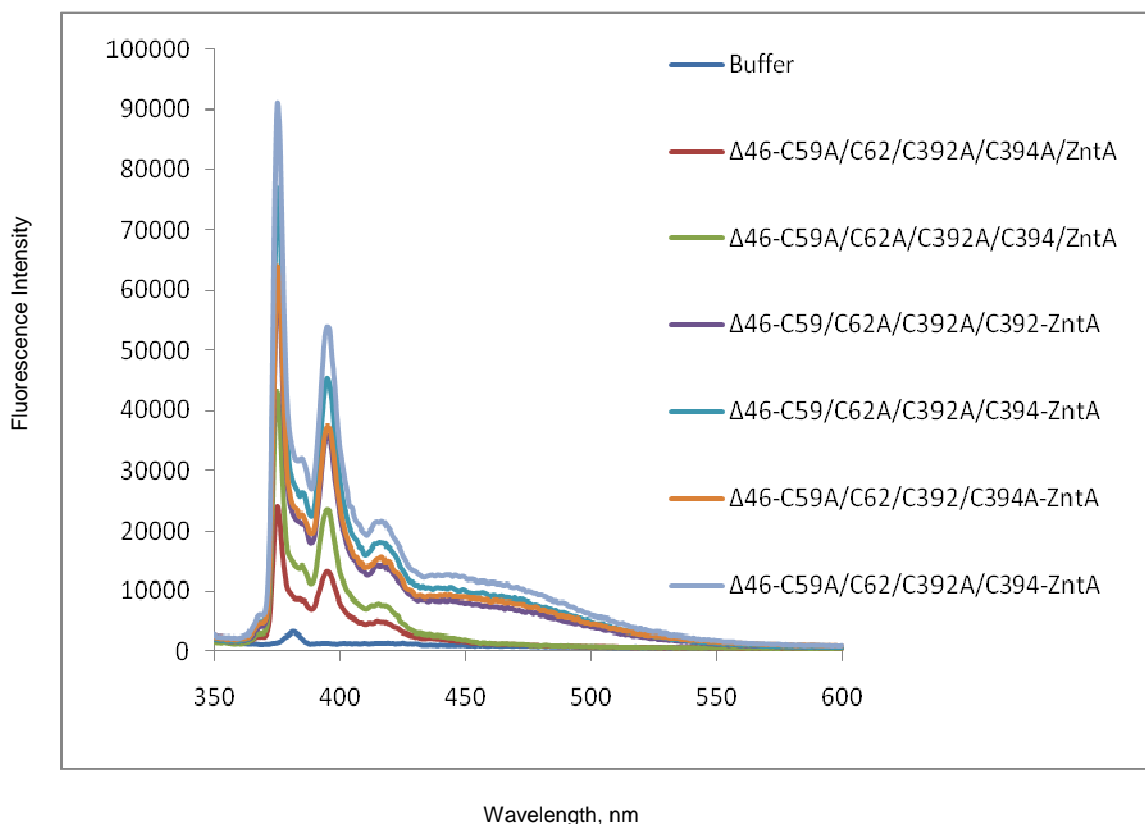


**Figure 3.12.** Emission spectra of pyrene maleimide labeled  $\Delta 46$ -ZntA cysteine mutants.

### 3.5 Discussion

Metal binding to the transmembrane region is an essential part of the ATPase reaction mechanism. ZntA, a  $P_{IB2}$  type ATPase involved in lead, zinc and cadmium transport, has a hydrophilic N-terminal domain. This domain has a conserved CXXC motif that has been shown to bind metal ions, which is conserved in the copper chaperone proteins like Atx1, Atox1, and CopZ. To date there has been no evidence of metallochaperones involved in zinc homeostasis and lead and cadmium detoxification. The aim of this work was to test our theory that the N-terminal domain acts an attached chaperone to the transporter; the N-

terminal domain efficiently binds metal ions from the cytosol and then directly delivers them to the metal binding site in the transmembrane region.

Early studies in the lab have shown that deletion of the entire N-terminal domain of ZntA does not inactivate the transporter; also its metal specificity is not affected (56). In vivo results show  $\Delta N$ -ZntA is able to complement the  $Pb^{2+}$ ,  $Zn^{2+}$  and  $Cd^{2+}$  sensitivity of a zntA deleted strain, but the growth rate is slower than ZntA. To investigate this further, we compared the ability of ZntA and  $\Delta N$ -ZntA to confer survival advantage to *E.coli* in toxic metal concentrations. In a competition assay, by day 3, only cells with ZntA survived (Figure 3.4), indicating that presence of the N-terminal domain gave ZntA a competitive advantage for survival in the presence of zinc. Additionally we also constructed a vector where both  $\Delta N$ -ZntA and N1-ZntA were co-expressed. The co-expression vector has a similar resistance profile (Figure 3.5) to  $\Delta N$ -ZntA, indicating that the N-terminal domain needs to be directly attached to the rest of the transporter in vivo, for it to display any growth advantage in the presence of toxic concentrations of lead, cadmium and zinc.

In vitro, the activity of truncated protein ( $\Delta N$ -ZntA) is 2-3 fold lower than that of ZntA (56). ICP measurements on N1-ZntA and  $\Delta N$ -ZntA have shown that both sites bind metal ions with a stoichiometry of 1; also the metal affinities for both the sites are similar. These results suggest that metal ion transfer between the two domains is feasible. If the N1-ZntA does deliver metal ions directly to the membrane region, the two metal binding sites in the N-terminal domain and transmembrane domain must come close to each other and interact for metal

transfer to occur. To investigate this we used cysteine specific fluorophores. Coumarin maleimide and pyrene maleimide were used to examine the interaction between the two domains. N1-ZntA labeled with coumarin maleimide was added to  $\Delta$ N-ZntA labeled with pyrene maleimide; this mixture was excited at 340 nm and showed an emission peak at ~470 which is characteristic of coumarin maleimide, in addition to the expected pyrene maleimide emission peak. The coumarin emission peak was observed because the emission energy from pyrene labeled  $\Delta$ N-ZntA was transferred to the coumarin labeled N1-ZntA, indication that the two domains can approach close in our in vitro assays (Figure 3.10). To examine the proximity of the two metal binding sites in the full-length ZntA, we made double and single cysteine mutations in a truncated form of ZntA ( $\Delta$ 46-ZntA) where the first 46 residues were deleted (Figure 3.11). These mutants were labeled with pyrene maleimide, a thiol specific fluorophore. When the labeled mutants were excited at 340 nm, the emission spectra for double mutants showed a peak at 480 nm which corresponds to characteristic excimer emission peak for pyrene maleimide (Figure 3.12). This excimer or “excited state dimer” is formed due to the interactions between the excited state of one monomer and the ground state of a second monomer (77). Distance and orientation are the two reasons that lead to formation of pyrene excimer. The pyrene excited state monomer must be within 6-10Å to interact with the ground state monomer and after excitation the monomers must orient themselves in the correct way or else the fluorescence will be quenched. This is a very useful method to examine the distance between the two sites. The excimer formation



observed for the pyrene labeled double cysteine mutants demonstrates that the two metal binding domains come close to each other and should be able to facilitate metal transfer.

A major goal of this work was to look at metal transfer by the N-terminal domain to the membrane region, by metal uptake assays using everted membrane vesicles of  $\Delta$ N-ZntA and ZntA and also ATPase activity measurements. In both the experiments the metal substrate provided was metal bound N1-ZntA. Everted  $\Delta$ N-ZntA and ZntA membrane vesicles both exhibited ATP dependent lead, zinc and cadmium accumulation by using metal bound N1-ZntA as the metal substrate (Figure 3.7). The everted membrane vesicles have an orientation opposite to that of intact cells; metal accumulation into the vesicle is same as extrusion from cells (Figure 3.3). Also, metal loaded N1-ZntA was used in the ATPase activity assay.  $Pb^{2+}$ ,  $Zn^{2+}$  and  $Cd^{2+}$  loaded N1-ZntA stimulated the ATPase activity of the transporter. A comparison of the  $V_{max}$  and  $K_m$  parameters for the ATPase activities of  $\Delta$ N-ZntA and ZntA in the presence of metal bound N1-ZntA as the substrate with those in the presence of free metal ion as substrate shows that the metal bound N1-ZntA stimulated activities of  $\Delta$ N-ZntA were higher than free metal stimulated activities of  $\Delta$ N-ZntA. But in the case of ZntA the activities in the presence of metal bound N1-ZntA was lower than in the presence of free metal. This may be because the intact N-terminal domain in ZntA has to first acquire metal ion from the N1-ZntA and then transfer it to the metal binding site in the membrane; this extra step slows down the rate. It is possible that for full-length ZntA, the attached N-terminal domain does not allow

the N1-ZntA fragment from delivering metal ion directly to the transmembrane site.

All the experiments shown here point towards the fact that the N-terminal metal site of ZntA comes within a distance of 6-10 Å of the transmembrane site to deliver metal ions to the membrane transport site (Figure 3.13). The amino terminal domain of ZntA is important for survival; it functions as an attached chaperone to the transporter and thus makes the process of metal binding and hence, transport, more efficient.

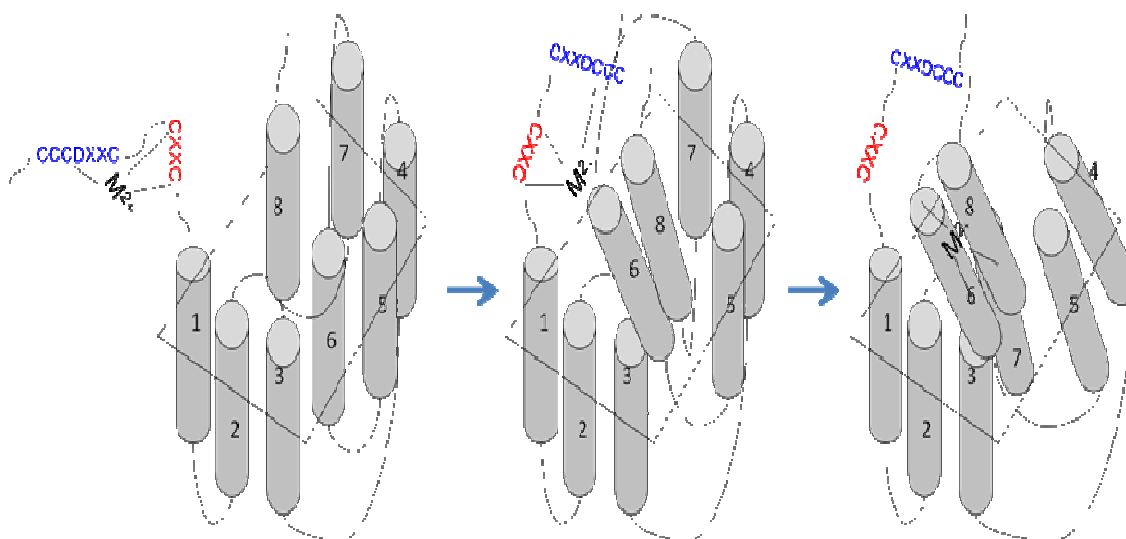


**Figure 3.13.** Model for Metal delivery to transmembrane metal binding site in ZntA.

### 3.6 REFERENCES

1. Maret, W. (2009) Molecular aspects of human cellular zinc homeostasis: redox control of zinc potentials and zinc signals, *Biometals* 22, 149-157.

2. Rosenzweig, A. C. (2002) Metallochaperones: bind and deliver, *Chem Biol* 9, 673-677.
3. Waldron, K. J., and Robinson, N. J. (2009) How do bacterial cells ensure that metalloproteins get the correct metal?, *Nat Rev Microbiol* 7, 25-35.
4. Shi, H., Bencze, K. Z., Stemmler, T. L., and Philpott, C. C. (2008) A cytosolic iron chaperone that delivers iron to ferritin, *Science* 320, 1207-1210.
5. Rensing, C., Mitra, B., and Rosen, B. P. (1997) The zntA gene of *Escherichia coli* encodes a Zn(II)-translocating P-type ATPase, *Proc Natl Acad Sci U S A* 94, 14326-14331.
6. O'Halloran, T. V., and Culotta, V. C. (2000) Metallochaperones, an intracellular shuttle service for metal ions, *J Biol Chem* 275, 25057-25060.
7. Liu, J., Stemmler, A. J., Fatima, J., and Mitra, B. (2005) Metal-binding characteristics of the amino-terminal domain of ZntA: binding of lead is different compared to cadmium and zinc, *Biochemistry* 44, 5159-5167.
8. Arnesano, F., Banci, L., Bertini, I., Ciofi-Baffoni, S., Molteni, E., Huffman, D. L., and O'Halloran, T. V. (2002) Metallochaperones and metal-transporting ATPases: a comparative analysis of sequences and structures, *Genome Res* 12, 255-271.
9. Ledwidge, R., Patel, B., Dong, A., Fiedler, D., Falkowski, M., Zelikova, J., Summers, A. O., Pai, E. F., and Miller, S. M. (2005) NmerA, the metal binding domain of mercuric ion reductase, removes Hg<sup>2+</sup> from proteins,

- delivers it to the catalytic core, and protects cells under glutathione-depleted conditions, *Biochemistry* 44, 11402-11416.
10. Fan, B., Grass, G., Rensing, C., and Rosen, B. P. (2001) Escherichia coli CopA N-terminal Cys(X)(2)Cys motifs are not required for copper resistance or transport, *Biochem Biophys Res Commun* 286, 414-418.
  11. Fan, B., and Rosen, B. P. (2002) Biochemical characterization of CopA, the Escherichia coli Cu(I)-translocating P-type ATPase, *J Biol Chem* 277, 46987-46992.
  12. Gonzalez-Guerrero, M., and Arguello, J. M. (2008) Mechanism of Cu<sup>+</sup>-transporting ATPases: soluble Cu<sup>+</sup> chaperones directly transfer Cu<sup>+</sup> to transmembrane transport sites, *Proc Natl Acad Sci U S A* 105, 5992-5997.
  13. Mitra, B., and Sharma, R. (2001) The cysteine-rich amino-terminal domain of ZntA, a Pb(II)/Zn(II)/Cd(II)-translocating ATPase from Escherichia coli, is not essential for its function, *Biochemistry* 40, 7694-7699.
  14. Liu, J., Dutta, S. J., Stemmler, A. J., and Mitra, B. (2006) Metal-binding affinity of the transmembrane site in ZntA: implications for metal selectivity, *Biochemistry* 45, 763-772.
  15. Sharma, R., Rensing, C., Rosen, B. P., and Mitra, B. (2000) The ATP hydrolytic activity of purified ZntA, a Pb(II)/Cd(II)/Zn(II)-translocating ATPase from Escherichia coli, *J Biol Chem* 275, 3873-3878.
  16. Foster, R. J., Poulouse, A. J., Bonsall, R. F., and Kolattukudy, P. E. (1985) Measurement of distance between the active serine of the thioesterase

- domain and the pantetheine thiol of fatty acid synthase by fluorescence resonance energy transfer, *J Biol Chem* 260, 2826-2831.
17. Ludi, H., and Hasselbach, W. (1987) Excimer formation in pyrenemaleimide-labeled sarcoplasmic reticulum ATPase, *Biophys J* 51, 513-515.
  18. Ishii, Y., and Lehrer, S. S. (1985) Fluorescence studies of the conformation of pyrene-labeled tropomyosin: effects of F-actin and myosin subfragment 1, *Biochemistry* 24, 6631-6638.
  19. Lin, Y. F., Walmsley, A. R., and Rosen, B. P. (2006) An arsenic metallochaperone for an arsenic detoxification pump, *Proc Natl Acad Sci U S A* 103, 15617-15622.
  20. Han, M. K., Knutson, J. R., Roseman, S., and Brand, L. (1990) Sugar transport by the bacterial phosphotransferase system. Fluorescence studies of subunit interactions of enzyme I, *J Biol Chem* 265, 1996-2003.

## CHAPTER 4

**CHARACTERIZING THE METAL BINDING PROPERTIES OF A TRUNCATED FORM OF ZNTA THAT IS STRUCTURALLY SIMILAR TO THE PINEAL NIGHT SPECIFIC ATPASE ENCODED BY A SPLICE VARIANT OF THE WILSON DISEASE GENE, ATP7B**

The work presented in this chapter is preliminary in nature. The experiments performed involve characterizing a truncated form of ZntA that lacks the first 4 transmembrane helices.

#### 4.1 Introduction

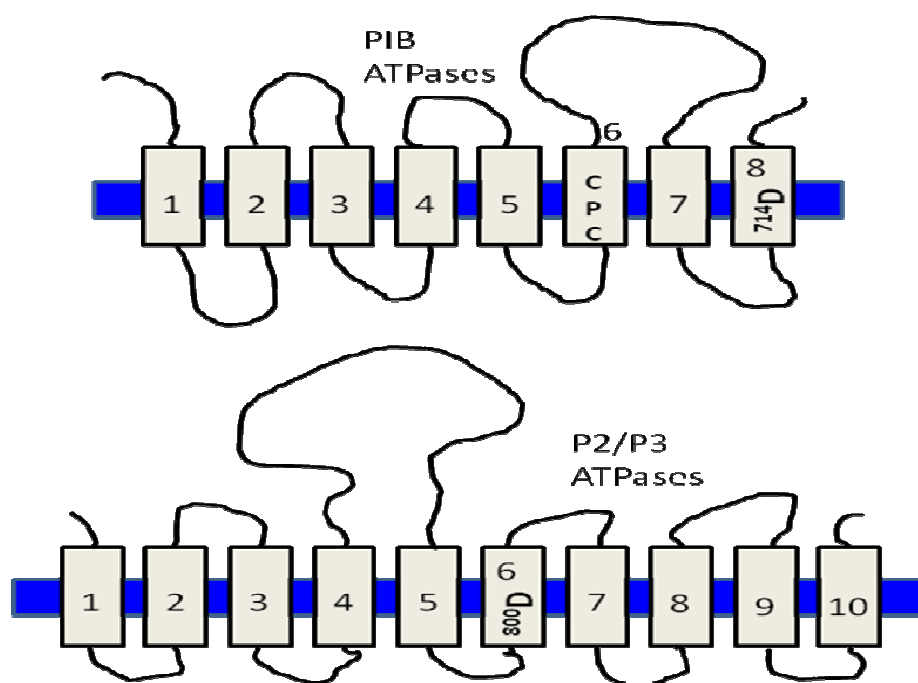


**Figure 4.1.**Membrane Topology of P<sub>1B</sub> and P<sub>2/P3</sub> ATPases.

ZntA has two metal binding sites, one in the N-terminal region and the other in the transmembrane region (63). The transmembrane metal site is essential for activity of the pump. All P<sub>1B</sub> ATPase family members have eight transmembrane helices and a few characteristic conserved charged residues in

the transmembrane region depending on the specific subgroup. All  $P_{1B}$  ATPases contain a conserved motif (C, S, T) P(C, H) in helix 6 (45). In the  $P_{1B-1}$  subfamily, which is selective for  $Cu^+$ ,  $Ag^+$ , and the  $P_{1B-2}$  subfamily, which is selective for  $Pb^{2+}$ ,  $Zn^{2+}$  and  $Cd^{2+}$ , the motif is conserved as CPC. Previous work in our laboratory on the conserved motif CPC has demonstrated that the alanine mutations at each of the two cysteine residues resulted in complete loss in activity and the proteins were also unable to bind metal ion at the transmembrane metal binding site, indicating that each of the cysteine residues are important metal-binding ligands (55).

Sequence alignment of helix 8 for  $P_{1B}$ -type ATPases shows the presence of a strictly conserved aspartate residue in the  $P_{1B-2}$  subfamily, which is not conserved in any other subgroup of the  $P_{1B}$ -ATPases. However this aspartate residue is strictly conserved in the transmembrane helix 6 of  $P_2$  and  $P_3$  family of ATPases, which corresponds to helix 8 in  $P_{1B}$ -ATPase (62) (Figure 1). Previous work from our laboratory has shown that Asp714 in ZntA residue is essential for the overall activity of the protein and it provides ligands to metal ions in the transmembrane site (62). Studies on the corresponding conserved Asp residue in the calcium ATPase, which belongs to the  $P_{2A}$  family, has shown that this residue is essential for activity of the pump. Structural studies on the calcium ATPase has shown the aspartate residue acts as a bridge to the two  $Ca^{2+}$  ions in the membrane (40). In other members of the  $P_2$  family such as the  $Na^+/K^+$  ATPase and the  $H^+/K^+$  pumps mutation of this aspartate residue leads to loss in activity of the protein (78). In the plasma membrane proton pumps which belong

to the P<sub>3</sub> family of ATPases, the aspartate residue is involved in conformational change of the transporter during catalysis (62).

Thus, in the ZntA subgroup of P<sub>1B</sub>-type ATPases, both the CPC motif in helix 6 and the Asp in helix 8 are part of the metal binding site in the transmembrane domain; these residues are involved in conferring metal selectivity to the pump.

The pineal gland is an endocrine organ of the brain that is responsible for the synthesis and secretion of melatonin mainly at night (79). Experiments to investigate the pineal circadian rhythms led to the identification of a novel protein called pineal night-specific ATPase (PINA), a night-specific and pineal/retina-specific splice variant of the ATP7B gene, defects in which cause Wilsons disease (80). Wilsons disease is an inherited disorder related to copper transport; it leads to accumulation of copper in the liver and hence, toxicity (20). Copper is also accumulated in the brain and is thought to be responsible for neurological and psychiatric abnormalities in some Wilson disease patients (20). The gene for Wilsons disease encodes a copper transporting ATPase (ATP7B), which belongs to the P<sub>1B-1</sub> subfamily of P<sub>1B</sub> ATPases, which are selective for Cu<sup>+</sup> and Ag<sup>+</sup>. From sequence analysis it was observed that PINA is identical to the C-terminal half of ATP7B (79). The 5' region upstream of the open reading frame of PINA has a 300 bp sequence which is not found in ATP7B and is pineal specific (79). Unlike ATP7B, PINA lacks the entire N-terminal domain which contains six CXXC motifs that are involved in copper binding. Also the first four transmembrane helices are absent (79). PINA however still retains some



important elements of P-type ATPases such as the phosphorylation domain, the ATP binding domain and the conserved CPC motif, which is important in metal binding in both the P<sub>IB-1</sub> and P<sub>IB-2</sub> subfamilies. Indirect in vivo studies suggested that although the N-terminal copper binding region and half the transmembrane helices are absent, the PINA protein may be able to transport copper in a yeast system but at a much lower efficiency than the ATP7B (79-80); however no direct proof exists that the PINA protein is an active transporter. So far, very little is known about the role of the first four transmembrane helices in P<sub>IB</sub> ATPases; helices 3 and 4 correspond to helices 1 and 2 in the Ca<sup>2+</sup> ATPase. In the Ca<sup>2+</sup> ATPase, helices 1-5 undergo major structural changes on metal binding and phosphorylation (37). With the discovery of PINA, we wanted to test a similar truncated form of ZntA that lacked the amino terminal domain and the first four transmembrane helices, Del231-ZntA, in order to investigate if the loss of upstream four transmembrane helices would affect the activity and the metal binding ability of the transporter.

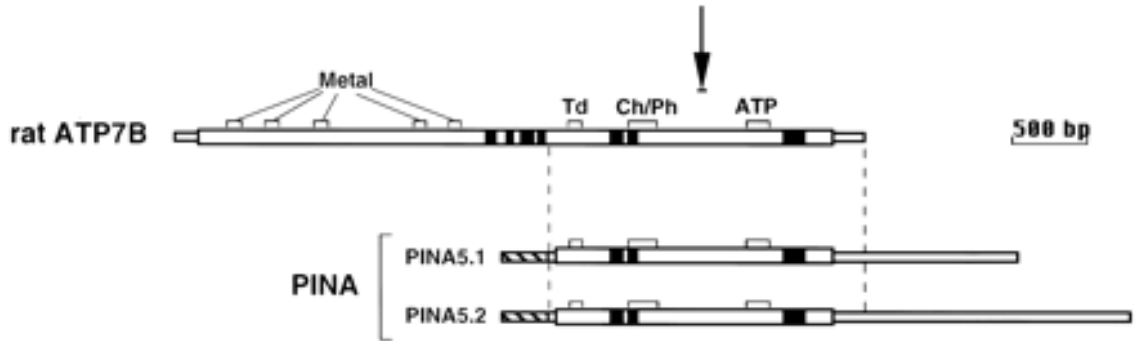


**Figure 4.2.** Structure of PINA in comparison with ATP7B. PINA is made up of 3.5kb (PINA5.1) and 4.3(PINA5.2) transcripts that are similar to the C-terminal portion of ATP7B. The regions conserved in the copper transporters are: Metal: metal binding domains (CXXC motifs); Td:transduction domain (TGEA); Ch/Ph:metal binding, CPC motif; phosphorylation domain (DKTGT); ATP:ATP-binding domain (GDGXNDXP) (79).

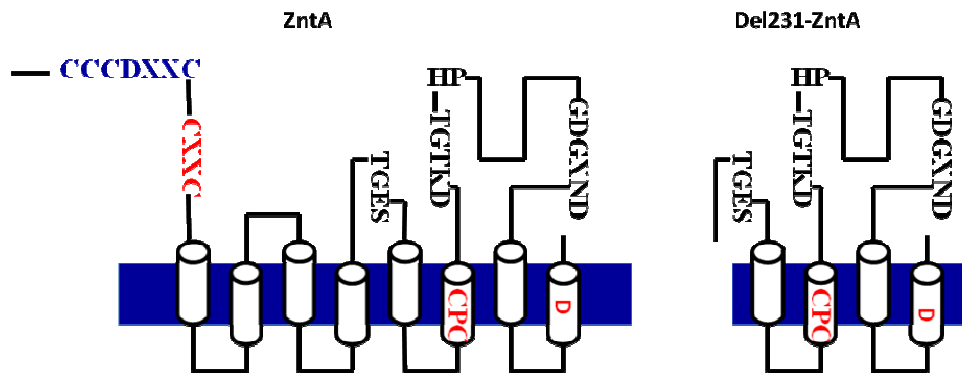


**Figure 4. 3.** Structures representing ZntA and the truncated form, Del231-ZntA

#### 4.2 Materials

Plasmid pBAD/mycHis-C and *E.coli* strain LMG194 were obtained from Invitrogen; plasmid pET16B was obtained from Novagen. Chemicals for the ATPase activity assay and standard metal solutions were purchased from

Sigma. Metal standards used for inductively coupled plasma mass spectrometry (ICP-MS) were from VWR.

### **4.3 Methods**

#### **4.3.1 Construction of Del231-ZntA with a carboxyl-terminal His tag and carboxyl terminal strep tag**

Del231-ZntA with a 6 His tag was created by PCR using the plasmid  $\Delta$ N-ZntA as template and the oligonucleotides 5'-CGT GCC ATG GCG CTG AAA CC- 3' as forward primer and 5'-GAA TTC TCT CCT GCG CAA CAA TCT TTA ACG-3' as the reverse primer. The PCR product and the vector were digested with Nco1 and EcoR1, after which the amplified DNA fragment and the vector were ligated together to generate his tagged Del231-ZntA.

Strep tagged Del 231-ZntA was created by using the plasmid  $\Delta$ N-ZntA as template and the primers 5'-CGT GCC ATG GCG CTG AAA CC- 3' as forward primer and 5' GCG CTC GAG TTA TTT TTC GAA CTG CGG GTG GCT CCA CAG GGA ATA GCC TGC 3' as the reverse primer. The PCR product and the vector were digested with Nco1 and EcoR1, after which the amplified DNA fragment and the vector were ligated together to generate strep tagged Del231-ZntA. The sequence of both Del-ZntA with the C-terminal his tag and C-terminal strep tag were confirmed using DNA sequencing analysis; both the genes were in frame with the corresponding tags at the carboxyl terminus.

#### **4.3.2 Protein expression of Del231-ZntA (his tag and strep tag)**

Both the His-tagged and strep tagged Del231-ZntA were expressed by growing LMG194 (zntA::cat) transformed with Del231-ZntA at 37° C in Luria-

Bertani medium supplemented with 100 µg/ml ampicillin to mid-log phase and then induced with 0.02% arabinose. Cells were harvested 4 h after induction, washed with ice-cold buffer containing 25 mM Tris, pH 7 and 100 mM KCl, and stored at -20°C till further use (50).

#### 4.3.3 Protein Purification of Del231-ZntA

Protein purification procedures were all performed at 4°C. Frozen cells were thawed and resuspended in buffer A (25 mM Tris, pH 7.0, 100 mM sucrose, 1 mM PMSF, 1 mM EDTA and 1 mM β-mercaptoethanol (BME)) at 0.2g/ml. The cells were broken at 20,000 p.s.i with a French press, the lysed cells were then incubated with DNase 1 (0.02mg/ml) and 2mM MgCl<sub>2</sub> for 30 min. The lysed cells were then centrifuged at 8000 rpm for 30 min. The supernatant was then centrifuged at 40,000 rpm for 1 h to separate the membranes from the soluble fraction of cells. The pellet from this centrifugation was resuspended in buffer B (1 mM Tris pH 7.0, 100 mM sucrose, 1 mM EDTA, 1 mM PMSF, and 1 mM BME), stirred for 1 hr at 4°C, and then centrifuged at 40,000 rpm for 1 h. The membrane fraction was resuspended in buffer C (25 mM Tris pH 7.0, 100 mM sucrose, 500 mM NaCl, 1 mM PMSF and 1 mM BME). Triton-X-100 was added to a final concentration of 1% and the suspension was stirred for 1 h at 4°C. The solubilized membranes were then centrifuged at 40,000 rpm for 1 h to remove the insoluble fraction.

For the His tagged protein: The supernatant was then loaded on a charged Ni<sup>2+</sup>-pro-bond column. The column was washed successively with buffer C, buffer C + 50 mM imidazole, buffer C + 100 mM imidazole. Finally the protein was eluted

using 30 ml of buffer C with 300 mM imidazole. 1ml fractions were collected and analyzed for protein. Protein containing fractions were pooled and loaded on 40 ml Sephadex G-25 columns to remove imidazole. Protein fractions were collected and concentrated using YM-100 centricons. The protein was stored at -80°C with 10 % glycerol as a cryoprotectant.

For the Strep tagged protein: The Triton-X-100 solubilized fraction was loaded on a strep-tactin column that was pre-equilibrated with buffer D (buffer C + 0.2% Triton-X-100). The resin was subsequently washed with 25ml of Buffer D. The protein was finally eluted with 20ml of buffer D containing 2.5 mM desthiobiotin. 1 ml fractions were collected and analyzed for protein. Protein containing fractions were pooled and loaded on a 40 ml Sephadex G-25 column pre-equilibrated with Buffer E (25 mM Tris pH 7.0, 100 mM sucrose, 50 mM KCl, 0.2% Triton-X-100) to remove the desthiobiotin. 1ml fractions were collected and assayed for protein. The protein containing fractions were pooled and concentrated using Centricon concentrators. The concentrated protein was then stored at -70°C using glycerol as the cryoprotectant.

#### **4.3.4 Determination of Protein Concentration**

Protein concentrations were determined by the bichinonic acid assay, using bovine serum albumin as standard. This assay is a modified Lowry assay, where the proteins reduce  $\text{Cu}^{2+}$  to  $\text{Cu}^{+}$  in a concentration dependent manner. Bichinonic acid forms a purple complex with  $\text{Cu}^{+}$ , which has an absorbance maximum at 562 nm. This absorbance is proportional to the protein concentration. BSA is used to generate a standard curve.

#### 4.3.5 Sensitivity to metal salts

The sensitivity of *E. coli* strains LMG194, LMG194 (zntA::cat) and LMG194 (zntA::cat) transformed with pZntA or Del231-ZntA, to lead, cadmium and zinc was measured. The cells were grown in low phosphate media, pH 7.5. Cells were grown overnight and then diluted 100 fold in the same media in the presence of lead acetate, zinc chloride, and cadmium chloride. Cell growth at 37 °C was monitored at 600 nm over a period of 24 hours (56, 69).

#### 4.3.6 ATPase Activity Measurements

The activity of Del231-ZntA was measured by a coupled spectroscopic assay, involving pyruvate kinase and lactate dehydrogenase. The regeneration of ATP is coupled to the oxidation of NADH, which is monitored at 340 nm (50). The buffer for the reaction was 0.05 M Bis tris, 0.1 M acetic acid, and 0.05 M triethanolamine at pH 7.0. The reaction mixture (1 ml) also contained 0.1% asolectin, 0.2% Triton-X-100, 10 % glycerol, 5 mM ATP, 0.25 mM NADH, 1.25 mM phosphoenolpyruvate, 7 units of pyruvate kinase, and 10 units of lactate dehydrogenase, with or without metal ion ( $Zn^{2+}$ ,  $Pb^{2+}$ ,  $Cd^{2+}$ ). The proteins were reduced by incubation with 2 mM DTT for 1 h prior to the reaction. About 0.5-2 mg/ml protein was used per assay. The reaction mixture was incubated for 5 mins at 37°C before initiating the reaction with 5 mM  $MgCl_2$ .

Thiolates in the assay buffer are known to increase the ATPase activity (50). The activity of the mutant was also investigated in the presence of thiolates. Along with the other assay ingredients, thiolates were also added. The concentration of the thiolate form of cysteine required to generate a constant

metal ion: thiolate ion ratio was calculated using the Henderson-Hasselbach equation, using a pKa of 8.33 for cysteine and a pH of 7.0. The data obtained was fit to the Michaelis-Menten equation,

$$v = V_{\max} \times S / (K_M + S)$$

where,  $V_{\max}$  equals the maximum velocity, S is the concentration of metal,  $K_M$  is the Michaelis constant for the substrate metal ion (50).

#### **4.3.7 Preparation of Metal bound Del231-ZntA**

To measure the stoichiometry of metals bound to Del231-ZntA, the protein was reduced with 1 mM TCEP for 1 h at 4 °C. The reduced protein was then incubated with metal salts for 1 hour at 4 °C, and then excess metal was removed by passing through a Sephadex G-25 column (56).

#### **4.3.8 Measurement of Metal Binding Stoichiometry of Del231-ZntA by ICP-MS**

The metal content was measured by a PE Sciex Elan 9000 ICP-MS (inductively coupled mass spectrometry) with a cross-flow nebulizer and Scott type spray chamber. The RF power was 1000 W, and the argon flow was optimized at 0.92 L/min. The optimum lens voltage was centered on rhodium sensitivity. The data were collected as counts per second. Lead, Cadmium and Zinc standards were obtained from VWR. Standard calibration curves were determined from samples diluted from stock solutions of 1000 ppm standard solutions. The samples and standards solutions were all diluted in 2% HNO<sub>3</sub>.

## 4.4 Results

### 4.4.1 The in vivo resistance activity of Del2310ZntA mutant to Pb<sup>2+</sup>, Zn<sup>2+</sup> and Cd<sup>2+</sup> in the growth medium

The *zntA* deleted *E.coli* strain, LMG194 (*zntA::cat*) is sensitive to toxic levels of Pb<sup>2+</sup>, Zn<sup>2+</sup> and Cd<sup>2+</sup>; it is unable to grow even after 24-30 h and this sensitivity can be complemented by *wzntA*. However when this *zntA* deleted strain was complemented with the *del231-zntA* gene, it was unable to confer resistance to Pb<sup>2+</sup>, Zn<sup>2+</sup> and Cd<sup>2+</sup>.

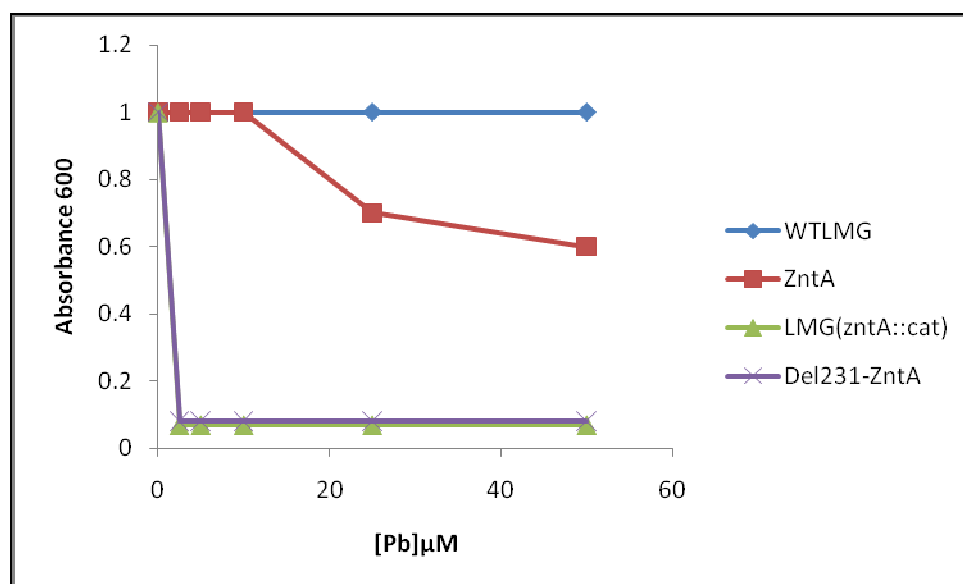


**Figure 4.4.** Resistance to Lead, Zinc and Cadmium salts by the wild type strain LMG194, the *zntA*-deleted strain LMG194(*zntA::cat*), and the deleted strain transformed with plasmids containing *wzntA* and *del231-ZntA*. The strains were grown in the presence of varying metal concentrations and the absorbance was measured after 24 hours.



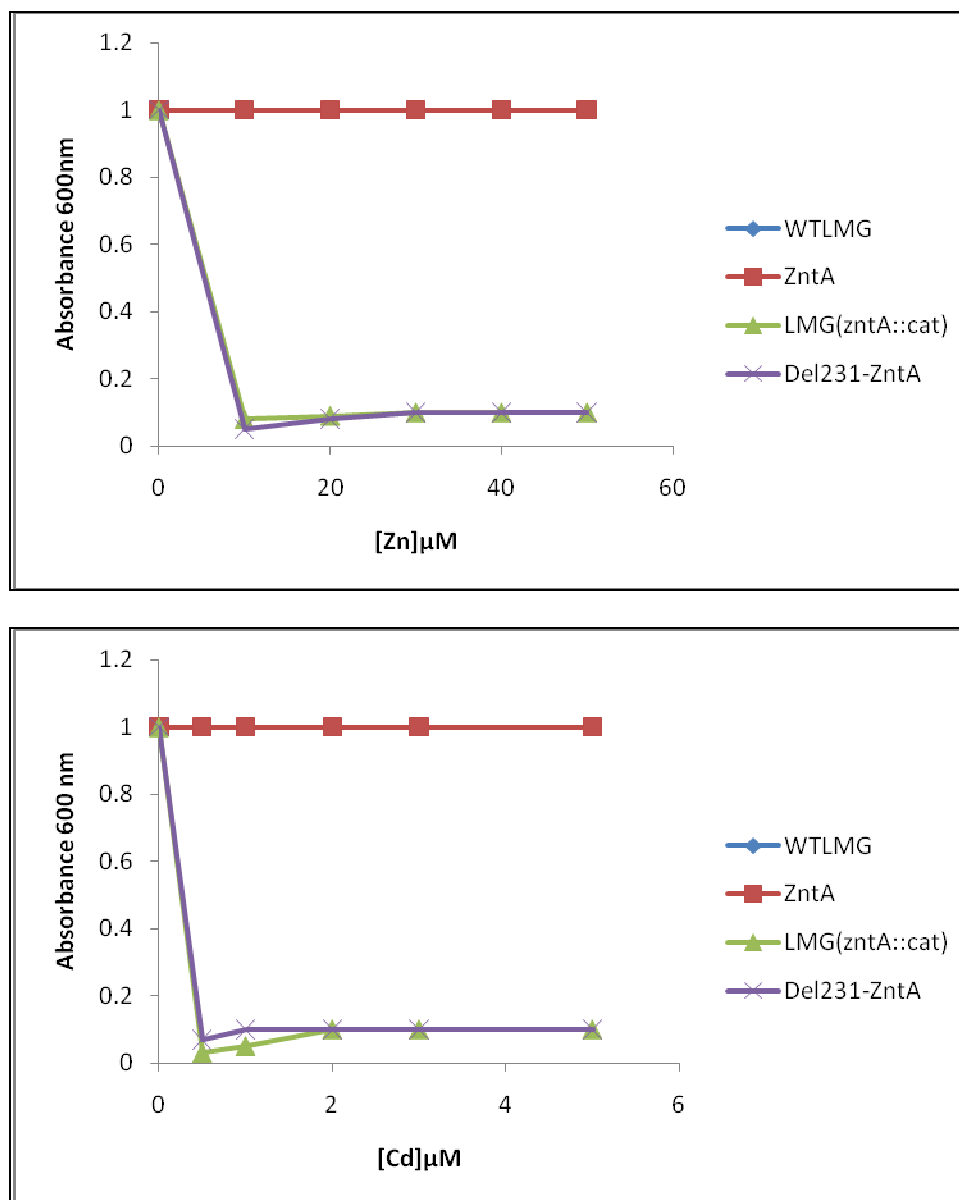


**Figure 4.4.** Resistance to Lead, Zinc and Cadmium salts by the wild type strain LMG194, the *zntA*-deleted strain LMG194(*zntA::cat*), and the deleted strain transformed with plasmids containing *wzntA* and *del231-ZntA*. The strains were grown in the presence of varying metal concentrations and the absorbance was measured after 24 hours.

#### 4.4.2 Activity of the purified Del231-ZntA

The ATPase activity of Del231-ZntA and ZntA was measured for the metal ions  $Pb^{2+}$ ,  $Zn^{2+}$  and  $Cd^{2+}$ . Previous studies showed that the metals ions stimulate the ATP hydrolysis activity of wtZntA, with  $Pb^{2+}$  exhibiting the highest activity (50). Del231-ZntA did not show any metal induced ATPase activity. There is a 4-8 fold increase in the ATPase activity of ZntA in the presence of thiolate forms of cysteine or glutathione in the assay medium (50). The activities for wtzntA and Del231-ZntA were measured in the presence of metal ions and thiolate form of cysteine in the ratio 1:1 for  $Pb^{2+}$ ,  $Zn^{2+}$  and  $Cd^{2+}$ . The Del231-ZntA showed extremely small but measurable activities in the presence of the thiolate form of cysteine (Table 4.1).

**Table 4.1.** Kinetic Parameters obtained for ZntA and Del231-ZntA, in the presence of the thiolate form of cysteine present at a concentration equal to the  $M^{2+}$  concentration.

	<b>Pb<sup>2+</sup> + Thiolate</b>	
	<b>V<sub>max</sub></b> nmoles/mg/min	<b>K<sub>M</sub></b> μM
<b>ZntA</b>	2500 ± 70	166 ± 16
<b>Del231-ZntA</b>	15 ± 0.6	109 ± 15
	<b>Zn<sup>2+</sup> + Thiolate</b>	
	<b>V<sub>max</sub></b> nmoles/mg/min	<b>K<sub>M</sub></b> μM
<b>ZntA</b>	710 ± 28	96 ± 11
<b>Del231-ZntA</b>	5 ± 0.16	45 ± 7.2
	<b>Cd<sup>2+</sup> + Thiolate</b>	
	<b>V<sub>max</sub></b> nmoles/mg/min	<b>K<sub>M</sub></b> μM
<b>ZntA</b>	1025 ± 25	252 ± 16
<b>Del231-ZntA</b>	2 ± 0.11	53 ± 12

#### 4.4.3 Stoichiometry of Metal Binding to Del231-ZntA using ICP-MS

Del231-ZntA has the conserved metal binding motif (CPC) and the conserved Asp714 (original ZntA numbering). To investigate if the truncated protein was able to bind metal ions, we determined the metal binding stoichiometries of the truncated protein purified with a strep-tag. Wild-type ZntA can bind to two metal ions with high affinity.  $\Delta$ N-ZntA which lacks the amino terminal domain, binds to  $Pb^{2+}$ ,  $Zn^{2+}$  and  $Cd^{2+}$  with a stoichiometry of 1. It was observed that Del231-ZntA bound to  $Pb^{2+}$ ,  $Zn^{2+}$  and  $Cd^{2+}$  with a stoichiometry of 0.5.

**Table 4.2.** Stoichiometry of Metal bound to N1-ZntA and Del231-ZntA using Inductively Coupled Plasma Mass Spectrometry (ICP-MS)

	<b>Lead</b>	<b>Zinc</b>	<b>Cadmium</b>
<b>ZntA</b>	2 ± 0.0	2 ± 0.1	2 ± 0.0
<b><math>\Delta</math>N-ZntA</b>	1 ± 0.1	1 ± 0.0	1 ± 0.0
<b>Del231-ZntA</b>	0.5 ± 0.0	0.5 ± 0.1	0.5 ± 0.0

#### 4.5 Discussion

Most P-type ATPases contain metal binding motifs (CXXC, histidine and methionine rich motifs) in their amino terminal domains. Transporters in the  $Zn^{2+}/Pb^{2+}/Cd^{2+}$  and  $Cu^{+}/Ag^{+}$  subgroups all have an N-terminal metal-binding domain containing 1-6 copies of the CXXC motif. Both these subgroups also have the CPC motif in TM 6, and a conserved Asp in TM 8 for the  $Zn^{2+}/Pb^{2+}/Cd^{2+}$  subgroup. So far, our investigation showed that these three residues are

involved in binding the metal ion in the transmembrane domain and conferring selectivity to the bound metal in ZntA. The function of the first four TM helices in the P<sub>1B</sub>-type ATPases is unclear; also it is not known whether they contribute to metal binding or not. They do not have any conserved residues that are polar. In order to test whether TMs 5-8 were adequate in metal binding and transport, we created a truncated form of ZntA which is similar to PINA. In vivo, Del231-ZntA did not confer resistance to Pb<sup>2+</sup>, Zn<sup>2+</sup> and Cd<sup>2+</sup>; its resistance profile was similar to the zntA deleted strain, indicating that both the amino terminal and the first four transmembrane helices are necessary for growth and survival. The truncated protein did not display any activity in the presence lead, zinc and cadmium. When the metal thiolate complex was used as the substrate, very low levels of activity were observed. Given that the in vitro activity of del231-ZntA is very low compared to ZntA, it is not surprising that in vivo, this truncated mutant is unable to provide resistance to metal salts.

However, the fact that some activity was observed in vitro, suggested to us that Del231-ZntA would be able to bind metal ions. Our results show that Del231-ZntA was indeed able to bind lead, zinc and cadmium, but surprisingly, with a stoichiometry of 0.5, unlike  $\Delta$ N-ZntA, which binds metal ions with a stoichiometry of 1. This result shows that TMs 5-8 are able to bind metal ions without the presence of TMs 1-4. It is possible that TMs 1-4 provide a fourth metal binding ligand, which when absent, forces the transporter to dimerize, with a second monomer providing the fourth ligand, leading to a stoichiometry of 0.5. It is also possible that TMs 1-4 do not provide a metal-binding ligand, but in their

absence, the transmembrane region folds in such a way that the transporter is able to dimerize easily in the membrane region, and therefore accommodates only one metal ion per dimer, again resulting in a stoichiometry of 0.5. Further studies are needed to show whether the CPC motif as well as Asp714 are all metal ligands in Del231-ZntA, and whether the metal binding affinity in Del231-ZntA is similar to that of ZntA or  $\Delta$ N-ZntA. It is clear though, that the first four transmembrane helices of ZntA are necessary for high activity of the transporter, and hence, growth in vivo in the presence of toxic concentrations of  $\text{Pb}^{2+}$ ,  $\text{Zn}^{2+}$  and  $\text{Cd}^{2+}$ . This suggests that the PINA protein may not be a good  $\text{Cu}^+$  transporter, but may be able to bind and transfer  $\text{Cu}^+$  to other  $\text{Cu}^+$ -binding proteins, especially membrane-bound  $\text{Cu}^+$ -binding proteins.

#### 4.6 REFERENCES

1. Liu, J., Dutta, S. J., Stemmler, A. J., and Mitra, B. (2006) Metal-binding affinity of the transmembrane site in ZntA: implications for metal selectivity, *Biochemistry* 45, 763-772.
2. Arguello, J. M., Eren, E., and Gonzalez-Guerrero, M. (2007) The structure and function of heavy metal transport P1B-ATPases, *Biomaterials* 20, 233-248.
3. Dutta, S. J., Liu, J., Hou, Z., and Mitra, B. (2006) Conserved aspartic acid 714 in transmembrane segment 8 of the ZntA subgroup of P1B-type ATPases is a metal-binding residue, *Biochemistry* 45, 5923-5931.

4. Dutta, S. J., Liu, J., Stemmler, A. J., and Mitra, B. (2007) Conservative and nonconservative mutations of the transmembrane CPC motif in ZntA: effect on metal selectivity and activity, *Biochemistry* 46, 3692-3703.
5. Toyoshima, C., Nomura, H., and Sugita, Y. (2003) Structural basis of ion pumping by Ca(2+)-ATPase of sarcoplasmic reticulum, *FEBS Lett* 555, 106-110.
6. Moller, J. V., Juul, B., and le Maire, M. (1996) Structural organization, ion transport, and energy transduction of P-type ATPases, *Biochim Biophys Acta* 1286, 1-51.
7. Borjigin, J., Payne, A. S., Deng, J., Li, X., Wang, M. M., Ovodenko, B., Gitlin, J. D., and Snyder, S. H. (1999) A novel pineal night-specific ATPase encoded by the Wilson disease gene, *J Neurosci* 19, 1018-1026.
8. Ahmed, S., Deng, J., and Borjigin, J. (2005) A new strain of rat for functional analysis of PINA, *Brain Res Mol Brain Res* 137, 63-69.
9. DiDonato, M., and Sarkar, B. (1997) Copper transport and its alterations in Menkes and Wilson diseases, *Biochim Biophys Acta* 1360, 3-16.
10. Toyoshima, C., and Inesi, G. (2004) Structural basis of ion pumping by Ca<sup>2+</sup>-ATPase of the sarcoplasmic reticulum, *Annu Rev Biochem* 73, 269-292.
11. Sharma, R., Rensing, C., Rosen, B. P., and Mitra, B. (2000) The ATP hydrolytic activity of purified ZntA, a Pb(II)/Cd(II)/Zn(II)-translocating ATPase from *Escherichia coli*, *J Biol Chem* 275, 3873-3878.

12. Poole, R. K., Williams, H. D., Downie, J. A., and Gibson, F. (1989) Mutations affecting the cytochrome d-containing oxidase complex of *Escherichia coli* K12: identification and mapping of a fourth locus, *cydD*, *J Gen Microbiol* 135, 1865-1874.
13. Liu, J., Stemmler, A. J., Fatima, J., and Mitra, B. (2005) Metal-binding characteristics of the amino-terminal domain of ZntA: binding of lead is different compared to cadmium and zinc, *Biochemistry* 44, 5159-5167.



## CHAPTER 5

### CONCLUSIONS AND FUTURE DIRECTIONS

The major aims of this thesis have been to study the structural, and biochemical aspects of ZntA which has given us an insight into the different mechanisms adopted by metal transporting proteins to achieve metal selectivity. I have been able to answer some of the many questions by characterizing the conserved cysteine residues (CCCDXXC and GMDCXXC) in the cytoplasmic N-terminal domain of ZntA and the interaction of this domain with the core transporter. This work is presented in Chapters 2 and 3. We began by altering the individual cysteine residues to alanines and the individual aspartate residues to alanine and asparagine. These mutants were fully characterized for in vivo resistance, ATPase activity, lead, zinc and cadmium binding (Fluorescence spectroscopy, ICP-MS) and the lead, zinc, cadmium binding site structures were examined by XAS. Our results suggested that Cys31 from the CCCDXXC motif, as well as the GMDCXXC conserved motif play important roles in metal selectivity to metal ions of highly different sizes.

Research presented in Chapter 3 sheds light on the role of the N-terminal domain as an attached chaperone to the core transport domain. The interaction between the two domains has been characterized using vivo assays, FRET studies; ATPase activity measurements. From the results obtained we can conclude that the amino terminal domain of ZntA is important for survival and it efficiently transports metal ion to the membrane domain.

In ongoing studies, solving the structure of the  $Pb^{2+}$ -bound N-terminal domain will give us detailed structural information about the positions of the two cysteine-rich motifs in this domain. So far there is no available structural data with regards to the metal binding site in the transmembrane domain of ZntA; X-ray absorption studies on the metal bound form of  $\Delta N$ -ZntA will provide us an insight into ligand environment and geometry. Within the cell, other than metalloproteins, there are several small-molecule chelating agents; we have studied the effect of two such agents (glutathione and cysteine) on the ATPase activity of ZntA. The metal:thiolate complex increases the activity of the transporter 4-5 fold. Another aspect to study would be to look at the effect of different chelating agents (citrate, histidine, imidazole etc) on the activity of the transporter in order to learn if metal complexes of sulfur-containing chelators behave differently from those of oxygen or nitrogen-containing chelators with respect to being efficient substrates of ZntA..

The fourth chapter presented in the thesis is work in progress. The role of the first four transmembrane helices in  $P_{IB}$ -ATPases is not known. In  $P_2$  and  $P_3$  ATPases, the helices 1 to 5 undergo important conformational changes on metal binding. Loss of these helices in ZntA leads to very low activity of the pump and also the metal binding stoichiometry is reduced to 0.5. Further studies such as determining the  $Pb^{2+}$ ,  $Cd^{2+}$  and  $Zn^{2+}$  binding affinities for  $\Delta I231$ -ZntA by competition titration experiments and determining the metal binding ligands in this mutant, will provide details regarding the role of these helices. Our results

may be able to provide an indication about the biological function of PINA, the splice variant of the Wilson  $\text{Cu}^+$ -ATPase.

**ABSTRACT****INVESTIGATING THE METAL BINDING SITES IN ZNTA,  
A ZINC TRANSPORTING ATPASE**

by

**SANDHYA MURALIDHARAN****August 2010****Advisor:** Dr. Bharati Mitra**Major:** Biochemistry and Molecular Biology**Degree:** Doctor of Philosophy

ZntA from *Escherichia coli* is a member of the P<sub>1B</sub>-type ATPase family of transporters. The P<sub>1B</sub>-type ATPase pumps maintain cellular homeostasis of heavy metals such as Zn<sup>2+</sup>, Co<sup>2+</sup>, Cu<sup>2+</sup>, Cu<sup>+</sup>, and mediate resistance to toxic metals such as Pb<sup>2+</sup>, Cd<sup>2+</sup> and Ag<sup>+</sup>. ZntA confers resistance to Pb<sup>2+</sup>, Cd<sup>2+</sup> and Zn<sup>2+</sup> by pumping these ions out of the cytoplasm. ZntA has two metal binding sites, one in the hydrophilic N-terminal domain and the other in the transmembrane region. The cysteine-rich N-terminal domain has ~110 amino acids and the conserved motifs –CCCDXXC- and –DCXXC-. The role of these motifs in metal-binding specificity was determined by site-specific mutagenesis, metal-binding studies, functional assays and EXAFS. Our results show that both motifs play a role in metal binding and conferring the broad metal selectivity shown by ZntA.

The N-terminal domain and the N-terminal metal-binding site are not essential for activity, but increase the kinetics of the pump and therefore, confer

a survival advantage to the organism. The transmembrane metal-binding site is essential for functioning of the pump. We investigated the role of the N-terminal metal-binding site in the overall function of the pump, and any possible interactions with the transmembrane site. Our results show that the isolated N-terminal domain is capable of transferring its bound metal ion to both *wtZntA* and to a *ZntA* mutant lacking the N-terminal domain. Activities obtained with the metal ion bound to the N-terminal domain are much higher than when the metal ion is present as low-affinity complexes in the assay buffer. Together with metal binding affinities of the two sites, these data show that the N-terminal metal site is capable of transferring metal ions directly to the transmembrane metal site. Thus the N-terminal domain acts as a metal chaperone to the transport site in this class of pumps. The function of this “attached” chaperone appears to be to increase the rate of metal binding to the transmembrane site and thus increase the overall kinetics of the pump.

In the last chapter, our studies on a truncated form of *ZntA* (Del231-*ZntA*), which lacks the first four transmembrane helices, are presented. This truncated form was based on the natural PINA splice variant of the copper-transporting Wilson disease-associated protein. Del231-*ZntA* had very low *in vitro* activity but was able to bind metal ions with a stoichiometry of 0.5, instead of the expected 1.

## AUTOBIOGRAPHICAL STATEMENT

I was born in Kerala, a place also known as the Venice of India and raised in Mumbai, the commercial capital of India. I completed my education from the University of Mumbai. My mother, Indira is a teacher by profession and my father, Murali is retired.

### **EDUCATION**

Ph.D., Biochemistry and Molecular Biology, Wayne State University, Detroit, Michigan (2010)

M.Sc., Biochemistry, University of Mumbai, India (2002)

### **HONORS AND AFFILIATIONS**

- Student member, American Academy for the Advancement of Sciences (2005-2008)
- Student member, American Chemical Society (2008, 2009)
- Student member, Society for Zinc Biology (2008, 2009)
- Wayne State University School of Medicine Graduate Student Travel Award (2008, 2009)
- 2005-2006 Student Representative, Graduate Program in Biochemistry and Molecular Biology
- Post-Graduate Merit Scholarship, University of Mumbai (2000-2002)

### **PUBLICATIONS**

- **Muralidharan, S.**, Haldar, S., and Mitra, B. and Penner-Hann, JE (Manuscript in preparation) EXAFS studies of the zinc, lead and cadmium sites of the cytosolic amino terminal domain of the Zinc transporting ATPase (ZntA)
- **Muralidharan, S.**, and Mitra, B. (Manuscript in preparation) Elucidating the role of metal transfer from the N-terminal domain to the membrane domain of *ZntA*, a Zinc transporting ATPase
- **Muralidharan, S.**, Haldar, S., and Mitra, B. (Manuscript in preparation) Characterizing the role of metal binding motifs in the N-terminal domain of *ZntA*